UNIVERSITEIT VAN PRETORIA
UNIVERSITY OF PRETORIA
YUNIBESITHI YA PRETORIA

Development of an *in vitro* mechanistic toxicity screening model using cultured hepatocytes

by
Jacob John van Tonder

A thesis submitted in partial fulfilment of the requirements for the degree

Doctor of Philosophy
in
Pharmacology

in the
Faculty of Health Sciences
at the
University of Pretoria

Supervisor: Prof. V. Steenkamp

Co-supervisors: Dr. A.D. Cromarty
Prof. M. Gulumian

Pretoria
November 2011

UNIVERSITEIT VAN PRETORIA
UNIVERSITY OF PRETORIA
YUNIBESITHI YA PRETORIA

Declaration

University of Pretoria

Faculty of Health Sciences

Department of Pharmacology

I, Jacob John van Tonder,

Student number: 21038491

Subject of the work: Development of an *in vitro* mechanistic toxicity screening model using cultured hepatocytes

Declaration

1. I understand what plagiarism entails and am aware of the University's policy in this regard.
2. I declare that this project (e.g. essay, report, project, assignment, dissertation, thesis etc.) is my own, original work. Where someone else's work was used (whether from a printed source, the internet or any other source) due acknowledgement was given and reference was made according to the departmental requirements.
3. I did not make use of another student's previous work and submitted it as my own.
4. I did not allow and will not allow anyone to copy my work with the intention of presenting it as his or her own work.

Signature:

Acknowledgments

- Prof. Vanessa Steenkamp and Dr. Duncan Cromarty for their guidance in the scientific process and taking the necessary steps to safeguard the quality of the results from this study. Teaching me the importance of objectivity and proving that my observations are accurate. For their patience and commitment.

- Prof. Mary Gulumian for her time and effort, ensuring that the interpretation of the results were accurate.

- Tracy Snyman, Clinical Chemistry at WITS, for her generous help regarding the propagation of the HepG2 cell line.

- Prof. Francois Steffens for pointing me in the right direction concerning statistical analyses and interpretation.

- My wife, Alet van Tonder, for her support, patience and understanding.

- God, for His faithfulness.

"Science is facts; just as houses are made of stones, so is science made of facts; but a pile of stones is not a house and a collection of facts is not necessarily science."

Henri Poincare

Abstract

In vitro testing includes both cell-based and cell-free systems that can be used to detect toxicity induced by xenobiotics. *In vitro* methods are especially useful in rapidly gathering intelligence regarding the toxicity of compounds for which none is available such as new chemical entities developed in the pharmaceutical industry. In addition to this, *in vitro* investigations are invaluable in providing information concerning mechanisms of toxicity of xenobiotics. This type of toxicity testing has gained popularity among the research and development community because of a number of advantages such as scalability to high throughput screening, cost-effectiveness and predictive power. Hepatotoxicity is one of the major causes of drug attrition and the high cost associated with drug development poses a heavy burden on the development of new chemical entities. Early detection of hepatotoxic agents by *in vitro* methods will improve lead optimisation and decrease the cost of drug development and reduce drug-induced liver injury. Literature highlights the need for a cell-based *in vitro* model that is capable of assessing multiple toxicity parameters, which assesses a wider scope of toxicity and would be able to detect subtle types of hepatotoxicity.

The present study was aimed at developing an *in vitro* procedure capable of mechanistically profiling the effects of known hepatotoxin dichlorodiphenyl trichloroethane (DDT) and its metabolites, dichlorodiphenyl dichloroethylene (DDE) and dichlorodiphenyl dichloroethane (DDD) on an established liver-derived cell line, HepG2, by evaluating several different aspects of cellular function using a number of simultaneous *in vitro* assays on a single 96 well microplate. Examined parameters have been suggested by the European Medicines Agency and include: cell viability, phase I metabolism, oxidative stress, mitochondrial toxicity and mode of cell death (apoptosis *vs.* necrosis). To further assess whether the developed method was capable of detecting hepatoprotection, the effect of the known hepatoprotectant, *N*-acetylcysteine, was determined.

Viability decreased in a dose-dependent manner yielding IC_{50} values of 54 µM, 64 µM and 44 µM for DDT, DDE and DDD, respectively. Evaluation of phase I metabolism showed that

cytochrome P4501A1 activity was dose-dependently induced. Test compounds decreased levels of reactive oxygen species, and significantly hyperpolarised the mitochondrial membrane potential. Assessment of the mode of cell death revealed a significant elevation of caspase-3 activity, with DDD proving to be most potent. DDT alone induced dose-dependent loss of membrane integrity.

These results suggest that the tested compounds produce apoptotic death likely due to mitochondrial toxicity with subsequent caspase-3 activation and apoptotic cell death. The developed *in vitro* assay method reduces the time it would take to assess the tested parameters separately, produces results from multiple endpoints that broadens the scope of toxicity compared to single-endpoint methods. In addition to this the method provides results that are truly comparable as all of the assays utilise the same batch of cells and are conducted on the same plate under the exact same conditions, which eliminates a considerable amount of variability that would be unavoidable otherwise. The present study laid a solid foundation for further development of this method by highlighting the unforeseen shortcomings that can be adjusted to improve scalability and predictive power.

Keywords: *Apoptosis, CYP1A1, DDD, DDE, DDT, hepatotoxicity, mechanistic profiling, mitochondrial hyperpolarisation, necrosis, organochlorine, reactive oxygen species.*

Table of Contents

List of Abbreviations

%	percentage
°C	degrees Celsius
$\bullet O_2^-$	superoxide
•OH	hydroxyl radical
7-ER	7-ethoxyresorufin
AAPH	2',2'-azobis(2-methylpropionamidine) dihydrochloride
Ac-DEVD-AMC	Acetyl-Asp-Glu-Val-Asp-7-amino-4-methylcoumarin
ADP	adenosine diphosphate
AhR	aryl hydrocarbon receptor
AIDS	acquired immune deficiency disease
AMC	7-amino-4-methylcoumarin
Apaf-1	apoptotic protease activating factor-1
Arnt	aryl hydrocarbon receptor nuclear translocator
ATP	adenosine triphosphate
Bad	Bcl-2 associated death promoter
Bax	Bcl-2 associated X protein
Bcl-2	B-cell lymphoma 2 protein
BH3	Bcl-2 homology domain 3
Bid	BH3 interacting-domain death agonist
Ca^{2+}	calcium
Cas-3	caspase 3
CAT	catalase
CHAPS	3-[(3-Cholamidopropyl)dimethylammonio]-1-propanesulfonate
cm	centimeter
CO_2	carbon dioxide
Cu^{2+}	copper(II)
Cu^{3+}	copper(III)
CYP	cytochrome P450
cyt C	cytochrome C
d	days
DCFDA	2'7'-dchlorofluorescein diacetate
DDA	bis(*p*-chlorophenyl)acetic acid
DDD	dichlorodiphenyl dichloroethane
DDE	dichlorodiphenyl dichloroethylene
DDT	dichlorodiphenyl trichloroethane
DISC	death-inducing signalling complex
DMSO	dimethylsulfoxide
DNA	deoxyribonucleic acid
$\Delta\psi_m$	mitochondrial membrane potential

EDTA	ethylenediaminetetraacetic acid
EMEA	European Medicines Agency
EMEM	Eagle's minimum essential medium
EROD	ethoxyresorufin-*O*-deethylase
$FADH_2$	flavin adenine dinucleotide (reduced)
FCS	foetal calf serum
Fe^{2+}	iron(II)
Fe^{3+}	iron(III)
g	gram
g	gravity
G-6-PD	glucose-6-phosphate dehydrogenase
GR	glutathione reductase
GSH	glutathione
GSH-Px	glutathione peroxidase
GSSG	glutathione disulfide
h	hour
H^+	proton
H_2O	water
H_2O_2	hydrogen peroxide
HEPES	2-[4-(2-hydroxyethyl)piperazin-1-yl]ethanesulfonic acid
HIV	human immunodeficiency virus
HSP90	heat shock protein 90
IC_{50}	concentration at which 50% of cells are not viable
JC-1	5,5',6,6'-tetrachloro-1,1',3,3'- tetraethylbenzimidazolylcarbocyanine iodide
KH_2PO_4	potassium dihydrogen orthophosphate
l	litre
LD_{50}	dose at which 50% of the population does not survive
LDH	lactate dehydrogenase
M	molar
m	milli-
MEIC	Multicentre evaluation of *in vitro* cytotoxicity program
Mg^{2+}	magnesium (II)
min	minutes
MMO	microsomal monooxygenase system
mPTP	mitochondrial permeability transition pore
mRNA	messenger ribonucleic acid
MTT	3-(4,5-Dimethylthiazol-2-yl)-2,5-diphenyltetrazolium bromide
n	sample size
Na^+	sodium
NAC	*N*-acetylcysteine
NADH	nicotinamide adenosine dinucleotide (reduced)
NADPH	nicotinamide adenosine dinucleotide phosphate (reduced)
NFI	nuclear factor I

NRU	neutral red uptake
O_2	oxygen
OH^-	hydroxyl
p	probability
p53	tumour protein 53
PBS	phosphate buffered saline
pH	negative logarithm of the hydrogen ion concentration
PI	propidium iodide
ppm	parts per million
Puma	*p53* up-regulated modulator of apoptosis
r^2	coefficient of determination
RFI	relative fluorescence intensity
RLW	relative liver weight
RNS	reactive nitrogen species
ROS	reactive oxygen species
RSA	Republic of South Africa
SEM	standard error of the mean
SOD	superoxide dismutase
t	test statistic
TCDD	2,3,7,8-tetrachlorodibenzo-*p*-dioxin
U	units
UK	United Kingdom
US$	US dollars
USA	United States of America
v	volume
V	volts
w	weight
XRE	xenobiotic response element
β	beta
γ-GCS	γ-glutamylcysteine synthase
λ_{em}	emission wavelength
λ_{ex}	excitation wavelength
µ	micro

List of Figures

Changes in $\Delta\psi_m$ in HepG2 cells following a 1 h exposure to various concentrations of DDT, DDE and DDD relative to untreated controls. Dark green bars represent cells exposed to test compounds alone and light green bars those with a 1 h pre-treatment with NAC (mean ± SEM). * = ***p*** < 0.05, ** = ***p*** < 0.01 and *** = ***p*** < 0.001 as determined by Mann-Whitney tests. Dashed horizontal lines represent Y = 100%.

Active caspase-3 in HepG2 cells following 6 h exposure to Control *vs.* Staurosporine (11 µM) (mean ±SEM). Staurosporine significantly induced caspase-3 activity with ***p*** < 0.001 (***).

Caspase-3 activity in HepG2 cells following 6 h exposure to DDT (A), DDE (B) and DDD (C) (mean ±SEM). Caspase-3 activity was used as a measure of cell death by apoptosis. Graphs (D), (E) and (F) represent the PI staining of cells exposed to DDT, DDE and DDD, respectively. Propidium iodide was used as a measure of membrane integrity and cell death by necrosis. Dashed horizontal lines represent untreated control values. Results are given as mean ± SEM. ** indicates ***p*** < 0.01 and *** ***p*** < 0.001 as determined by Mann-Whitney and Student's ***t***-tests, where applicable.

Propidium iodide staining as a measure of membrane integrity in HepG2 cells following treatment with 0.5% (v/v) Triton X-100 (TX-100) (mean ±SEM). *** = ***p*** < 0.001.

Caspase-3 activity in HepG2 cells following 6 h exposure to DDT (A), DDE (B) and DDD (C) (mean ±SEM). Graphs (D), (E) and (F) represent the PI staining of cells exposed to DDT, DDE and DDD, respectively. Caspase-3 activity and propidium iodide were used as a measure of cell death by apoptosis and necrosis, respectively. Dashed horizontal lines represent Control values. Results are given as mean ± SEM. * indicates ***p*** < 0.05, ** indicates ***p*** < 0.01 and *** ***p*** < 0.001 as determined by

List of Tables

Chapter 1: Literature review

1.1. Introduction

A significant advance in the field of early medicine was Paracelsus' recognition that all compounds have the capacity to be poisonous depending upon dosage. This has made toxicity testing a necessary and critical industry practice to identify and define safety thresholds for all new potential chemotherapeutics (Niles *et al.*, 2009). As there are a number of ways in which a substance can induce toxicity in an organism, there are a number of toxicities that can be tested for with any given substance. Within the scope of life sciences, toxicity generally refers to cellular toxicity that may result from a number of adverse alterations at a sub-cellular level. This type of toxicity is usually related to an organ or tissue type such as the kidney, brain, heart and liver. Apart from direct xenobiotic cytotoxicity, cardiotoxicity may also be the result of alterations in contractility or ventricular arrhythmias (Gwathmey *et al.*, 2009; Mandenius *et al.*, 2011). Of these, drug-induced ventricular arrhythmias have received the most attention of late, especially from regulatory authorities (Mandenius *et al.*, 2011). The reason for this is QT-interval prolongation, which is associated with the potentially fatal arrhythmia known as *torsades de pointes* (Liu *et al.*, 2011).

Other types of toxicity that are not due to cytotoxicity but rather perturbed signalling between systems within an organism as a whole include developmental toxicity, endocrine toxicity and allergenicity. In addition to these, there is also genotoxicity, which is related to genetic mutations and cancer. Collectively, the afore-mentioned serves to demonstrate the fragility of homeostasis and how easily it can be disrupted by the introduction of xenobiotics.

1.2. Safety evaluation

Considerable time, effort and expenses are spent on safety evaluation of pharmaceuticals in development. Pharmaceutical safety evaluation includes pre-clinical testing, clinical safety assessment and post-marketing safety evaluation. Pre-clinical testing involves both *in vitro* and *in vivo* safety assessment. The usual sequence of testing involves: *in vitro*, *in vivo* animal testing (rodent + non-rodent), clinical safety evaluation (Phase I - III trials) and finally post-marketing safety evaluation (adverse event reporting etc.). At the one end of the spectrum, clinical and post-marketing safety evaluations provide 'true' toxicity data that may be difficult to explain, whereas *in vitro* testing that may lack predictive power provides very specific (mechanistic) toxicological information. This illustrates why all of the afore-mentioned areas of safety evaluation are necessary to provide comprehensive information regarding the safety of a particular compound.

In vitro toxicology simply describes a field of endeavour that applies technologies inclusive of isolated organs, isolated tissues, cell culture, biochemistry, and chemistry to the study of toxic or adverse reactions to xenobiotics. This type of safety assessment is used principally for two reasons: 1) to generate more comprehensive toxicological profiles of a compound and 2) for screening purposes. *In vitro* methods are invaluable in providing mechanistic information on toxicological findings for both in experimental animals and in humans and they are also of potential use for studying local or tissue and target specific effects (Eisenbrand *et al.*, 2002). Cell-based approaches to toxicity testing generally involves cytotoxicity testing using one of the many assays that are prevalent in literature such as the neutral red uptake, dimethylthiazol diphenyltetrazolium (MTT), sulforhodamine B and lactate dehydrogenase (LDH) leakage assays, to name a few. As with any assay, each have advantages and disadvantages but all of them are relatively easy and fast to perform.

One area of toxicology in particular for which whole cell cultures are required is cardiotoxicity, the reason being that intact cells are necessary for researchers to study and detect xenobiotic-induced arrhythmias. Evaluating cardiotoxicity *in vitro* is made difficult for a number of reasons. There is significant interspecies variation and the lack of predictive

power prevents data derived from animal models being directly extrapolated to humans. This is further complicated by the fact that human cardiomyocytes are very difficult to obtain and highly differentiated with extremely low proliferative capacity and rapid loss of phenotypical characteristics in culture. Apart from the normal cytotoxicity testing, screening assays in cardiotoxicity also include electrophysiological measurements of action potentials of the cultured cells, from which the potential of a compound to induce arrhythmias is deduced (Mandenius *et al.*, 2011).

Cytotoxicity testing has proven to be accurate in predicting lethal human blood concentrations (Ekwall *et al.*, 1998). Realising that cytotoxicity testing alone has limited potential in detecting some subtle types of toxicity, researchers have developed cell-based strategies that examine more than one endpoint (Flynn and Ferguson, 2008; Wu *et al.*, 2009). Flynn and Ferguson (2008) tested the predictive power of their method and found good correlation with *in vivo* data, which is promising for this type of "expanded" cytotoxicity testing. However, some of the parameters were not very specific with regards to the endpoint that was examined. For example, rhodamine 123 was used to assess both mitochondrial effects and P-glycoprotein function in the same cell sample. The question arises that should a change be detected in this sample, would that be the result of mitochondria or P-glycoprotein function being affected? Although the advantages of a multiparametric cell-based model are obvious, minor oversights, such as the example given, and limited scalability have restricted the use of these techniques for screening purposes.

Apart from cytotoxicity, *in vitro* testing is also capable of examining the effects that xenobiotics may have on specific biochemical / signalling pathways at a sub-cellular level, which may be a difficult proposition *in vivo*, especially when human tissues are involved. Recently, commercially available molecular toxicology screening technology has made it possible to screen xenobiotics for affects they may have on up to 45 molecular pathways in microplate format (Panas *et al.*, 2011). This type of advancement is responsible for the growing significance of *in vitro* testing in safety assessment. Furthermore, because this type of testing is likely to be scalable to high-throughput screening, it may greatly enhance current understanding of molecular toxicology provided that enough classes of toxic compounds are screened and data deposited in appropriate databases.

Databases form a fundamental part of another technique that has gained popularity in toxicology over the last decade or two - *in silico* computational toxicology. Quantitative structure-activity relationship (QSAR) models generate equations by statistically identifying molecular descriptors and/or sub-structural molecular attributes that are correlated with toxicity (Kruhlak *et al.*, 2007). This type of toxicity prediction is especially useful when no previous toxicological information is available with regards to a particular molecule or to gather some initial information while proper toxicity testing is underway. In the pharmaceutical industry, computational toxicology is used as a sentinel tool for the early assessment of the toxicological potential of candidate molecules in lead selection and drug discovery (Pearl *et al.*, 2001).

1.3. The burden of hepatotoxicity on the pharmaceutical industry

More than 600 drugs have been associated with hepatotoxicity. The clinical picture is diverse, even for the same drug when given to different patients. The manifestations range from mild, asymptomatic changes in serum transaminases, which occur at a relatively high frequency with a number of drugs, to fulminant hepatic failure, which although rare, is potentially life threatening and may necessitate a liver transplant (Park *et al.*, 2005).

From a pharmaceutical viewpoint toxicology plays a major role during early drug development, from the initial pre-clinical development of lead compounds through to the late clinical evaluation (phase III trials). Between 1992 and 2002, 43%, 25%, and 35% of drugs undergoing Phase I, II, and III studies, respectively, were terminated due to the development of mostly hepatic injury (Schuster *et al.*, 2005). Also, the most common cause of drug attrition is drug-induced liver injury and between 1992 and 2002, 27% of market withdrawals in the United States and the European Union were due to hepatotoxicity (Lasser *et al.*, 2002; Schuster *et al.*, 2005). The pharmaceutical industry spends more than US$ 20 billion on drug discovery and development per year, with approximately one fifth of this amount is being used in initial screening assays and toxicity testing. To alleviate this financial burden, knowledge concerning the early events in drug-induced toxicity is required

to aid in the decision-making processes during the development of new therapeutic agents (Hakimelahi and Kodarahmi, 2005). It is desirable to detect toxicity as early as possible, preferably during the pre-clinical phase, which will aid lead optimisation and subsequently increase the successful output of the entire process. Boosting the output from drug development programs is a necessity as there is a global need for faster drug development and nowhere is this more urgent than in the pharmaceutical field of antibiotics. Resistance to currently available antibiotics is rising and the arsenal of drugs seems to be shrinking as the development of novel antibiotics is not able to keep up with the increasing rate of microbial resistance (Livermore, 2004; Finch and Hunter, 2006; Baiden *et al.*, 2010). Market withdrawals due to hepatotoxicity of antibiotics like Temafloxacin and Trovafloxacin (Peters, 2005) are only contributing to the problem.

Toxicity testing during preclinical drug development is intended to identify target tissues and then assess potential risks prior to introduction of new molecular entities into the human population. The standard regimen is testing at different doses in at least two species of animals, one rodent (rats or mice) and one non-rodent (dogs, nonhuman primates, minipigs or rabbits) for at least two weeks of repeated dosing. Although experience has shown that this regimen “works” most of the time, in many cases hepatotoxicity is detected later in animal toxicity studies or clinical trials (Ballet, 1997). However, animal testing is financially burdensome and because hundreds of compounds are synthesized each year, the cost of animal testing, which may exceed several million dollars to test a single substance for safety assessment, needs to be reduced (Davila *et al.*, 1998).

1.4. Hepatotoxicity

The clinical patterns of hepatotoxicity are hepatocellular damage, cholestasis, a mixed hepatocellular and cholestatic injury, and steatosis (Abboud and Kaplowitz, 2007). Clinical signs relate back to the underlying molecular mechanisms, which can be invoked in hepatocyte injury induced by a xenobiotic itself or by any of its metabolites, leading to cell death by necrosis or apoptosis.

The critical synthetic, metabolic, and detoxifying functions of the liver partly explain its unique vulnerability to injury by xenobiotics (Hardisty and Brix, 2005; Gomez-Lechon *et al.*, 2010a). Liver injury can manifest in various ways, with the two main types of injury being cytotoxicity and cholestasis. The former refers to the death of hepatocytes following loss of cellular homeostasis mainly due to damage to cellular organelles such as mitochondria. After the ingestion of sufficient amounts of an intrinsic hepatotoxin the afore-mentioned damage on a cellular level may then lead to liver injuries such as zonal hepatocellular necrosis (Tsui, 2003). Cholestatic injury involves reduced formation or secretion of bile. Most cases of drug-induced cholestatic injury result from a drug- or metabolite-mediated inhibition of hepatobiliary transporters located in the plasma membranes of hepatocytes (Pauli-Magnus and Meier, 2006).

Intrinsic hepatotoxins exert toxic effects in all individuals in a predictable, dose-related manner either directly (active intrinsic hepatotoxins) or following biotransformation (latent intrinsic hepatotoxins)(Castell *et al.*, 1997). Examples of direct intrinsic hepatotoxins include: carbon tetrachloride (cytotoxic) and paraquat (cholestatic), whereas latent intrinsic hepatotoxins include: acetaminophen (cytotoxic) and steroids (cholestatic) (Tsui, 2003).

Unpredictable compound-induced liver damage is termed idiosyncratic hepatotoxicity and is not dose related. This type of liver injury is mostly attributed to host hypersensitivity and/or aberrant metabolism. It is usually a result of host genotype that results in either toxic metabolites or prolonged host exposure due to slow drug/xenobiotic metabolism (Tsui, 2003; Pauli-Magnus and Meier, 2006). Idiosyncratic reactions, which are qualitatively different from a drug's pharmacologic activity, are often immunologically mediated and have a host-dependent component (Peters, 2005). Symptoms may take weeks or months to manifest and is often characteristic of hypersensitivity-type reactions including eosinophilia and rash, such as seen with an amoxicillin-clavulinate hepatotoxic reaction. Idiosyncratic liver injury has been reported for the drugs Isoniazid and Troglitazone (Peters, 2005).

1.5. Molecular mechanisms of hepatotoxicity

1.5.1. Metabolic activation

The biotransformation of lipophilic compounds into hydrophilic derivatives, that are more readily excreted, is one of the physiological roles of the liver (Park *et al.*, 2005). There are two phases of metabolism. Phase I metabolism involves the cytochrome P450 enzymes (CYP), which are responsible for the functionalisation of xenobiotic compounds (Iyer and Sinz, 1999). This is accomplished by the introduction of polar and reactive groups into the specific compound through various reactions which include hydroxylation, oxygenation, dealkylation and epoxidation (Guengerich, 2001). Phase I metabolism is aimed at preparing the compound for phase II metabolism by making the molecule more polar and chemically reactive. Phase II metabolism is focused on the conjugation of the phase I metabolites to polar, charged molecules such as glutathione, sulphate, glycine and glucuronic acid. These reactions are catalysed by transferases like glutathione-*S*-transferase and render the phase I metabolite more polar and therefore biologically inactive as it cannot easily cross cell membranes. This polarity also aids in the elimination of the compound from the body through renal excretion (Jakoby and Ziegler, 1990).

Although xenobiotic metabolism is aimed at detoxification, some xenobiotics can undergo biotransformation to metabolites that have intrinsic chemical reactivity towards cellular macromolecules. A number of enzymes, and in particular CYPs, can generate reactive metabolites, even from inert substances (Ioannides and Lewis, 2004; Park *et al.*, 2005). The identity of the susceptible cellular macromolecules, and the physiological consequence of its covalent modification, will dictate the resulting toxicological response. Toxic responses may include carcinogenicity, cell death or hypersensitivity (Figure 1.1).

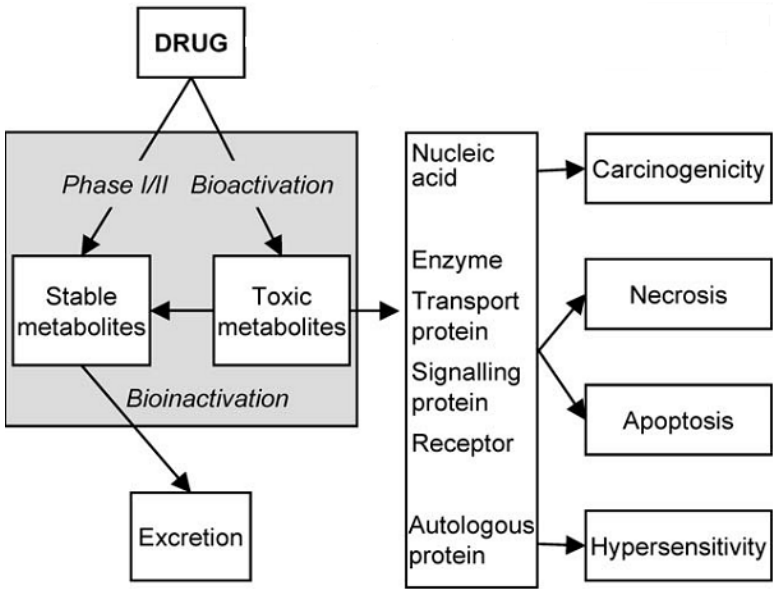

Figure 1.1. **The relationship between drug metabolism and toxicity. Toxicity may occur through accumulation of parent drug or via metabolic activation, through formation of a chemically reactive metabolite, which, if not detoxified, can effect covalent modification of biological macromolecules. The identity of the target macromolecule and the functional consequence of its modification will dictate the resulting toxicological response (Park *et al.*, 2005).**

A classic example of hepatotoxicity as a result of metabolic activation is acetaminophen (paracetamol) toxicity. At therapeutic doses, acetaminophen is well tolerated. However, at higher doses it can induce acute hepatotoxicity. This is due to the formation of the reactive metabolite *N*-acetyl-*p*-benzoquinone-imine, which depletes cellular antioxidants (glutathione) and results in cell death by necrosis (James *et al.*, 2003; Marzullo, 2005). Troglitazone, an antidiabetic drug, was withdrawn from the market due to idiosyncratic hepatotoxicity. It was found that metabolic activation of Troglitazone in patient populations with specific gene polimorphisms was responsible for the idiosyncratic hepatotoxicity of the drug (Ikeda, 2011).

Hepatotoxicity due to metabolic activation of drugs is prevalent enough that metabolite profiling in hepatic preparations from experimental species and humans has become a routine task which has been incorporated into drug discovery and development processes. Furthermore, the data constitutes an important section in regulatory filing to eliminate

hepatotoxic metabolites at an early stage of drug development (Kalgutkar and Soglia, 2005; Park *et al.*, 2005).

1.5.2. Mitochondrial toxicity

Mitochondria are present in almost all eukaryotic cells, their chief function being energy production for the benefit of the cell. Malfunctioning mitochondria present a hazard to any cell, not only due to depletion of energy stores but also because of disturbed signalling pathways (Wallace and Starkov, 2000). Mitochondria generate energy by actively producing an electrochemical proton gradient across the inner membrane of the mitochondrion, termed the mitochondrial membrane potential. The backflow of protons down the electrochemical gradient, from the intermembrane space into the mitochondrial cytosol is used to drive the enzyme ATP synthase and thus the synthesis of molecules that provide cellular energy.

Xenobiotics can affect hepatic mitochondria either directly or indirectly. Direct interaction may occur in one of two ways: either by inhibiting the production of the required electrochemical gradient or through its dissipation (Wallace and Starkov, 2000). Changes in this electrochemical gradient will manifest as either mitochondrial hyperpolarisation (steeper gradient) or depolarisation (loss of gradient). Examples of xenobiotics that affect mitochondria directly are diclofenac (Masubuchi *et al.*, 2002) and phenobarbital (Santos *et al.*, 2008). Diclofenac has been shown to inhibit enzymes involved in the mitochondrial electron transport chain, causing depolarisation of the mitochondrial inner membrane by acting as an uncoupler (Moreno-Sanchez *et al.*, 1999).

Xenobiotics can also affect mitochondria indirectly through cytosolic Ca^{2+} signalling. A number of researchers have established that mitochondria act as intracellular 'Ca^{2+} buffers', which eliminates excess cytosolic Ca^{2+} through active transport via a ruthenium red-sensitive uniporter (Parekh, 2003; Duchen, 2004). Furthermore, it has been demonstrated that mitochondrial Ca^{2+}concentrations influence mitochondrial respiration rate by directly modulating the activity of the various enzymes involved in the electron transport chain

(Brini, 2003). The latter implies that any xenobiotic affecting intracellular Ca^{2+} concentrations/signalling may possibly disturb mitochondrial respiration and thus adversely affect a cells energy homeostasis.

In recent years, considerable attention has been paid to mitochondria regarding both apoptotic and necrotic cell death because of the role of mitochondria in electrolyte homeostasis in cells (e.g. acting as 'Ca^{2+} buffers') and the myriad of proteins present inside the mitochondrial cytosol, one of which is cytochrome C (Cyt C). Disturbances in cellular electrolyte balance may lead to cellular swelling and necrotic death, whereas release of cyt C into the cytosol may trigger a signalling cascade leading to apoptotic death through caspase activation (Silva and Couthino, 2010).

1.5.3. Oxidative stress

Any atom/molecule with an unpaired valence electron(s) is referred to as a free radical. The widely used term reactive oxygen species (ROS) refers not only to oxygen-centred free radicals but also to other non-radical but reactive oxygen-centred molecules (Halliwell and Gutteridge, 2007). Under certain conditions the production of ROS is enhanced and/or the levels or activity of endogenous cellular antioxidant defences are reduced. The resulting state, which is characterized by a disturbance in the balance between ROS production, ROS removal, and repair of damaged complex molecules, is called oxidative stress (Cederbaum *et al.*, 2009). Oxidative stress has been implicated as a major cause of cellular injury in a variety of clinical abnormalities including cancer, neurological diseases, arthritis, and hepatitis and is also thought to accelerate the aging process (Droge, 2002; Wang and Weinman, 2006).

The major types of ROS in cells are superoxide anion ($\bullet O_2^-$), singlet oxygen, hydrogen peroxide (H_2O_2) and hydroxyl radicals ($\bullet OH$). The nitrogen-centred equivalents of ROS are referred to as reactive nitrogen species or RNS, which include molecules such as nitric oxide and peroxynitrite. The $\bullet OH$ radical is potentially the most reactive of the afore-mentioned

molecules because of its very strong oxidising potential (Powers and Jackson, 2006). This high reactivity also makes it likely to react very close to its site of generation causing DNA damage, initiating lipid peroxidation or causing protein residue modification (Zhang *et al.*, 2010). In order to generate •OH in a biological environment, H_2O_2 has to react with transition metals such as Fe^{2+} or Cu^{2+} (Zhao *et al.*, 2005) in the Fenton reaction where:

$$H_2O_2 + Fe^{2+}/Cu^{2+} \rightarrow Fe^{3+}/Cu^{3+} + OH^- + \bullet OH$$

H_2O_2 is generated from nearly all sources of oxidative stress and has the ability to diffuse freely in and out of cells and tissues (Barbouti *et al.*, 2002). Therefore, one way of probing for potentially damaging ROS generation would be to determine H_2O_2 generation, which is required for the formation of •OH in biological systems (Powers and Jackson, 2006).

Two major sources of ROS in cells are the mitochondria and CYPs. The main type of ROS produced by mitochondria is $\bullet O_2^-$. The major contributor of mitochondrial $\bullet O_2^-$ is the respiratory complex III, where it is believed that O_2 present within the lipid bilayer of the inner mitochondrial membrane is reduced by the ubisemiquinone radical to form $\bullet O_2^-$. A portion of the $\bullet O_2^-$ produced is then converted into H_2O_2 by mitochondrial superoxide dismutase (SOD) (Jezek and Hlavata, 2005). With regards to CYPs, ROS generation is the result of uncoupling of the redox cycle between the haem active site and nicotinamide adenine dinucleotide phosphate (NADPH), which causes the release of $\bullet O_2^-$ and H_2O_2. This type of event is highly substrate-specific and has been associated with tight binding of the substrate to the specific CYP catalytic site (Schlezinger *et al.*, 2006).

To protect against the adverse effects of ROS, cells possess a complex machinery of antioxidant compounds and enzymes, which include glutathione (GSH), SOD, catalase (CAT), glutathione peroxidase (GSH-Px) and glutathione reductase (GR) (Polaniak *et al.*, 2010). Figure 1.2 depicts the interaction between the various components of this machinery.

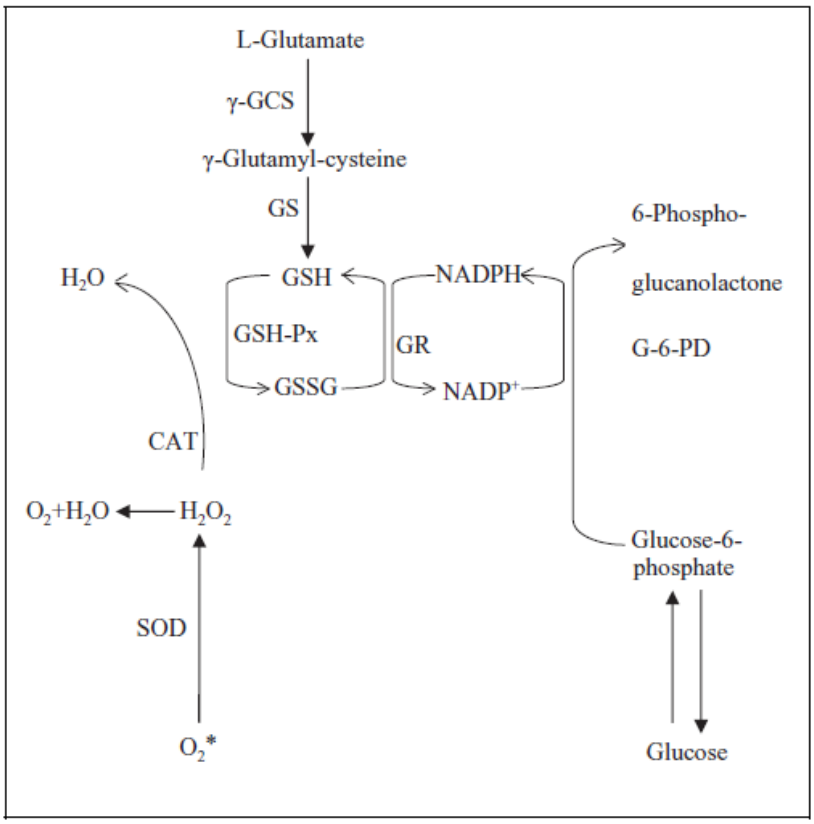

Figure 1.2. **Cooperation between various antioxidant enzymes and cofactors. SOD – superoxide dismutase, CAT – catalase, GSH – glutathione, GSSG – glutathione disulfide, GSH-Px – glutathione peroxidase, GR – glutathione reductase, γ-GCS – γ-glutamylcysteine synthase, GS – glutamine synthase, G-6-PD – glucose-6-phosphate dehydrogenase (Polaniak *et al.*, 2010).**

Glutathione (GSH), a tripeptide, is the most abundant non-protein thiol in cells (Meister and Anderson, 1983). It can counteract a state of oxidative stress in a number of ways:

- It can react directly with a radical by donating a hydrogen cation, thus eliminating the unpaired valence electron and rendering the free radical harmless (Yu, 1994)

- It serves as a substrate for GSH-Px to eliminate generated H_2O_2 (Meister and Anderson, 1983)

- It has the ability to reduce other oxidised antioxidant molecules such as vitamins E and C, replenishing their activity (Powers and Jackson, 2006)

Apart from excessive free radical generation, oxidative stress may also be induced by xenobiotics or their metabolites that diminish the cellular antioxidant capacity. This is done by inhibiting enzymes involved in generating endogenous antioxidant molecules (like GR) or depleting these endogenous antioxidant molecules (e.g. GSH), or other molecules required to generate endogenous antioxidant molecules (e.g. NADPH) (Figure 1.2). An example of a xenobiotic that is able to elicit this type of response is valproic acid, which is known to deplete cellular GSH content (Kiang *et al.*, 2011).

1.6. Need for improved cell-based hepatotoxicity screening

In light of the fact that hepatotoxicity is a major cause of drug attrition and drug development requires toxicity testing, evaluation of potential hepatotoxic effects represents a crucial step in the development of new drugs.

Human *in vitro* cellular models are valuable tools in understanding the molecular and cellular processes of drug-induced liver injury (Gomez-Lechon *et al.*, 2010a). The Multicentre Evaluation of In vitro Cytotoxicity program (MEIC) conducted a study in 29 different laboratories, where 50 reference chemicals were tested using 61 different *in vitro* cytotoxicity tests. The study concluded that *in vitro* cytotoxicity testing predicted the acute, lethal human blood concentrations just as well as mouse and rat LD_{50}s (Ekwall *et al.*, 1998). This demonstrates the potential of *in vitro* toxicity testing for reducing not only animal testing but also for reduction of post-commercialisation drug attrition due to hepatotoxicity. Furthermore, *in vitro* testing has the advantage over *in vivo* testing in being faster, more cost-effective and requiring less test material. These advantages show the vital and growing role *in vitro* testing is playing during early drug development, especially in light of the three R's of animal testing: replacement, reduction and refinement.

Gomez-Lechon *et al.* (2010a) stated: *"Current cytotoxicity assessments have been limited by their inability to measure multiple mechanistic parameters that capture a wide spectrum of potential cytopathological changes. By examining the effects on a hepatocyte-specific*

metabolism, it is possible to discover whether relevant hepatic functions are altered by the presence of a xenobiotic. However by addressing this issue, the development of robust in vitro-based multiparametric screening assays covering a wider spectrum of key effects will heighten the predictive capacity for human hepatotoxicity, and accelerate the drug development process". There is thus clearly a need for the development of a multiparametric hepatotoxicity screening model that assesses a wider spectrum of toxicity towards hepatic cells. The screening of multiple toxicity parameters should better reflect human *in vivo* hepatotoxicity and provide earlier safety assessment.

1.7. Model hepatotoxin

Dichlorodiphenyl trichloroethane (DDT) was originally synthesized in 1874 and put into use as an insecticide only in 1939. It was initially used by allied forces in the Second World War as vector control against malaria and was subsequently made available for commercial use in 1945 (World Health Orginisation, 1979). DDT was the most extensively used insecticide across the world until the 1960's and has been credited with the eradication of malaria from the USA and Europe (Attaran and Maharaj, 2001).

In order to be eliminated from the body, DDT has to be dechlorinated and oxidised by CYPs to intermediate metabolites such as dichlorodiphenyl dichloroethylene (DDE) and dichlorodiphenyl dichloroethane (DDD). DDE is a non-biodegradable and a highly fat-soluble molecule that accumulates in the adipose tissue of the organism. DDD on the other hand is biodegradable and with further metabolism it is converted intro bis(*p*-chlorophenyl)acetic acid (DDA), a water soluble molecule that is excreted in bile, faeces and urine (Klaassen *et al.*, 2001) (Figure 1.3).

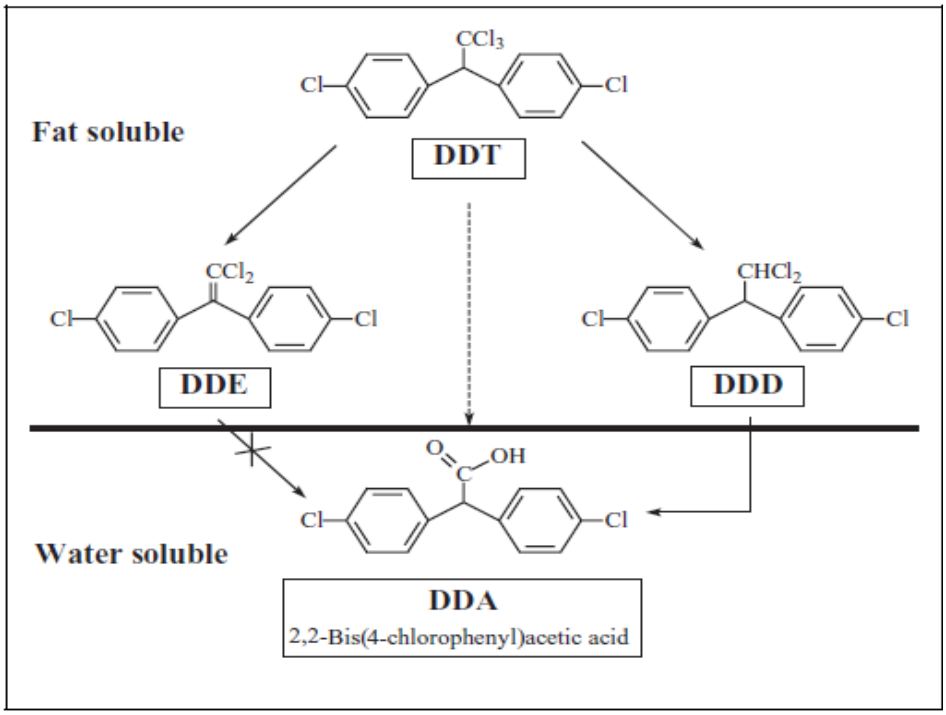

Figure 1.3. Illustration of the two routes of metabolism of DDT to produce either DDE or DDD, showing the structure of each of the test compounds utilised in this study (Chen *et al.*, 2009).

Studies have shown that DDT exposure increases the microsomal content and activity of CYP 2B1 and CYP 3A2 in liver tissue by enzyme induction (Klaunig and Ruch, 1987; Flodstrom *et al.*, 1990; Harada *et al.*, 2006). DDT partially exerts its anti-androgenic effects on the body by up-regulating the activity of, amongst others, these two enzymes (You *et al.*, 1999; Harada *et al.*, 2006). DDT has also been linked to increased oxidative stress by depleting cellular glutathione (GSH) content *in vitro* (Dehn *et al.*, 2005). It has been speculated that the depletion of GSH by DDT may be due to disruption of GSH regulation in the cell (Dehn *et al.*, 2005) and that there is a possible interaction between CYP induction and reduced GSH levels, which may lead to an increase in the generation of ROS (Bagchi *et al.*, 1993; Bagchi *et al.*, 1995) and depletion of cellular GSH stores. One of the major DDT metabolites, DDE, has also been shown to increase CYP activity, specifically the activities of CYP 2A1, CYP 2B1, CYP 2C11 and CYP 3A1 (You *et al.*, 1999).

Animal studies in rats have demonstrated that a single DDT dosage of 24 mg/kg body weight significantly increases relative liver weight (RLW) although a single dosage of 12 mg/kg body weight has no effect on RLW, (Kostka *et al.*, 1996). However, repeated dosages of 12 mg/kg

body weight do increase RLW (Kostka *et al.*, 1999). Histological examination revealed a high prevalence of cytoplasmic vacuolization and inflammatory infiltration, which is attributed to centrolobullar zonal necrosis whereas an increase in RLW is attributed to a regenerative liver response. Zonal necrosis was found to up-regulate both mitoses and DNA synthesis resulting in hepatomegaly. It is well known that cell proliferation plays a crucial role in the initiation of carcinogenesis in the liver (Butterworth *et al.*, 1992) and DDT has therefore been regarded as a hepatocarcinogen (Kostka *et al.*, 1999; Sukata *et al.*, 2002). DDT-induced liver toxicity is well documented.

DDT follows a similar mechanism of hepatotoxicity as some well-known hepatotoxic drugs in that biotransformation of DDT yields two major metabolites, DDE and DDD, which are also known hepatotoxins. Acetaminophen has long been established as a hepatotoxin at excessive dosages and also yields toxic metabolites after biotransformation (Ray *et al.*, 1999; Ray *et al.*, 2001). Another possible route of toxicity is that the process of DDT biotransformation may produce non-drug related reactive molecules that could result in hepatotoxicity, similar in mechanism to that of Isoniazid (Weisiger, 2010). The afore-mentioned similarities indicate that DDT was a suitable candidate for inducing toxicity in the present study. In addition, DDT as well as its two metabolites, DDE and DDD, are all commercially available as standards.

1.8. Hepatoprotective agent

N-acetylcysteine (NAC) is a thiol that is used in the clinical setting to treat drug toxicity and disease-associated oxidative stress. It is probably best known for its use during acetaminophen overdose but has also been used in the treatment of HIV/AIDS, cystic fibrosis and chronic obstructive pulmonary disease (Smilkstein *et al.*, 1991; Atkuri *et al.*, 2007). NAC is also used to alleviate some of the adverse effects associated with anti-cancer therapies such as doxorubicin, cyclophosphamide and phosphamide (De Flora *et al.*, 2001). The reason that NAC is used to counter a state of oxidative stress is two-fold. Not only is NAC able to scavenge free radicals itself by donating a hydrogen cation, but it is also able to replenish and maintain intracellular levels of glutathione by providing the necessary cysteine

for GSH synthesis (De Flora *et al.*, 2001; Carageorgiou *et al.*, 2004; Oh and Lima, 2006; Atkuri *et al.*, 2007).

In the present study NAC, was utilised to assess how a widely used hepatoprotectant may affect the toxicity parameters measured during the study. Due to its antioxidant activities (Wang *et al.*, 2000), authors have described NAC as being able to inhibit oxidative stress (Park *et al.*, 2002; Reliene *et al.*, 2004). Since DDT has been speculated to deplete intracellular GSH (Bagchi *et al.*, 1993; Bagchi *et al.*, 1995) it was postulated that NAC may be able to alleviate DDT-induced toxicity.

1.9. Research topic

Literature highlights the significance of hepatotoxicity in both drug development and attrition, which directs current research in this field towards early, accurate detection of hepatotoxicity, preferably during the pre-clinical stages of drug development. Literature also demonstrates how hepatotoxicity may come about through a number of different mechanisms. The diversity of processes that may lead to hepatotoxicity complicates cell-based *in vitro* detection using an assay that evaluates only a single endpoint. For this reason, there exists room for the development of a cell-based *in vitro* technique that assesses multiple endpoints in an attempt to detect subtle hepatotoxicity that an assay evaluating a single endpoint (such as the conventional cytotoxicity assay) may fail to detect.

1.10. Aims of the study

I. Develop an *in vitro* procedure capable of mechanistically profiling the effects of a model hepatotoxin on hepatocytes in culture by evaluating several different aspects of cellular function using a number of simultaneous *in vitro* assays on a single 96 well microplate.

II. To determine whether the model can detect hepatoprotective effects of NAC on hepatocytes exposed to a known hepatotoxin.

1.11. Study objectives

I. Assess a number of intracellular assays that test different aspects of toxin responses thereby allowing mechanistic profiling of the effect of a toxic compound on cultured hepatocytes.

II. Optimisation of the assays for compatibility with the proposed microplate assay method.

III. Stagger the hepatotoxicity assays in such a way that it allows simultaneous multiplexing of the selected assays using a single 96 well microplate.

IV. Determine whether the method provides acceptable sensitivity and mechanistic data when testing a known hepatotoxin.

V. Assess whether the developed assay method can detect the hepatoprotective effect on cultured hepatocytes pre-loaded with a known protective agent prior to hepatotoxin exposure.

Chapter 2: *In Vitro* Procedure

2.1. Introduction

2.1.1. Background

The use of *in vitro* methods/models has increased greatly in order to reduce the use of animal testing models (Davila *et al.*, 1998). Many hepatic *in vitro* test systems have been developed in the past including isolated perfused organs, tissue slices, cell culture/suspensions, isolated organelles/membranes/enzymes, invertebrates and non-living systems (Silber *et al.*, 1994).

Primary human hepatocytes are considered the ‘‘gold standard” in the pharmaceutical industry for rapid evaluation of new chemical entities for both liver-related pharmacokinetic and toxicity liabilities (Hewitt *et al.*, 2003). However, there are some drawbacks in using primary cultures. Most cryopreserved human hepatocyte preparations do not attach to the culture plate surface, thereby limiting their survival time (usually less than 24 h) (Flynn and Ferguson, 2008). Also, primary hepatocytes lose normal hepatocyte characteristics and functions, a few days after explantation, making them unsuitable for longer term studies (Katsura *et al.*, 2002). Furthermore, the availability of freshly plated human hepatocytes can be sporadic and different donors need to be used between temporarily separated batches of experiments (Flynn and Ferguson, 2008), leading to large donor-to-donor variability (Reid *et al.*, 2009).

The HepG2 hepatocarcinoma perpetual cell line has been widely used by many researchers for more than a decade in various *in vitro* models focusing on hepatotoxicity (Castell *et al.*, 1997; Sahu, 2003; Dambach *et al.*, 2005; Farkas and Tannenbaum, 2005; Baudoin *et al.*, 2007; Gomez-Lechon *et al.*, 2010b; Swift et al., 2010). Amongst others, the HepG2 cell line was chosen as one of the cell lines used in the LIINTOP project. This project is aimed at

establishing experimental *in vitro* models and protocols for testing hepatic metabolism and toxicity of molecules of pharmacological interest. This model also strives to replace animal experimentation with alternative models in the drug development process (Gomez-Lechon *et al.*, 2010b).

HepG2 cells display most of the genotypic and phenotypic features of normal liver cells (Sassa *et al.*, 1987) preserving many of the normal functions of human liver cells. These include aldehyde dehydrogenase regulation (Marselos *et al.*, 1987), high drug metabolising capacity (Dashti *et al.*, 1984; Knowles *et al.*, 1980), a functional glutathione system (Dierickx, 1987) and CYP subfamilies 1, 2 and 3, which are the major classes involved in drug and xenobiotic metabolism (Alexandre *et al.*, 1999; Westerink and Schoonen, 2007).

2.1.2. Hepatotoxic endpoints

There are a substantial number of endpoints that can be considered in hepatotoxicity studies. Scrutiny of relevant literature indicated that the toxicity endpoints suggested by "*The non-clinical guideline on drug-induced hepatotoxicity"* assembled by the European Medicines Evaluation Agency (EMEA) (Committee for medicinal products for human use, 2008) were the most appropriate. The parameters suggested by the EMEA together with the parameters that were tested in the present study are listed in Table 2.1.

In the present study one major substitution was made to the list of parameters suggested by the EMEA. "*Loss of critical macromolecules/small molecular scavengers*" was substituted with "*CYP1A1 induction*" (Table 2.1). ROS generation, which was already part of the panel of tests suggested by the EMEA, and cellular glutathione concentration, which would be a measure of "*Loss of critical macromolecules/small molecular scavengers*", evaluate the oxidative state of cells. To avoid duplication (two assays that assess oxidative status; ROS generation and GSH depletion), CYP1A1 was included in the panel of tests used in the present study. The broad xenobiotic selectivity of CYPs (Park *et al.*, 2005) increases the possibility to detect toxicity that may induce subtle adverse effects. Also, in HepG2 cells the

levels of CYP1A1, 1A2, 2B6 and 3A4 correlate well with primary cultures (Westerwink and Schoonen, 2007).

Table 2.1. **Parameters of cellular physiology that are suggested by the EMEA and those that were examined in the present study.**

Suggested by the EMEA	Examined in present study
Loss of membrane integrity	Loss of membrane integrity
Apoptosis induction	Apoptosis induction
Loss of critical macromolecules/small molecular scavengers	CYP1A1 induction
Increased ROS generation	Increased ROS generation
Mitochondrial effects	Mitochondrial effects
Anti-proliferative effects	Cell viability

2.1.3. Scope of toxicity

The toxicological parameters evaluated in the present study are graphically represented in Figure 2.1. Examining these parameters provides a good overview of the toxic response of the cells to the test compound. In an initial toxic response, cells (especially liver-derived cells) attempt to eliminate a xenobiotic through metabolic inactivation by especially CYPs, as these enzymes allow cells to adapt to changes in their chemical environment (Denison and Whitlock, 1995; Delescluse *et al.*, 2000). The focus in this study was on CYP1A1 as it is rapidly and highly induced by a wide range of substances (Whitlock, 1999; Ma, 2001), thereby increasing the chance of detecting an initial toxic response.

Another toxic response is the generation of ROS, which may originate either from the mitochondria (Liu *et al.*, 2002) or from CYP activity (Schlezinger *et al.*, 2006). ROS generation may induce a state of oxidative stress within the cell, which can disrupt homeostasis and in this way lead to cell death. Mitochondria are not only a source of ROS but may also be a

target for ROS under certain conditions, during which ROS mediates the release of cytochrome c from the mitochondrial intermembrane space. In turn, cytochrome c triggers caspase activation, leading to apoptosis (Simon *et al.*, 2000). However, if ROS generation produces excessive levels of radicals, these radicals may inactivate caspase activity, which could then favour necrosis as the mode of cell death (Samali *et al.*, 1999; Prabhakaran *et al.*, 2004).

Quantifying apoptotic and necrotic death provides valuable information regarding the mechanism of cell death. Furthermore, cell viability provides an indication of the concentration at which the test compound induces cell death.

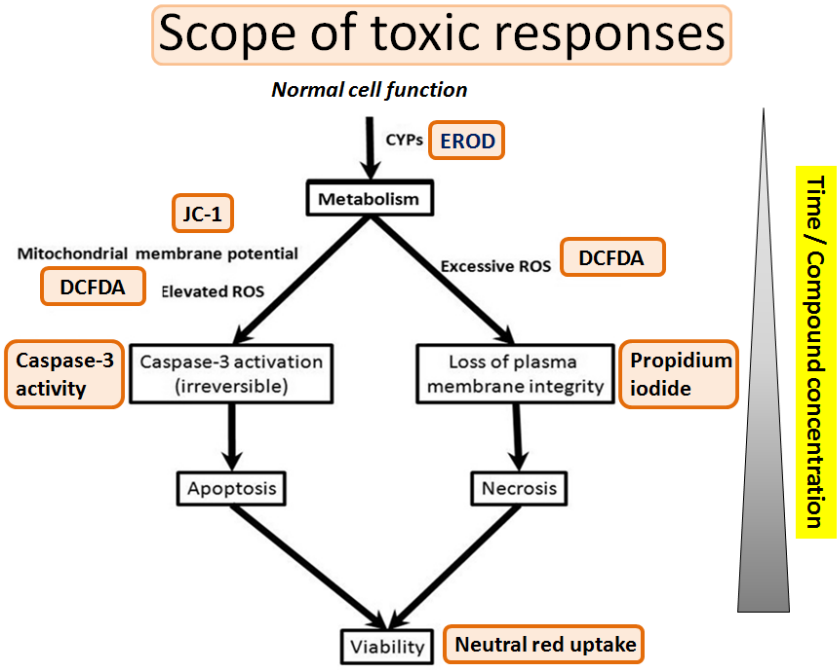

Figure 2.1. Diagram illustrating the scope of toxicity that the chosen parameters are expected to evaluate. As the concentration of test compound increases one would expect to see different cellular responses in an attempt to restore homeostasis. Initially, cells should respond by trying to eliminate xenobiotics through metabolic inactivation (Phase I metabolism). At higher concentrations ROS generation may occur, originating from either mitochondria or from CYP activity. If the mitochondria are affected, they may release factors that will initiate apoptotic death via caspase-3. On the other hand, excessive ROS may result in deactivating caspase activity and lipid peroxidation, which leads to cell death by necrosis. The degree of toxicity can then be assessed utilising an assay that enumerates viable cells. EROD - ethoxyresorufin-*O*-deethylase, JC-1 - 5,5′,6,6′-tetrachloro-1,1′,3,3′-tetraethylbenzimidazolylcarbocyanine iodide, DCFDA - 2'7'-dichlorofluorescein diacetate.

2.2. Methods

2.2.1. Propagation of Cells

Ethical approval for performing the work on a commercially available cell line was obtained from the Faculty of Health Sciences Research Ethics Committee (Annexure A). Cells were propagated in a CO_2 tissue culture incubator (Binder C150, USA) in EMEM containing non-essential amino acids and fortified with 10% FCS. Cells were grown in 75 cm^2 culture flasks and medium changed every 2-3 days, as required, until confluent before being harvested with trypsin-/versine and split 1:6. All experiments were performed on cells between passages 20 - 26.

2.2.2. Cell harvest

Propagation medium was discarded and the cell culture flask rinsed with sterile PBS to wash off excess FCS. This was followed by the addition of 2 ml of trypsin/versene and incubated for 5 - 7 min at 37°C. The suspension of detached cells was transferred to a sterile 15 ml tube, filled with EMEM containing 10% FCS to inactivate the trypsin/versene and then centrifuged at 200 *g* for 5 min. The supernatant was discarded and the cell pellet resuspended in 1 ml cell culture medium supplemented with 10% FCS. The suspension was mixed thoroughly with an autopipette to obtain a homogenous single-cell suspension.

2.2.3. Cell counting

A homogenous single-cell suspension was diluted 1:9 into Trypan blue counting solution. The mixture was immediately loaded onto a haemocytometer and a minimum of 200 cells were counted using a Reichert Jung MicroStar 110 microscope at 400x magnification. Trypan blue, a membrane impermeable dye, was used to improve assay consistency by eliminating

non-viable cells from the cell count by staining their cytoplasm blue. Dilutions of the cell suspension in EMEM (10% FCS) were then made to achieve the correct viable cell density required for the experiments.

2.2.4. Microplate setup

The microplate was set up as illustrated in Figure 2.2. The columns of each plate were divided to give 6 duplicate columns of 8 wells each. Each set of 16 wells was used to perform one of six *in vitro* assays. Additionally, each plate was divided into 8 rows spanning all 12 columns. Blanks, positive and negative controls and 5 different concentrations of each test compound (5, 10, 50, 100 and 150 µM) were allocated to each row. This setup allowed each assay to be performed in duplicate on each plate for each of the controls/test compound concentrations/blanks. Nine individual experiments were conducted, 6 for each of the test compounds (18 plates; 12 observations per parameter per compound) and 3 for each of the compounds in combination with NAC pre-treatment (9 plates; 6 observations per parameter per compound). Negative controls were exposed to vehicle solvent (0.5% DMSO) alone. Positive controls used were compounds different from the test compounds that demonstrate a predictable effect on each specific assay.

2.2.5. Test staggering

Depending on the plate row number, cells were exposed to either negative control (0.5% DMSO v/v), positive control (150 µM) or test compound at concentrations of 5, 10, 50, 100 and 150 µM (Figure 2.2). All procedures were carried out under sterile conditions and all incubations took place in a 5% CO_2 incubator at 37°C.

The times of treatment (test staggering) are provided in Table 2.2. The starting time of a specific assay (described individually in each relevant chapter) were different since the time to complete assays (exposure + incubation times), varied. The time lines were as follows:

Table 2.2. **A summary of the timing followed to perform the six *in vitro* toxicity assays on a single microplate. Columns refer to those shown in Figure 2.2.**

Time	Procedure	*Columns
-24 h	Expose for Viability + CYP + Necrosis determination	A-F
-6 h	Expose for Apoptosis determination	K-L
-4 h	ROS assay dye loading	G-H
-3 h	Wash + Expose for ROS determination	G-H
-2 h	Add Viability + CYP assay dyes	A-B; C-D
-1.5 h	Mitochondria assay dye loading	I-J
-1 h	Wash + Expose for Mitochondria determination	I-J
-15 min	Add Necrosis assay dye	E-F
-5 min	Wash Viability + Necrosis assays	A-B; E-F
0	Determine values for CYP + Necrosis + ROS + Mitochondria assays	C-J
+5 min	Lyse cells for Apoptosis assay	K-L
+20 min	Add Apoptosis assay dye	K-L
+ overnight	Determine values for Viability +Apoptosis assays	A-B; K-L

*Columns refer to those shown in Figure 2.2.

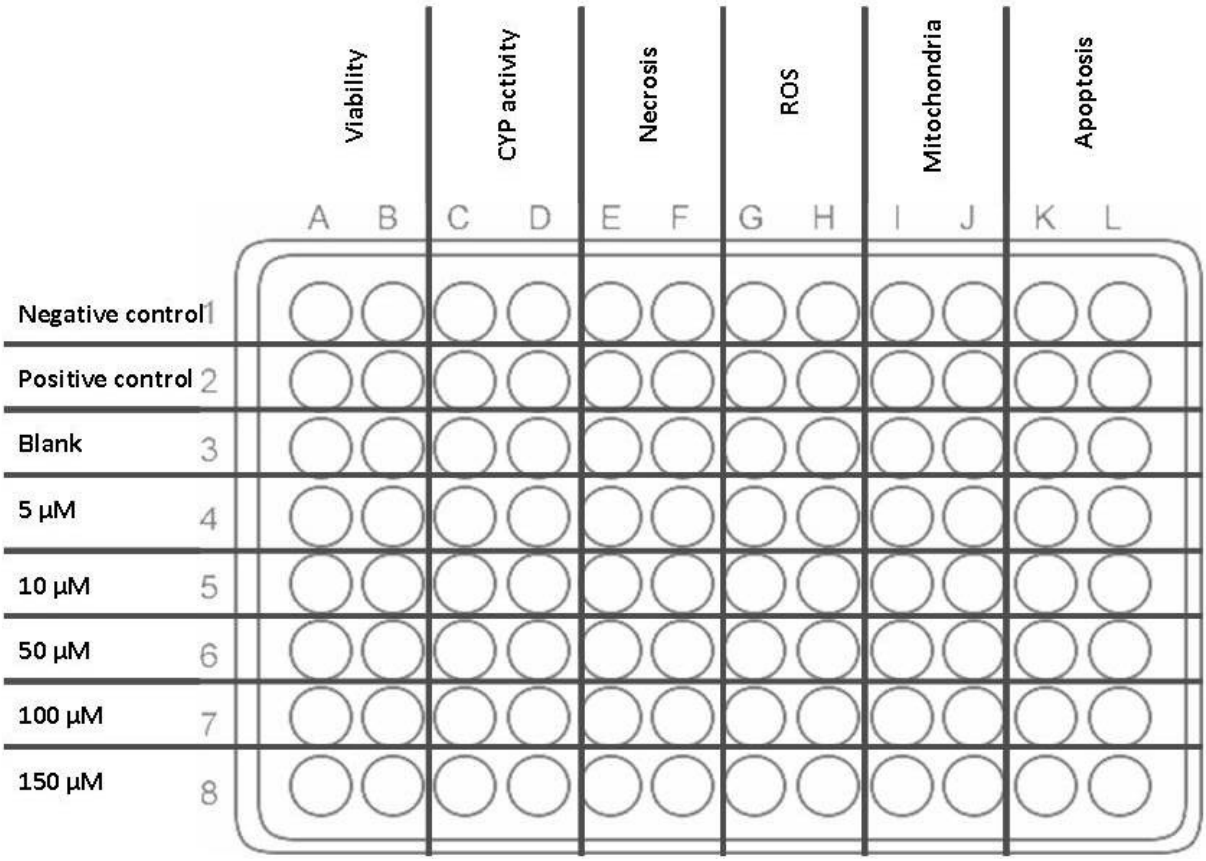

Figure 2.2. Diagram illustrating the plate setup. Plates were divided into six duplicate column sets, one for each of the six different assays to be performed and into eight rows, for the blanks, controls and various concentrations of test compound. Only one compound was tested on a single plate.

Initially cells (2×10^4 cells/well) were seeded into all wells (except for blank wells) and incubated for 48 h, to allow for proper cell adhesion.

-24 h: Cells in wells subjected to viability, CYP activity, and necrosis assays were exposed to control or test compounds.

-6h: After further 18 h of incubation, which was 6 h prior to the endpoints of the viability, CYP activity and necrosis determination, wells for determination of apoptosis were exposed to control or test compounds.

-4 h: After further 2 h incubation, cells in wells for ROS determination were loaded with 2', 7'-dichlorofluoresceindiacetate for 1 h.

-3 h: Wells for ROS determination were washed to remove excess dye and the control or test compounds added.

-2 h: Following a further one hour incubation, the dyes for only the cell viability and CYP determinations were added to the wells and incubation continued.

-1.5 h: After further 30 min incubation, wells used to determine possible mitochondrial toxicity were loaded with the relevant fluorescent dye.

-**1 h:** Following further 30 min incubation, cells in wells loaded for mitochondrial toxicity determination were washed to remove the excess dye and the control or test compounds added.

-15 min: After further 45 min incubation, propidium iodide was added to the wells, in which necrosis was to be determined, and incubated for 10 min.

-5 min: Wells used for necrosis and viability determination were rapidly washed.

Time 0: At 24 h after the initial control or test compound exposure, the following parameters were determined fluorometrically: CYP activity, necrosis, ROS and mitochondrial toxicity effects.

+5 min→ +20 min: Cells in wells used for determination of apoptosis were lysed on ice for 15 min followed by the addition of apoptosis assay substrate and incubation overnight.

+ 18 h: Fluorescence for the apoptosis assay was determined and the dye used for the viability assay was then eluted and the absorbance measured.

All wash steps were performed as follows:

- Aspirate well contents and discard
- Slowly add 200 µl of sterile PBS so as not to disturb the cell monolayer
- Aspirate well contents and discard

The entire procedure i.e. from seeding of the cells to obtaining the results took approximately 90 h (≈4 days).

When evaluating the possible hepatoprotective effects of NAC against test compound toxicity, the same procedure as described above was followed, except that the cells were pre-treated with NAC (100 µg/ml or approximately 620 nM) for 1 h (Souza *et al.*, 2004), prior to addition of the test compound for each assay.

Chapter 3: *In Vitro* Cytotoxicity

3.1. Background

Cytotoxicity testing is one of the major assays applied during *in vitro* toxin assessment, which focuses mainly on cell death or some measure of growth impairment. This type of testing is designed to evaluate the intrinsic ability of a compound to kill cells (Ferro & Doyle, 2001). Apart from dosage, two other factors play a major role in the toxicology of an entity: the duration of exposure to a compound and the compound's mechanism of toxicity (Riss & Moravec, 2004). At a cellular level, *in vitro* toxicity can manifest in a number of ways including (Horvath, 1980):

1. diminished cellular adhesion
2. dramatic morphological changes
3. a decrease in replication rate or
4. a reduction in overall viability

Many different assays have been developed to determine *in vitro* toxicity such as quantifying cell death/survival by assessing plasma membrane integrity, cell enumeration by total protein content and enumerating viable cells through assessing certain vital functions. Popular assays that are widely used are the total cellular protein assay (sulforhodamine B), the neutral-red uptake assay, the LDH leakage assay, and the tetrazolium dye assays (Murakami, 2000).

The best known of the tetrazolium assays is probably the MTT assay for mammalian cells in which 3-(4,5-Dimethylthiazol-2-yl)-2,5-diphenyltetrazolium bromide, a yellow tetrazolium salt is reduced by the mitochondria of viable cells to insoluble, purple formazan crystals. Although this is one of the most prevalent viability assays, its weakness lies in yielding false positives in the presence of a number of compounds including albumin and antioxidants such as ascorbic acid, cysteine and glutathione (Funk *et al.*, 2007).

The neutral red uptake (NRU) assay is also widely used to determine cell viability. Neutral red, a supravital (non-toxic) dye, relies on the principle of dye accumulation in the lysosomes and Golgi apparatus of viable, uninjured cells and has the following advantages:

1. it does not rely on a reduction reaction to determine viability, excluding susceptibility to making type I errors (false positives) in the presence of antioxidants or other reductive agents
2. it is cost-effective
3. it is quick
4. is reported to be more sensitive to changes in cell viability of hepatocyte cultures as compared to total protein content determination and the LDH leakage assay (Fotakis and Timbrell, 2006)

In this chapter the effects of DDT, DDE and DDD on hepatocyte viability are presented. Initial cytotoxicity testing was performed in order to establish a concentration range that would be used throughout the study. The concentration range that was selected covered a wide toxicity range, from merely affecting cell function to complete loss of cellular function and viability. This was done in order to assess the incremental effects of the test compounds on different parameters at different levels of toxicity, which may shed light on the optimal concentration range that can be utilised with the procedure developed in the present study.

3.2. Methods

3.2.1. Experimental design

After a 48 h incubation period (to allow cells to adhere to the wells), cells were exposed to DDT, DDE and DDD at concentrations of 5, 10, 50, 100 and 150 µM. Tamoxifen (150µM), which is known to induce cell death through apoptosis in HepG2 cells (Guo *et al.*, 2010), was used as positive control. DMSO (0.5%) was included as vehicle control. After exposure, cells were incubated for 24 h at 37°C until performing the viability assay. To assess the possible

hepatoprotective effects of NAC, three additional experiments were conducted, which included an additional 1 h pre-treatment with 620 nM NAC, prior to test compound exposure.

3.2.2. Viability assay

Exposure medium was aspirated and replaced with 100 µl EMEM containing 100 µg/ml Neutral red dye. Cells were incubated with the dye for 2 h at 37°C, after which medium was discarded and cells were washed with PBS (200 µl). Plates were dried overnight at 40°C and the accumulated dye dissolved by adding 100 µl of Neutral red elution buffer to each well and incubated at room temperature on an orbital shaker for 40 min (Fotakis and Timbrell, 2006). The amount of dye accumulated by the cells in each well was quantified by measuring the absorbance at 540 nm with a reference wavelength of 630 nm (Biotek XL plate reader).

3.2.3. Statistical analyses

Six experiments were carried out in duplicate (***n*** **=** 12) to assess viability response. All observed results were standardised to percentage of control values. Quality of the collected data was assessed by plotting the distributions for the tested concentration of each tested compound. Grubb's test was performed to remove outliers, after which a Shapiro-Francia test was used to assess normality based on a discrete number. Depending on the normality of the data, student's ***t***-tests (parametric) or Mann-Whitney *U*-tests (non-parametric) were performed across the respective concentration ranges to determine whether the different concentrations had any statistically significant influence on HepG2 viability. Three additional experiments were carried out in duplicate to assess the possible effects that NAC may have on the initially observed toxicity. These results were also standardised to percentage of control but no preliminary tests (Grubb's and Shapiro-Francia) were performed. Due to the

small sample size (***n*** **=** 6), no outliers were removed and normality of the data could not be established. Therefore, all NAC results were analysed using Mann-Whitney tests. The 50% Inhibitory concentrations (IC_{50}) were determined by fitting a Hill equation with variable slope to the observed data. Analyses were performed using GraphPad Prism 5.0 (www.graphpad.com) and the freeware package, R 2.12.1 (www.r-project.org). All reported results are given as mean ± standard error of the mean (SEM), unless stated otherwise.

3.3. Results

Normality testing revealed non-normal distributions, especially for the higher concentrations of the tested compounds. The different distributions for DDT, DDE and DDD are illustrated in Figures 3.1, 3.2 and 3.3, respectively. Non-normality of some distributions was confirmed with the Shapiro-Francia test (Table 3.1). The Shapiro-Francia test is based on hypothesis testing: the null hypothesis states that the collected data originates from a normal distribution, if the ***p***-value drops below the chosen alpha level, the null hypothesis is rejected and the data assumed to originate from a non-normal distribution. Concentrations between 50 µM and 150 µM for DDT and DDD and 100 µM for DDE were found to be significantly non-normal. The Control group in the DDT data set is an example of a perfectly normally distributed data set with ***p*** = 1.00 (Figure 3.1A).

DDT did not have any significant influence on viability up to concentrations of 10 µM but did produce slight cellular proliferation with enumeration results being 105.4 ± 3.5% and 103.4 ± 3.8% for concentrations of 5 µM and 10 µM, respectively (Figure 3.4). Higher concentrations resulted in significant (***p*** < 0.001) decreases in viability. Concentrations of 50, 100 and 150 µM DDT induced 54.3 ± 3.7%, 74.5 ± 4.8% and 74.4 ± 3.8% losses in viability, respectively (Figure 3.4). The Hill equation fitted the observed DDT results well with a coefficient of determination (r^2) of 0.86, meaning that 86% of the variance observed in the results can be accounted for by the fitted model (Figure 3.4). From the fitted equation it was deduced that DDT has an IC_{50} value of 54 ± 1 µM after 24 h exposure, if a cell density of 2×10^4 cells/well is used (Table 3.2).

NAC pre-treatment did not alleviate but rather aggravated DDT toxicity, decreasing the IC_{50} to 40 ± 1 µM, after 24 h exposure (Table 3.2 and Figure 3.4). Compared to DDT exposure alone, NAC pre-treatment significantly decreased the viability at low concentrations of 5 µM ($p < 0.05$) and 10 µM ($p < 0.01$) (Figure 3.4).

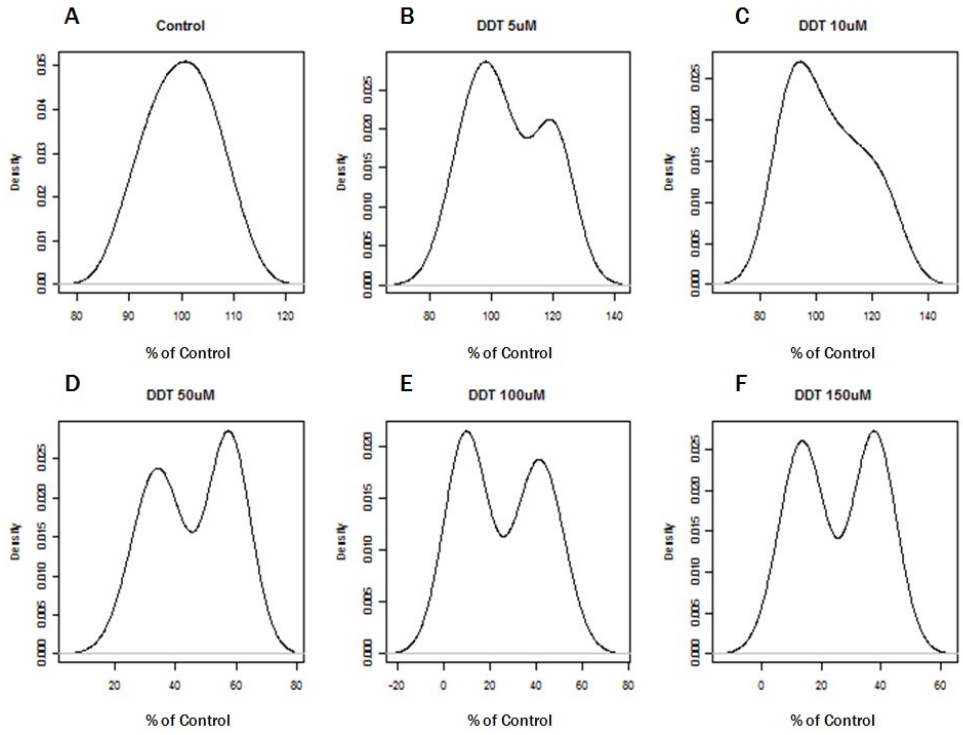

Figure 3.1. Histogram density plots of the observed viability data of HepG2 cells exposed to DDT demonstrating the distributions of the collected data. The control group is a good example of a normal distribution. The observations did not always follow a normal distribution, especially in the higher ranges of viability. X-axis represents observed values and Y-axis, the count.

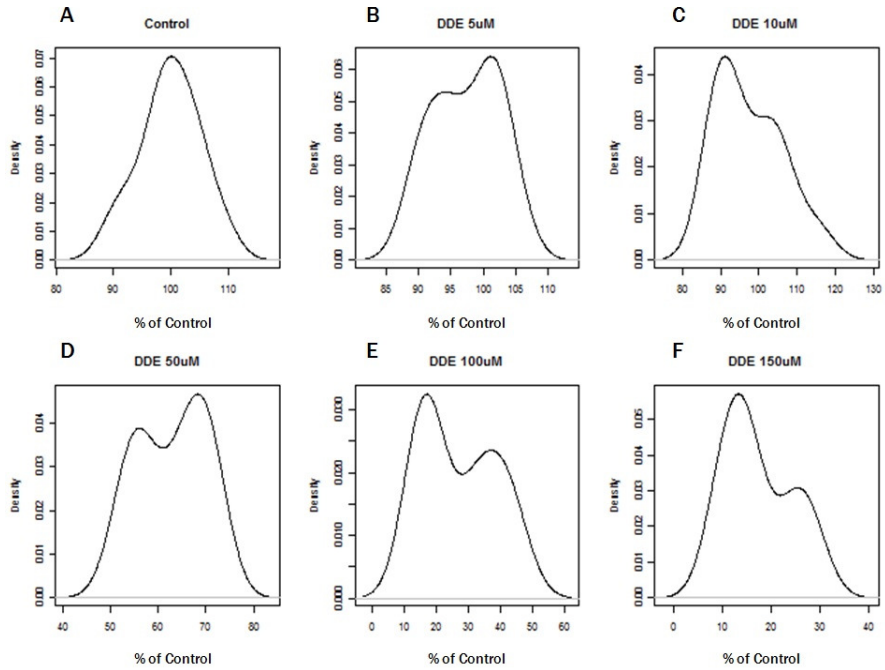

Figure 3.2. Histogram density plots of the observed viability data of HepG2 cells exposed to DDE demonstrating the distributions of the collected data. The results do not follow a normal distribution. X-axis represents observed values and Y-axis, the count.

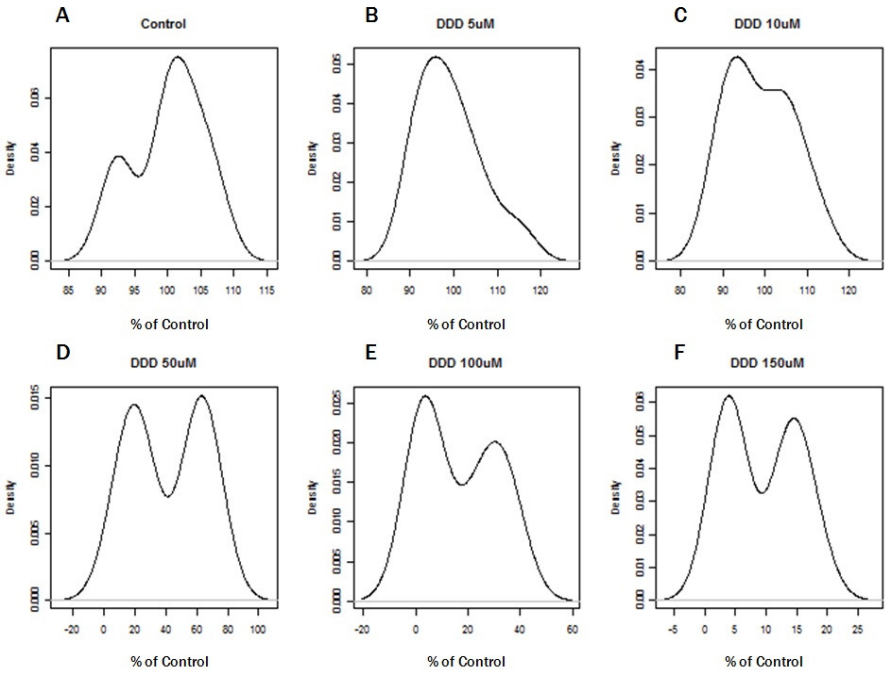

Figure 3.3. Histogram density plots of the observed viability data of HepG2 cells exposed to DDD demonstrating the distributions of the collected data. Data is non-normal as indicated with distinct multiple peaks instead of a single peak. X-axis represents observed values and Y-axis, the count.

Similar to the parent molecule, DDE produced a dose-dependent decrease in viability. Concentrations up to 10 µM did not produce any significant fluctuations in viability. However, unlike DDT, it caused a slight decrease in viability at the 5 µM and 10 µM concentrations, yielding 97.4 ± 1.5% and 97.5 ± 2.5% viability, respectively (Figure 3.4). Concentrations between 50 µM and 150µM produced significant deviation from the control mean ($p < 0.001$). A 50 µM concentration of DDE caused a 37.1 ± 2.0% decrease in viability, while 100 and 150 µM lowered cell viability by 73.1 ± 3.3% and 82.6 ± 2.0% respectively (Figure 3.4). At a cell density of 2×10^4 cells/well, DDE demonstrated an IC_{50} of 64 ± 1 µM ($r^2 = 0.95$) after 24 h exposure (Table 3.2 and Figure 3.4).

Again, NAC pre-treatment did not alleviate the toxicity of the test compound, decreasing the IC_{50} to 58 ± 1 µM, after 24 h exposure (Table 3.2 and Figure 3.4). When compared to DDE exposure alone, NAC pre-treatment significantly ($p < 0.05$) decreased the viability at concentrations of 10 µM and 50 µM (Figure 3.4).

Table 3.1. Shapiro-Francia test results for normality of the observed data. Values given in the table are p-values and instances where p < 0.05 are not normally distributed (*).

Concentration	DDT	DDE	DDD
Control	1.00	0.91	0.54
5µM	0.22	0.39	0.23
10µM	0.33	0.12	0.64
50µM	0.02*	0.33	0.02*
100µM	0.02*	0.03*	0.01*
150µM	0.02*	0.24	0.01*

Table 3.2. **IC_{50} values (±SEM) of cells with/without NAC pre-treatment prior to test compound exposure.**

Test compound	No pre-treatment (µM)	NAC pre-treatment (µM)
DDT	54 ± 1	40 ± 1
DDE	64 ± 1	58 ± 1
DDD	44 ± 1	33 ± 1

Similar to DDT and DDE, DDD also produced a dose-dependent decrease in HepG2 viability. DDD did not significantly affect HepG2 viability up to concentrations of 10 µM, with 5 µM and 10 µM concentrations yielding viabilities of 99.1 ± 2.1% and 99.0 ± 2.3%, respectively. However, concentrations of ≥ 50 µM induced significant ($p < 0.001$) decreases in viability (Figure 3.4). The Hill equation fitted the observed data well ($r^2 = 0.91$). From this analysis, DDD showed an IC_{50} of 44 ± 1 µM after 24 h exposure (Figure 3.4).

NAC pre-treatment produced results similar to those observed with DDT and DDE by not alleviating the toxicity of the test compound at low test compound concentrations. The IC_{50} was decreased to 33 ± 1 µM, after 24 h exposure (Table 3.2 and Figure 3.4). Compared to DDD exposure alone, NAC pre-treatment significantly ($p < 0.001$) decreased the viability at a concentration of 50 µM (Figure 3.4).

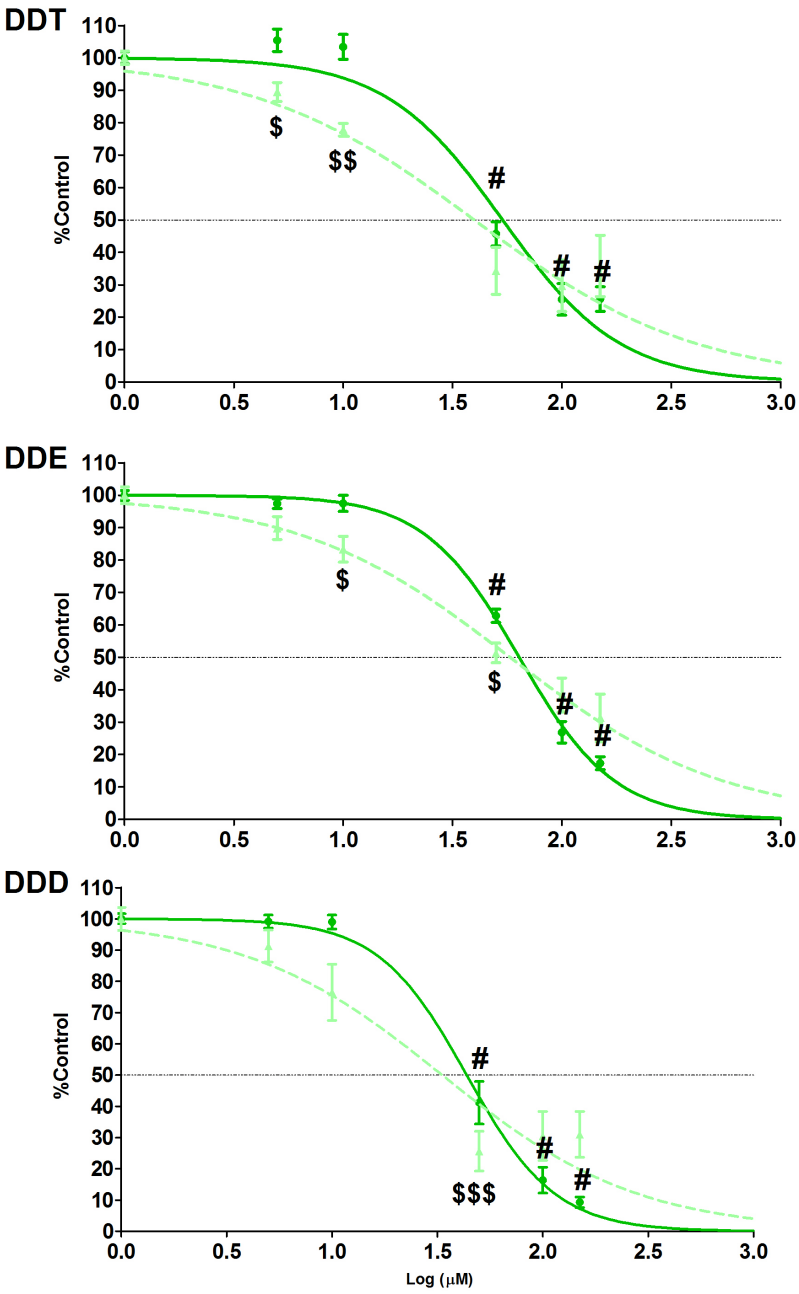

Figure 3.4. Fitted dose-response curves of viability of HepG2 cells after DDT, DDE and DDD treatment (mean ± SEM). Dark green curves represent the test compounds alone and light green curves, cells pre-treated with NAC. Curves were obtained by fitting viability results to a four-parameter Hill equation with variable slope and the following constraints: top = 100 and bottom = 0. Graphs are plotted on semi-logarithmic axes. Dashed horizontal lines represents Y = 50%. **#** = $p < 0.001$, treatment with test compound alone compared to controls. **$** = $p < 0.05$, **$$** = $p < 0.01$, **$$$** = $p < 0.001$, pre-treatment with NAC compared to treatment with test compound alone.

3.4. Discussion

Figures 3.1 - 3.3 present the data distribution plots of the observed data for the different concentrations of DDT, DDE and DDD, respectively. In an ideal situation these curves would resemble a bell-shaped curve. Rather than describing the endpoint, these curves are good for describing the observed data itself and provide guidance for subsequent statistical manipulation. Noticeable from the graphs of some of the data are more than one peak. This is indicative of more than one population being present in a particular set of data. For example, these curves are very closely related to histograms obtained from flow cytometry. If the X-axis of a histogram represents size and the Y-axis count or density, a mixture of oocytes and spermatozoa will present as two distinct populations in terms of size. In the same way, the curves presented here show the number of observations made at a particular value, which in this case would be a % of control value. However, unlike flow cytometry, increasing the number of repetitions would eventually produce a perfect bell-shaped curve.

More than one population indicates variability between experiments. In this way these curves can be interpreted as a measure of the robustness of an assay. However, care should be taken when interpreting these curves as multiple populations may also be the result of outliers. For this reason, outliers identified by the Grubb's test were removed prior to testing for normality (Shapiro-Francia test). Data collected for the three test compounds indicates a trend in that higher concentrations (50 - 150 µM) of all three test compounds demonstrated multiple peaks. This was confirmed with the Shapiro-Francia test (Table 3.1), where most of the 50 - 150 µM data sets proved to be significantly non-normal. The multiple populations that are observed here may have been the result of differences between the preparation of batches of NR dye, buffers or test compounds or differences between cell passages, incubation times, instrument conditions etc. These results should not be considered definitive as the SEMs are also indicative of reproducibility. Also, mean values obtained from the pooled individual assay results yielded good dose-response curves with r^2 values ≥ 0.86, which is acceptable considering it is a non-linear fit. This means that the maximum amount of variability that could not be attributed for was 14% in the case of

DDT, whereas it was 5% and 9% for DDE and DDD, respectively. Taken collectively, the above-mentioned indicates that the NRU assay yielded reproducible results but has its limitations.

With regards to the effects of the test compounds on cell viability, high concentrations of the test compounds were necessary to significantly decrease cell viability after 24 h of exposure. Significant cytotoxicity was only evident at concentrations above 10 µM with IC_{50} values of 40 - 60 µM. Medina-Diaz & Elizondo (2005), who studied the effects of DDT on HepG2 viability, also reported the onset of toxicity at concentrations higher than 10 µM. Results suggest that DDT (but not DDE or DDD) may induce cellular proliferation at sub-toxic concentrations. Although not significant, exposure to 5 µM DDT resulted in a 5% increase in cell number when compared to the control. A possible explanation for this can be found in the work of Kiyosawa *et al.* (2008), who demonstrated the up-regulation of the cell proliferation–related genes *Ccnb1*, *Ccnb2*, *Ccnd1*, *Stmn1*, and *Mdm2* in the livers of rats exposed to DDT. These authors concluded that up-regulation of these genes were facilitated by activation of the constitutive androgen receptor by DDT, which also resulted in the up-regulation of CYP3A4. As the exposure period was only 24 h, it is possible that a longer incubation time could increase proliferation significantly. Cellular proliferation induced by DDT has also been reported in MCF-7 cells (breast adenocarcinoma) (Diel *et al.* 2002). Surprisingly, this proliferative effect decreased at a concentration of 10 µM DDT, which, in the present study, was found to be the concentration that did not adversely affect cell viability. Diel *et al.* (2002) suggested that the decrease in proliferation might be due to the onset of toxicity at these concentrations. Rat mammary gland proliferation induced by DDT has also been reported *in vivo* (Upalla *et al.*, 2005).

In contradiction to the results from the present study, Delescluse *et al.* (1998) observed no toxicity in HepG2 cells exposed to DDT at concentrations as high as 100 µM of DDT. Dehn *et al.* (2005) reported an IC_{50} of 1 mM for DDT in HepG2 cells, which is approximately 20 times greater than the value determined in the present study (54 µM). This difference could possibly be attributed to the ten-fold difference in cell density used between the two

studies: 2×10^5 cells/well (Dehn *et al.*, 2005) *vs.* 2×10^4 cells/well, as well as the vehicle solvent concentration. In the present study the vehicle solvent, DMSO, did not exceed a final concentration of 0.5% (v/v) compared to a 2.5% (v/v) concentration in the study by Dehn *et al*. (2005). It has been reported that the addition of DMSO to culture medium improves the cell viability of isolated primary hepatocytes (Banic *et al.*, 2011), which may also contribute to the difference in IC_{50} values between the two studies.

The IC_{50} values reported for DDT in other hepatocyte cell cultures such as primary hepatocytes and HaCaT cells (rat liver) were 250 µM and 70 µM, respectively (Delescluse *et al.* 1998). These IC_{50} values and that reported in the present study suggest that different hepatocyte cultures may not necessarily respond in the same way to DDT (and other test compounds for that matter). Primary cell cultures are considered the 'gold standard' but as already mentioned, there are many drawbacks in terms of feasibility and predictability when utilising these hepatocytes.

At the highest concentration tested (150 µM) of all three test compounds some cells remained viable. This could demonstrate the resilience of hepatocytes but may also be a drawback of the assay that was employed; in that complete cell death was not achieved. Some of the NR dye did bind to the well surface, mimicking cell numbers. However, because the relevant blanks were included in the assay setup, this should have compensated for any non-specific staining. Nonetheless, the assay yielded good dose-response curves (Figure 3.4) and the results were reproducible (average coefficient of variation < 10), demonstrating the reliability of the NRU assay.

Noticeable from Figure 3.4 is the difference in slope of the dose-response curves of the test compounds alone compared to those of the cells that were pre-treated with NAC. When considering the IC_{50} values, NAC pre-treatment did not protect against toxicity induced by any of the three test compounds. Rather, it seemed to exacerbate it. On examination of the dose-response curves this exacerbating effect can be seen at concentrations of 5 - 50 µM of

all three test compounds. However, at higher concentrations (100 -150 µM), NAC pre-treatment appeared to have alleviated some of the toxicity induced by the three test compounds. Exactly how this may have happened is not obvious but these results suggest that different aspects of cellular physiology are involved. On the one hand, lower concentrations (5 - 10 µM) of the test compounds may appear non-toxic due to some cellular response that allows the cells to cope with the xenobiotics. This crucial response may be counteracted by NAC, which will then decrease the resistance of the cells to the exogenous stressor, causing the loss of cell viability observed at these concentrations.

On the other hand, above some threshold concentration the cells may not be able to counteract the effect of the test compounds, resulting in cell death. NAC may be able to counteract this mechanism of toxicity, which would alleviate some of the toxicity seen above this threshold concentration, as observed for concentrations of 100 - 150 µM of all three test compounds. No literature was found to compare/support any of the NAC pre-treatment results observed in the present study.

Chapter 4: Phase I metabolism

4.1. Background

Humans are constantly exposed to many different chemicals. A large percentage of these are hydrophobic in nature and would accumulate in the body if not converted to water-soluble derivatives that can be excreted via the kidneys (Delescluse *et al.*, 2000). The CYPs are a superfamily of hemethiolate enzymes, of which over 2000 individual members are currently known. It has been established that many of these CYPs play major roles in the metabolism of drugs and other xenobiotics. In humans and in other mammalian species, CYPs of the families 1, 2 and 3 are primarily associated with Phase I metabolism of exogenous compounds (Lewis, 2003). Phase I metabolism is responsible for the functionalisation of xenobiotic compounds (Iyer and Sinz, 1999). This is accomplished either by the introduction of polar and reactive groups through processes such as hydroxylation, oxygenation and epoxydation, or through the modification of existing groups on the specific compound through processes such as dealkylation and dechlorination (Guengerich, 2001; Westerink and Schoonen, 2007). Phase I metabolism is aimed at preparing the compound for and facilitating Phase II metabolism by making the molecule more chemically reactive. Whilst Phase I reactions generally result in a more polar metabolite, it is the conjugation reactions (e.g. glucuronidation and sulphonation) that result in marked increases in water solubility, which facilitate renal excretion (Westerink and Schoonen, 2007).

Some of the CYP enzymes are substrate inducible, which allows the cell to adapt to changes in its chemical environment (Denison and Whitlock, 1995; Delescluse *et al.*, 2000). The CYP1A subfamily of enzymes consists of only two members, CYP1A1 and CYP1A2, both of which are involved in oxidative metabolism of exogenous chemicals such as polycyclic aromatic hydrocarbons (PAHs), aromatic amines and heterocyclic amines, to name a few (Fujii-Kuriyama *et al.*, 1992). CYP1A2 accounts for approximately 13% of the total cytochrome P450 content in the liver (Shimada *et al.*, 1994) whereas CYP1A1 is expressed at low levels in the liver (Nakamura *et al.*, 2005) but is highly inducible (Morel *et al.*, 1999; Vrzal *et al.*, 2009). Although CYP1A1 and CYP1A2 have many inducers in common, the

difference between them lies in their tissue expression. When host animals are treated with the relevant inducers, CYP1A1 is not only expressed in liver tissue, but also in many extra-hepatic tissues such as lung, skin and kidney, whereas the expression of CYP1A2 is essentially limited to liver tissue (Fujii-Kuriyama *et al.*, 1992).

The ubiquitous form of CYP1A, one of the most studied CYP enzymes due to its involvement in generating reactive metabolites as a result of xenobiotic metabolism, has been implicated in both cytotoxicity and cancer induction. CYP1A1 can be induced by various environmental factors, such as smoking, dioxin exposure as well as the ingestion of charred meat (Nakamura *et al.*, 2005). A good example demonstrating CYP1A's role in toxicity would be the oxygenation of polycyclic aromatic hydrocarbons, originating from combustion, including cigarette smoke, to generate arene oxides. These are chemically reactive electrophiles capable of covalently binding different cellular components, such as DNA, which gives rise to their tumorigenic effect (Whitlock, 1999). The cancer-promoting role of CYP1A1 is probably best illustrated in the review of bezo(a)pyrene carcinogenicity (Androutsopoulis *et al.*,2009). Apart from its apparent role in cancer, an increase in CYP1A1 activity (similar to CYP2E1 (Chen and Cederbaum, 1998) and CYP3A4 (Perret and Pompon, 1998)), has been shown to release H_2O_2 during its catalytic cycles (Morel *et al.*, 1999), which may lead to oxidative stress and result in cell death. Due to its possible implication in both short and long-term toxicity, assessing CYP1A1 activity would be beneficial to any study evaluating potential hepatotoxicity as the liver is the major detoxifying organ of the body, implicating a major role in Phase I metabolism and, as such, it would be prone to toxic insult from a CYP1A1 inducing agent, which may generate reactive radicals in more than one way.

The best cell type for studying the detoxification and activation processes of compounds are hepatocytes (Westerink and Schoonen, 2007). There are many different techniques for performing the CYP1A1-specific ethoxyresorufin-*O*-deethylase (EROD) assay described in literature (Kennedy and Jones, 1994; Alexandre *et al.*, 1999; Jonsson *et al.*, 2006; Shiizaki *et al.*, 2008; Rudzok *et al.*, 2009). EROD activity is indicative of the rate of the CYP1A-mediated *O*-deethylation of the substrate 7-ethoxyresorufin (7-ER) to form the fluorescent product resorufin. The catalytic activity is an indication of the amount of enzyme present (Kennedy and Jones, 1994). Described methods include techniques for use with microsomal fractions,

fish gills (Jonsson *et al.*, 2006) and HepG2 cells (Alexandre *et al.*, 1999; Shiizaki *et al.*, 2008; Rudzok *et al.*, 2009). However, consistency among the techniques used by various researchers (specifically on the HepG2 cell line) is lacking.

4.2. Methods

4.2.1. Experimental design

Exposure conditions were similar to those previously described in Chapter 3; with the exception that omeprazole (150 µM) was used as positive control due to reports of CYP1A1 induction. Omeprazole produces its inductive effect by activating the aryl hydrocarbon receptor (AhR) pathway (Shiizaki et al., 2008).

Techniques for performing the EROD assay differ mainly in the amount of substrate used and the cofactors used in the final assay solution. For the purposes of this study, three different techniques (Alexandre *et al.*, 1999; Dubois *et al.*, 2006; Jonsson *et al.*, 2006) were tested but failed to detect increased CYP1A1 activity after treatment with the known modulator, omeprazole (Linden *et al.*, 2010; Fujii-Kuriyama *et al.*, 2010). An excessive 7-ER concentration (10 µM) was assumed to be the cause due to the fact that the background fluorescence intensities from blank wells were too high compared to the fluorescence intensities from wells seeded with cells. Consequently, Step 1 of the optimisation aimed at determining the role that 7-ER concentrations play in the EROD assay. HepG2 cells were seeded at a density of 2×10^4 cells/well and allowed to acclimatise for 24 h. White microplates were setup to include blank wells (no cells) along with the ones in which cells were seeded as before. Medium was then aspirated and replaced with 100 µl of fresh EMEM (no FCS) containing various concentrations (0.5 nM - 1000 nM) of 7-ER and incubated for 2 h at 37°C. Resorufin fluorescence was detected using a FluoStar Optima at λ_{ex} = 520 nm and λ_{em} = 595 nm.

Step 2 of optimisation focused on cofactors included in the final assay solution, specifically the use of NADPH in the EROD assay as an electron donor (Nakamura *et al.*, 2005; Rudzok *et*

al., 2009; Lemaire *et al.*, 2011). The use of NADPH in EROD assays performed on microsomal fractions may be a prerequisite because the necessary biochemical co-factors, co-enzymes etc. may not be present because only a sub-fraction of the cell is used. On the other hand, when performing the EROD assay on whole cell cultures, the use of NADPH as a cofactor may not be required as a complete, whole cell is already present with all of its biochemical functions intact. To test this hypothesis, experiments were setup to include both blanks (no cells) and untreated cells, as in Step 1 of optimisation. After the acclimatisation period, cells were then treated with 150 µM Omeprazole in EMEM for 24 h. Medium was then aspirated and replaced with 100 µl EMEM containing 150 nM 7-ER, either with or without 100 nM NADPH (Rudzok *et al.*, 2009). Thereafter, cells were incubated at 37°C for 2 h and fluorescence was monitored using a FluoStar Optima at λ_{ex} = 520 nm and λ_{em} = 595 nm.

4.2.2. Statistical analyses

For optimisation experiments, results were analysed for normality using the Shapiro-Francia test, after which hypothesis testing was applied in the form of Mann-Whitney tests to assess differences between means of the distributions. For CYP1A1 induction by the compounds in question, outliers were detected using Grubb's test. Following removal of the relevant outliers, normality of the data distributions were evaluated with the Shapiro-Francia test. Hypothesis testing was then performed utilising both Mann-Whitney and ***t***-tests, where applicable, to determine whether any observable differences between means were statistically significant.

Three additional experiments were carried out in duplicate to assess the possible effects that NAC may have on pesticide-induced changes in CYP1A1 activity. These results were also standardised to percentage of control but no preliminary tests (Grubb's and Shapiro-Francia) were performed due to the small sample size (***n*** **=** 6). Normality of distribution of the NAC pre-treatment data could not be established, therefore, Mann-Whitney tests were performed.

4.3. Results

4.3.1. Optimisation

Step 1 of optimisation showed that as the amount of 7-ER, the CYP1A1 substrate, increased from 0.5 - 1000 nM, the amount of resorufin cleaved by the cells also increased in a concentration-dependent manner. From approximately 4 nM up to 1000 nM the fluorescence appeared to increase in a linear fashion as depicted in Figure 4.1. From this figure it is apparent that substrate concentrations of 1 nM and lower were insensitive to changes in enzyme concentration and would yield similar results, which indicated that 7-ER concentrations of ≤ 1 nM are below the limit of quantitation for CYP1A1 activity. The relative fluorescence intensity (mean ± SEM values) of the different concentrations of 7-ER are presented in Table 4.1.

As illustrated in Figure 4.1, background fluorescence increased at 7-ER concentrations of greater than 250 nM. For this reason, further optimisation of the assay was performed at a substrate concentration of 150 nM 7-ER as this would most likely provide the greatest sensitivity and assay range while avoiding increased background fluorescence due to high substrate concentrations.

Table 4.1. Relative fluorescence intensity of resorufin as a result of 7-ER cleavage by untreated HepG2 cells. [7-ER] = concentration (nM) of substrate employed. Compared to 1 nM, all higher concentrations yielded significantly different results with $p < 0.05$.

[7-ER]	0.5	1.0	2.0	3.9	7.8	15.6	31.3	62.5	125.0	250.0	500.0	1000.0
Mean	766	764	829	905	1078	1260	1471	1613	1824	1831	2023	2251
SEM	12	6	8	9	21	43	48	69	62	89	44	63

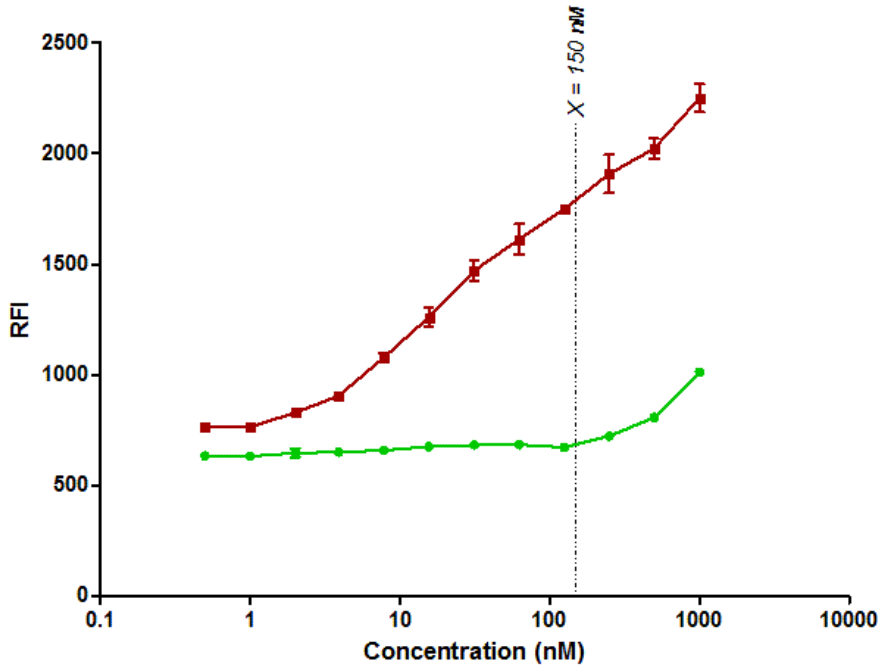

Figure 4.1. **Semi-logarithmic scatterplot of EROD assay optimisation for fluorescence substrate concentration. Following 24 h incubation, after seeding, wells were exposed to different concentrations of 7-ER, ranging from 0.5 - 1000 nM, for 1 h and monitored fluorometrically at λ_{ex} = 520 nm, λ_{em} = 595nm. The green line represents blank wells and the red line wells with untreated cells. The dashed vertical line indicates X = 150 nM and the Y-axis represents relative fluorescence intensity (RFI). Values differed significantly from blanks at all points along the graph with $p < 0.01$.**

Step 2 of the optimisation focused on the use of the cofactor NADPH. Results revealed that the presence of NADPH significantly ($p < 0.001$) decreased fluorescence (Figure 4.2). NADPH also significantly ($p < 0.01$) decreased the relative fluorescence intensity in assay blanks, although the difference was not as large as in the case of treated cells (Table 4.2). The difference in fluorescence intensities (y-axes) between Figures 4.1 and 4.2 are due to treatment with 150 µM omeprazole, which was only applicable in Step 2 of the optimisation.

Table 4.2. Effect of the cofactor NADPH on EROD assay results. In Step 2 of optimisation substrate (150 nM), with or without the addition of 100 nM NADPH was utilised to perform an EROD assay. Results are presented as mean ± SEM of the relative fluorescence intensity. Statistical analyses of these results are shown in Figure 4.2.

	Blank +NADPH	Blank	Cells + NADPH	Cells
Mean	824	863	4469	7631
SEM	± 9	± 8	± 286	± 374

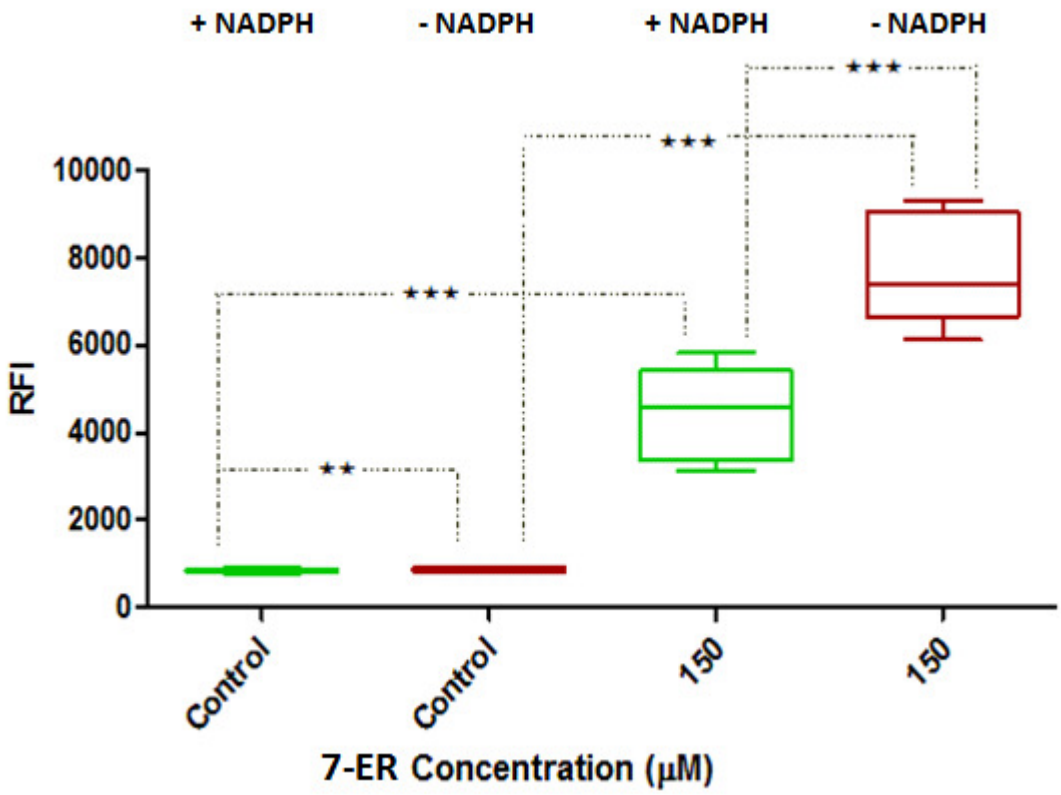

Figure 4.2. Boxplot of EROD assay with the addition or absence of the cofactor NADPH. To induced CYP1A1 activity, cells were exposed to 100 µM omeprazole (except controls) for 24 h before performing the EROD assay. Groups represented on the X-axis were exposed to 0 and 150 nM 7-ER for 1 h and fluorometrically monitored at λ_{ex} = 520 nm, λ_{em} = 595 nm. Red boxplots represent wells that received 7-ER only, while green boxplots represent those that received 7-ER and 100 nM NADPH. Y-axis represents relative fluorescence intensity (RFI), ** indicates $p < 0.01$, *** indicates $p < 0.001$.

4.3.2. CYP1A1 induction

The frequency distributions of data obtained for the CYP1A1 activity in DDT exposed cells shows that the 5 µM data set provides evidence for the presence of outliers, seen as a small peak to the far right of the bulk of the data (Figure 4.3B). Data was subjected to Grubb's test in order to detect outliers (Table 4.3). Testing revealed that three data sets in the DDT group (5, 10 and 100 µM), one in the DDE group (5 µM) and one in the DDD group (Control) contained outliers.

Table 4.3. Grubb's test results for detecting outliers in the observed CYP1A1 data. Values given in the Table are *p*-values. Instances where $p < 0.05$ (*) indicates the presence of outliers.

Concentration	DDT	DDE	DDD
Control	0.53	0.62	0.04*
5 µM	0.00*	0.01*	0.14
10 µM	0.01*	0.31	0.34
50 µM	0.43	0.26	0.43
100 µM	0.02*	0.88	0.35
150 µM	0.06	0.64	0.40

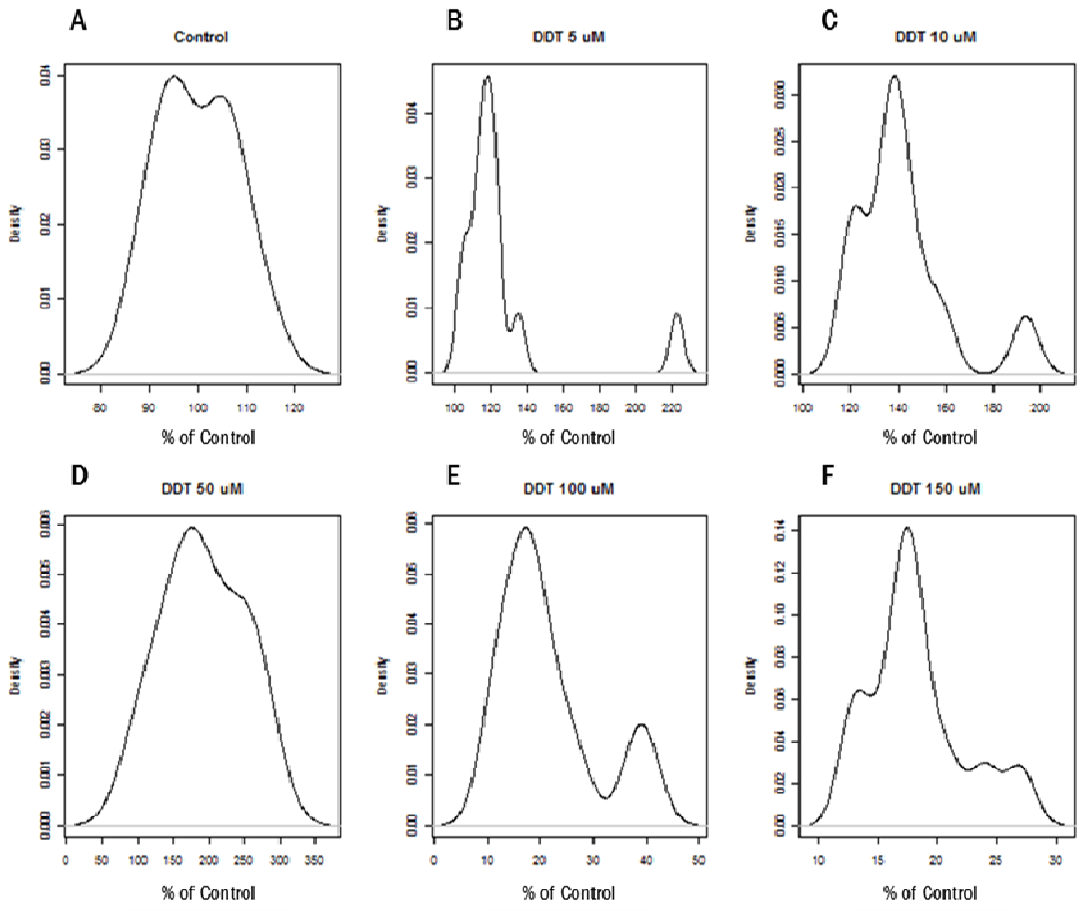

Figure 4.3. Histogram density plots of the observed CYP1A1 data of HepG2 cells exposed to DDT demonstrating the distributions of the collected data, prior to the removal of outliers detected by Grubb's test. The X-axis represents observed values and the Y-axis the count or density.

Relevant outliers were removed and the distributions re-plotted (Figure 4.4). When comparing the distributions in Figures 4.3 and 4.4, a marked difference can be observed as distributions in Figure 4.4 more closely resemble a typical normal distribution. However, visual assessment of graphs alone is not sufficient to claim normality and the data was subjected to a second evaluation of normality, the Shapiro-Francia test. Results from this test are presented in Table 4.4. Normality testing revealed that, after removal of outliers, the DDT group of data sets demonstrated normal distributions, whereas some of the data sets in the DDE (100 µM) and DDD (50 µM) groups still manifested as significantly non-normal. As a result, these two groups of data were tested using non-parametric Mann-Whitney tests, while the DDT group could be tested using unpaired, two-tailed ***t***-tests.

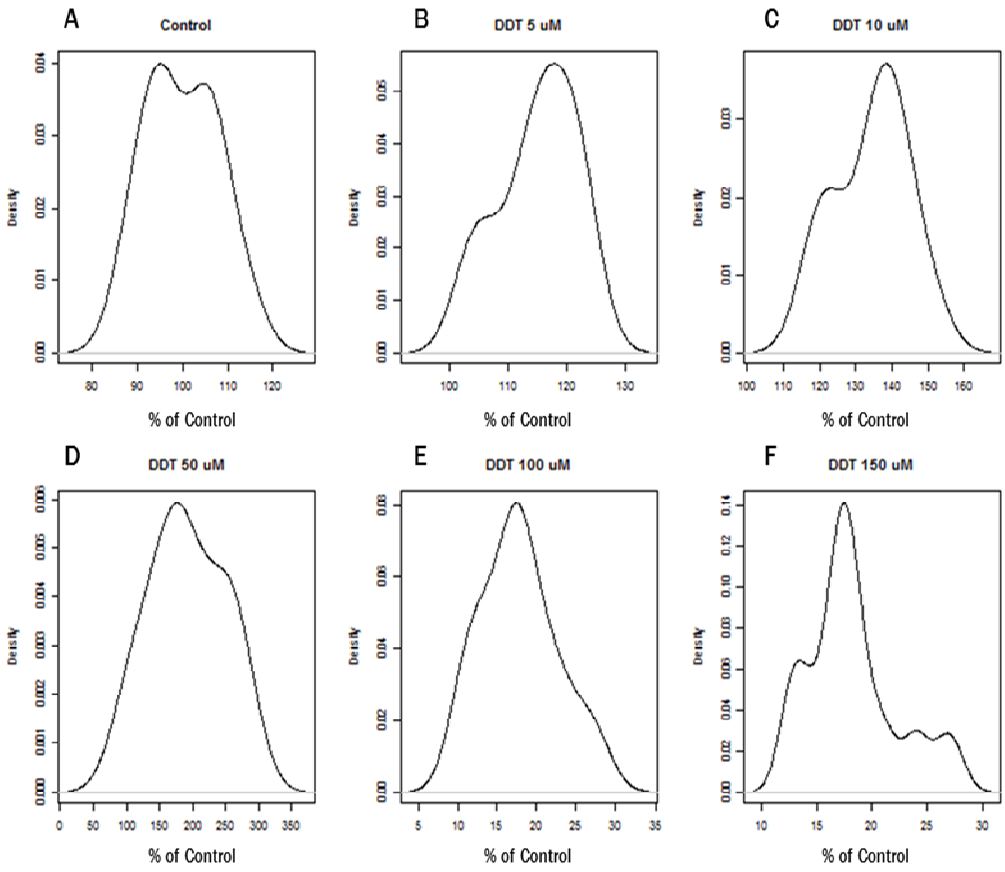

Figure 4.4. Histogram density plots of the observed CYP1A1 data of HepG2 cells exposed to DDT after the removal of outliers detected by Grubb's test. The X-axis represents observed values and the Y-axis the count or density.

Table 4.4. Shapiro-Francia test results for normality of the observed CYP1A1 data after removal of outliers as detected using Grubb's test. Values given in the Table are p-values. Instances where $p < 0.05$ (*) are significantly non-normal.

Concentration	DDT	DDE	DDD
Control	0.67	0.85	0.20
5 µM	0.50	0.75	0.68
10 µM	0.58	0.76	0.70
50 µM	0.87	0.33	0.03*
100 µM	0.80	0.01*	0.76
150 µM	0.25	0.05*	0.72

Relative percentage changes in CYP1A1 activity, as determined using the optimised EROD assay conditions is presented in Table 4.5 and Figure 4.5. Omeprazole, a well-known up-regulator of CYP1A1 activity (Ma and Lu, 2007; Linden *et al.*, 2010; Fujii-Kuriyama *et al.*, 2010), produced a seven-fold increase ($p < 0.001$) in CYP1A1 activity compared to untreated controls. All of the tested compounds significantly ($p < 0.001$) induced CYP1A1 activity up to concentrations of 10 µM. A 50 µM concentration of DDT and DDE caused a further increase in activity ($p < 0.001$), whereas 50 µM DDD did not produce any significant shift in the mean CYP1A1 activity when compared to controls. The highest CYP1A1 activity, other than that from the positive control, was induced by 50 µM DDE (258 ± 21%), representing a two-and-a-half fold increase. High concentrations (100 and 150 µM) of all three test compounds significantly ($p < 0.001$) inhibited CYP1A1 activity.

Table 4.5. Percentage CYP1A1 induction in HepG2 cells following 24 h exposure to DDT, DDE, DDD and the established CYP1A1 inducer, omeprazole (mean ± SEM). * indicates $p < 0.001$ as determined by Mann-Whitney tests.**

Concentration	DDT	DDE	DDD	Omeprazole (150 µM)
Control	100 ± 2	100 ± 1	100 ± 2	
5 µM	126 ± 9***	140 ± 7***	127 ± 5***	
10 µM	141 ± 6***	174 ± 12***	151 ± 6***	692 ± 78***
50 µM	192 ± 16***	258 ± 21***	92 ± 20	
100 µM	21 ± 3***	15 ± 3***	7 ± 1***	
150 µM	18 ± 1***	11 ± 2***	7 ± 1***	

NAC pre-treatment significantly decreased changes in CYP1A1 activity at concentrations of 50 µM for all three test compounds ($p < 0.01$) (Table 4.6 and Figure 4.6). At higher concentrations of the test compounds (100 - 150 µM), NAC pre-treatment showed no significant changes on test compound-induced CYP1A1 activity. In summary, CYP1A1 activity was raised at lower concentrations (5 - 10 µM) of DDT and DDD, however only being

significant in the 5 µM DDT group ($p < 0.05$). Conversely, CYP1A1 activity was decreased at similar concentrations when treated with DDE.

Table 4.6. **Percentage CYP1A1 induction in HepG2 cells by DDT, DDE, DDD relative to untreated controls, with or without 1 h pre-treatment with NAC (mean ± SEM). *, ** and *** represents $p < 0.05$, < 0.01 and < 0.001, respectively (Mann-Whitney tests).**

	DDT		DDE		DDD	
	--	NAC	--	NAC	--	NAC
5 µM	126 ± 9	137 ± 6*	140 ± 7	133 ± 2	127 ± 5	156 ± 14
10 µM	141 ± 6	169 ± 12	174 ± 12	155 ± 7	151 ± 6	201 ± 24
50 µM	192 ± 16	30 ± 9***	258 ± 21	95 ± 12***	92 ± 20	9 ± 3**
100 µM	21 ± 3	22 ± 9	15 ± 23	29 ± 5	7 ± 1	10 ± 3
150 µM	18 ± 1	15 ± 5	11 ± 2	18 ± 4	7 ± 1	10 ± 3

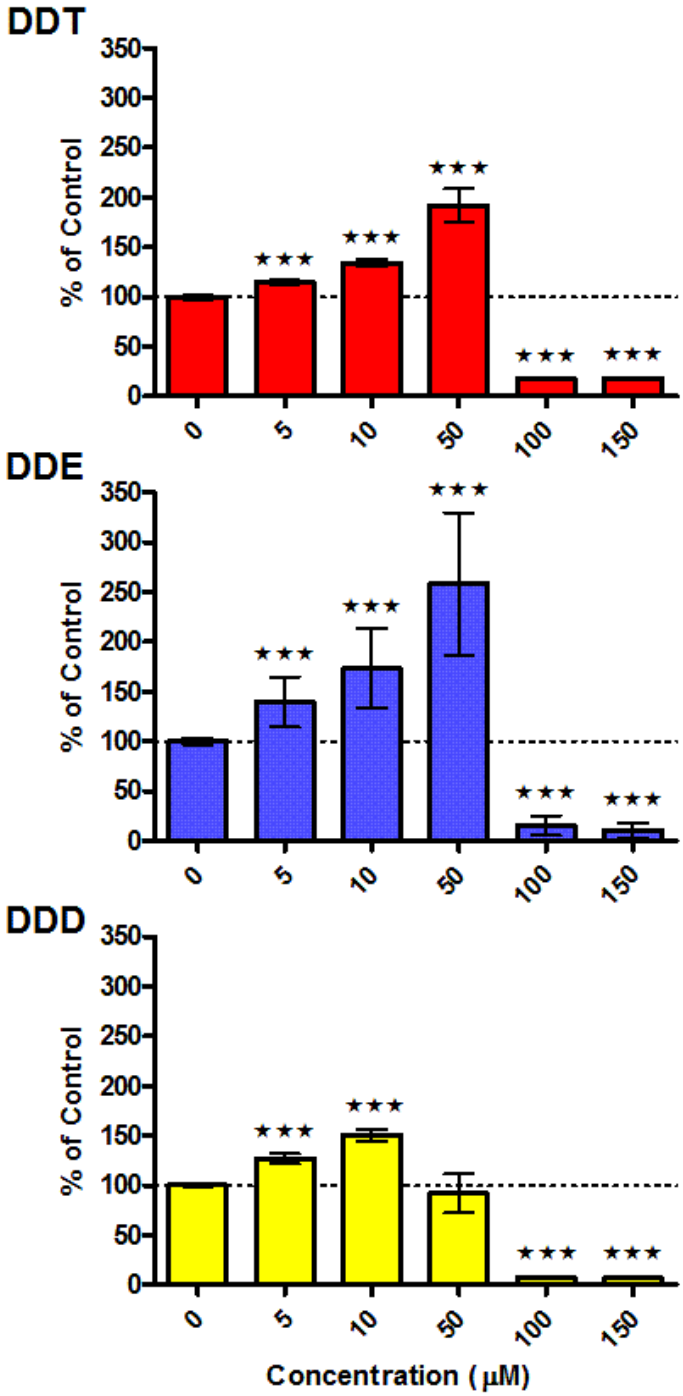

Figure 4.5. Graphical representation of CYP1A1 induction in HepG2 cells exposed to DDT, DDE and DDD mean ± SEM. *** indicates $p < 0.001$ and the dashed horizontal line Y = 100%.

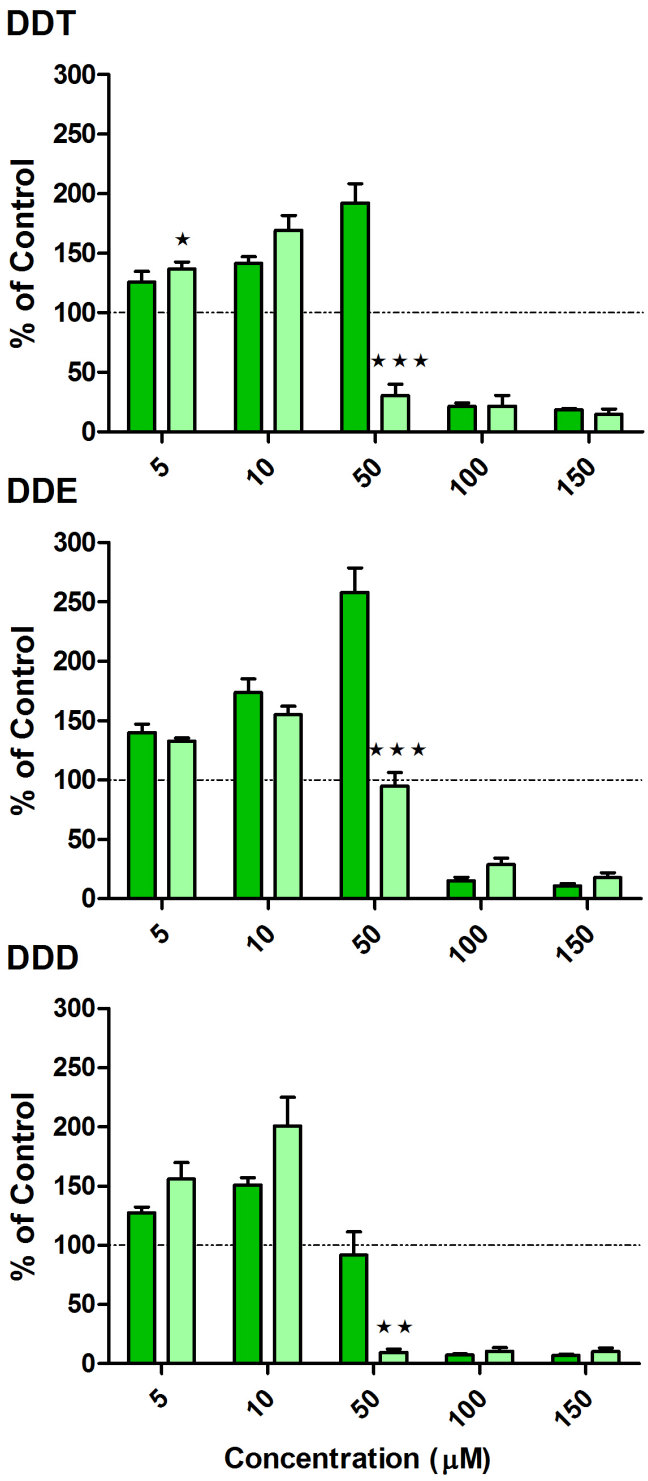

Figure 4.6. CYP1A1 induction in HepG2 cells exposed to DDT, DDE and DDD after 1 h pre-treatment with NAC. * indicates $p < 0.05$, ** indicates $p < 0.01$, *** indicates $p < 0.001$, compared to corresponding dose with no pre-treatment. Dashed horizontal lines show Y = 100%.

4.4. Discussion

4.4.1. Optimisation

Although CYP mRNA levels are much lower in HepG2 cells when compared to primary human hepatocytes, this cell line has been shown to still retain enough CYP function for use in CYP induction studies, specifically CYP1A1, 1A2, 2B6, 2D6, 2E1 and 3A4 (Westerwink and Schoonen, 2007). Initially, tests in the present study for determination of CYP1A1 activity used substrate concentrations of 1 - 10 µM (Alexandre *et al.*, 1999; Dubois *et al.*, 2006; Jonsson *et al.*, 2006), which was not able to detect omeprazole-induced elevations in CYP1A1 activity. The reason for this was excessive CYP1A1 substrate concentrations, which produced considerable background fluorescence, thus limiting the sensitivity of detection of cleaved resorufin and the ability to detect elevated CYP1A1 activity. Optimisation showed that 7-ER concentrations of 2 - 250 nM yielded a steady rise in fluorescence produced by the cells, while the background fluorescence remained essentially constant (Table 4.1 and Figure 4.1). Whether this rise in background fluorescence from 250 - 1000 nM of 7-ER is the result of non-specific release of resorufin or due to direct fluorescence of the substrate itself is not clear and is beyond the scope of this study. Subsequent experiments in the present study have therefore utilised a substrate concentration of 150 nM as this maximised the linear sensitivity and range of the assay while still excluding excessive background fluorescence.

Step 2 of optimisation focused on the use of NADPH as a co-factor in the EROD assay. Results confirmed that performing the EROD assay on whole cell cultures does not require NADPH as a co-factor. The presence of NADPH decreased the sensitivity of the assay by almost 50%. A possible explanation for this may be that the presence of NADPH in the solution quenches the fluorescence. The decrease seen in untreated cells may also be due to quenching but it cannot be excluded that some other biochemical change(s) elicited by excessive NADPH may have occurred. Consequently, NADPH was excluded from the EROD assays in this study when evaluating CYP1A1 induction in intact HepG2 cells by the test compounds.

4.4.2. CYP1A1 activity

Figures 4.3 and 4.4 present the density plots of the observed CYP activity data for DDT. These graphs are shown to demonstrate the presence and effect that outliers may have on a particular data set. Some of the data sets presented in Figure 4.3 clearly show more than one population, especially Figure 4.3B In this graph the majority of observations tend to be around 120% of the control with a second small population that presents with 220% as the mean. After removal of the relevant outliers using Grubb's test, this density plot changes to resemble a more bell-shaped curve, consisting of only one population as seen in Figure 4.4B, illustrating the importance of assessing the data prior to statistical manipulation in order to remove any bias that may be present and in this way decrease the probability of making type I or II errors (false positives and negatives, respectively). The density plots presented in Chapters 3 and 4 were added to demonstrate the importance of assessing data quality. Throughout the rest of the manuscript only the Grubb's and Shapiro-Francia test results will be presented as a measure of data quality.

The three test compounds appeared to induce CYP1A1 activity in HepG2 cells as all three test compounds were able to significantly increase CYP1A1 activity at the lower concentrations assayed (5 - 10 µM). DDT and DDE induced even greater activity at concentrations of 50 µM, yielding approximately 200% and 250% of the activity of the untreated cells, respectively. DDD, on the other hand, did not produce a significant effect at this concentration. At the higher concentrations assayed, a large and statistically significant decrease in CYP1A1 activity was seen for all three test compounds which could be ascribed to cell death due to the toxic effects before CYP 1A1 could be induced. Despite the fact that at test compound concentrations of 50 µM, approximately half of the cells were no longer viable, a significant increase in CYP1A1 activity was still observed.

The up-regulation of CYP1A1 due to DDT exposure has been described *in vitro* (Dehn *et al.*, 2005), *in vivo* (Nims *et al.*, 1998; Sierra-Santoyo *et al.*, 2000) and even in plants when using cultured cells of the common onion, *Allium cepa* (Riffat and Masood, 2006). In contrast to

findings from this study, Dehn *et al.* (2005), who also performed EROD assays on HepG2 cells following DDT exposure, detected no CYP1A1 activity in cells exposed to 10 and 50 µM of DDT, but found a significant increase of CYP1A1 activity from 100 µM up to 1 mM. This may once again be attributed to the considerable difference in cell density used in the two studies, 2×10^5 cells/well (Dehn *et al.*, 2005) *vs.* 2×10^4 cells/well. Additional sources of discrepancy could have resulted from NADPH presence and/or substrate concentrations for 7-ER. However, the authors did not elaborate on their methods, therefore the substrate concentration they used and whether or not they added NADPH as a cofactor, both of which have already been shown to significantly affect EROD assay results, could not be established. Observations from the present study showed that exposure to 100 µM of DDT resulted in a significant decrease in CYP1A1-associated EROD activity, most probably due to cell death. On the other hand, Dehn *et al.* (2005) reported significant increases in EROD activity from concentrations of 100 - 1000 µM of DDT. These findings could implicate that, in the present study concentrations of 100 and 150 µM of DDT may also have induced further CYP1A1 activity, had cell death due to toxicity not been observed. The findings of Dehn *et al*. (2005) that 1 mM of DDT increases CYP1A1 activity is disputable as DDT has a solubility limit of approximately 200 µM in aqueous media at a vehicle solvent concentration of 0.5% (v/v).

Delescluse *et al.* (1998) reported findings similar to the present study in that DDT at 10 µM could induce CYP1A1 activity in HepG2 cells but this increase was found to be statistically insignificant. Following three days incubation with 10 µM of DDT, treated cell cultures were lysed using a freeze-thaw cycle and EROD activity measured in a similar manner to that performed on microsomal fractions with a concentration of 2 µM 7-ER and the addition of 500 µM NADPH. The authors, however, did not report the seeding cell density. The prolonged exposure to DDT, difference in approach to the EROD assay and high substrate concentration may explain why a significant increase was not detected by Delescluse *et al.* (1998), as was the case in the current work. Despite some discrepancies, results from this study and those in literature suggest that DDT does induce CYP1A1 activity *in vitro*, but the concentration at which this occurs seems to be dependent on various experimental conditions when performing the EROD assay.

With regards to the *in vitro* effects of DDE and DDD on CYP1A1, no literature was found in order to compare with the findings from the present *in vitro* study. However, effects on CYP1A1 induced by these two metabolites, as well as DDT, have been described *in vivo*. Nims *et al.* (1998) conducted a study using male F344 rats exposed to dietary DDT, DDE and DDD. Although this was an *in vivo* study, there were some similarities to the observations made in the present study in that these authors also observed dose-dependent increases in hepatic CYP1A1 activity induced by all three test compounds. In addition to this, DDT and DDE were almost equipotent inducers with CYP1A1 activities reaching 3.45- and 3.55-fold increases compared to untreated control animals, whereas DDD was the least potent reaching a maximum CYP1A1 activity of 2.18 times that of untreated control animals. Despite the fact that these experiments were conducted *in vivo*, the potency of the three compounds correlated with what was observed in the present study where (in terms of potency of inducing CYP1A1 activity) the compounds were ranked DDE > DDT > DDD. Dickerson *et al.* (1999) also reported potent, dose-dependent induction of CYP1A1 by DDE *in vivo* while Sierra-Santoyo *et al.* (2000) reported findings that suggest that the CYP1A1 induction by DDT, DDE and DDD may also be gender-dependent.

NAC pre-treatment increased CYP1A1 activity at low concentrations (5 - 10 µM) for both DDT (significant at 5 µM, $\boldsymbol{p} < 0.05$) and DDD but had the opposite effect when cells were exposed to DDE (Table 4.6 and Figure 4.6). However, these observations were not significant. NAC pre-treatment caused significant reductions in CYP1A1 activity at 50 µM for all three test compounds. Previous reports have shown that NAC is able to inhibit heavy metal-mediated CYP1A1 induction (Elbekai and El-Kadi, 2005; Wu *et al.*, 2009). However, results from the present study do not support the fact that NAC inhibited CYP1A1 induction by the test compounds because if this was the case, NAC would have inhibited CYP1A1 induction across the entire test concentration range of the test compounds. Contrarily, the decrease in CYP1A1 activity was only statistically significant at one particular concentration for all three test compounds (50 µM). This observation is more likely to be due to decreases in cell viability as NAC pre-treatment exacerbated the toxic effects of all three test compounds, as was demonstrated in the cytotoxicity assays.

In summary, results from the present study indicate that DDT is capable of up-regulating CYP1A1 activity. Like DDT, its two metabolites also induced CYP1A1 activity, which is expected as all three compounds are similar in structure. In terms of potency of inducing CYP1A1 activity the three test compounds can be ranked as follows: DDE > DDT > DDD. Pre-treating cells with NAC induced CYP1A1 activity at low concentrations of DDT and DDD but not DDE, suggesting that there may be different mechanisms of activation involved. NAC did cause hepatoprotective, significant decreases in CYP1A1 activity at concentrations of 50 µM of all three test compounds, which corresponds with the decreases in cell viability observed earlier.

Chapter 5: Oxidative Stress

5.1. Background

ROS are unstable molecules, which make them highly reactive. These molecules are naturally generated in small amounts during metabolic reactions of the body. ROS can react with and damage cellular molecules such as lipids, proteins and DNA. Four chemical reactions have been reported through which reactive molecules can modify other molecules and include (Wu and Cederbaum, 2003):

- *Hydrogen abstraction:*

  A radical reacts with a hydrogen donor, to yield a stable molecule, which in turn makes the hydrogen donor reactive.
- *Addition:*

  A radical binds to an originally stable molecule converting the combined molecule into a reactive one.
- *Termination:*

  Two radicals react with each other to form a stable compound.
- *Disproportionation:*

  A radical reacts with another identical radical and donates its unpaired electron to the other, thereby yielding two stable compounds.

Under certain conditions the production of ROS is enhanced and/or the level or activity of antioxidants is reduced. The resulting state, which is characterized by a disturbance in the balance between ROS production, on the one hand and ROS removal and repair of damaged molecules on the other, is called oxidative stress (Cederbaum *et al.*, 2009).

The principal source of ROS production in mammalian cells is the mitochondria, which produces reactive species including $\bullet O_2^-$, H_2O_2 and the highly reactive $\bullet OH$. Mitochondrial ROS are produced by the electron transport chain, which consists of four electron carrier complexes, I-IV. Electrons derived from metabolic reducing equivalents are fed into the

electron transport chain through either complex I or complex II, and eventually pass to molecular O_2 to form H_2O in complex IV (Liu *et al.*, 2002). Theoretically, all of these complexes are able to transfer electrons to O_2 to form $\bullet O_2^-$, which is quickly dismutated to H_2O_2 by mitochondrial superoxide dismutase. However, studies have shown that mitochondrial ROS originate mainly from carrier complexes I and III (Turrens and Boveris, 1980; Turrens *et al.*, 1985).

Another major source of ROS, especially in the liver, is the membrane-bound microsomal monooxygenase system (MMO) (Wu and Cederbaum, 2003). This system, which catalyses the oxygenation of a wide variety of exogenous and endogenous compounds, contains CYPs as the terminal oxidases. Monooxygenation reactions typically require the input of two electrons that are transferred to P450 by the flavoprotein NADPH-P450 reductase but may also come from cytochrome b_5, a small hemoprotein, and its NADH-dependent reductase. The efficiency of electron transfer from NADPH through the electron carriers to the CYP for monooxygenation of substrate is referred to as coupling (Zangar *et al.*, 2004). Although the degree of coupling of NADPH consumption to substrate oxidation varies for different P450 species, it is usually less than 50%. An uncoupled state leads to ROS production as electrons that enter the system do not end in the oxygenation of substrate but escape their natural reaction sequence, finally affecting other molecules present through one of the four reactions mentioned at the beginning of this chapter.

Results from the CYP1A1 experiments show that the test compounds in question are able to induce CYP activity. As mentioned above, MMO is a major source of ROS, especially in the liver, and the up-regulation of CYP1A1 activity is suggestive of possible increased ROS generation and a resultant state of oxidative stress. For this reason, examining DDT/DDE/DDD-induced ROS generation could illuminate the mechanism of the cytotoxicity of the three test compounds.

5.2. Methods

5.2.1. Detection of intracellular ROS by fluorometery

Nine independent endpoint fluorometry experiments were carried out in duplicate, six with the test compounds alone (*n* = 12) and three that included a 1 h NAC pre-treatment (*n* = 6). Intracellular ROS was detected according to the method described by Zhang et al. (2009), with slight modifications. Following the 48 h seeding incubation, 40 µl of 2',7'-dichlorofluorescein diacetate DCFDA (20 µM) in PBS was added to each well and incubated for 1 h at 37°C. The loading medium was then carefully removed and cells washed with 200 µl PBS. Cells were kept hydrated by the addition of 50 µl of PBS to each well followed by the addition of 50 µl of either PBS (1% DMSO), 2',2'-azobis(2-methylpropionamidine) dihydrochloride AAPH (300 µM) or test compound (10 - 300 µM) to yield final concentrations of 0.5% DMSO, 150 µM AAPH and 5 - 150 µM of the relevant test compounds. Cells were incubated for 3 h before fluorescence was measured on a FluoStar Optima fluorescent plate reader using λ_{ex} = 492 nm and λ_{em} = 525 nm at a gain setting of 750. AAPH was used as positive oxidant control (Ximenes *et al.*, 2009).

5.2.2. Detection of intracellular ROS by flow cytometry

To confirm the findings obtained with fluorometry, ROS detection with DCFDA was repeated using flow cytometry. After harvesting cells by trypsinisation, 1×10^7 cells were pooled into a single centrifuge tube and incubated with 5.7 µM DCFDA in 1 ml EMEM for 1 h at 37°C. This was done to ensure that all the cells for a particular experiment were pre-loaded with the same concentration of the oxidant sensitive dye.

While the cells were being incubated to pre-load with DCFDA, 5 µl of DMSO (vehicle solvent), AAPH (30 mM) or test compound (1 - 30 mM), were added to individual flow cytometry tubes.

Following DCFDA pre-loading, cells were diluted to 2×10^5 cells/ml (same cell density as used in all other experiments) using PBS. Of this cell suspension, 1 ml was added to each of the prepared flow cytometry tubes. Cells were then incubated for 3 h at 37°C, after which the fluorescence was measured using channel FL1 (525 nm) on a Beckman Coulter FC500 flow cytometer. A total number of 5000 events were recorded per sample, from which a mean was obtained. Three individual experiments on individual batches of cells were performed.

5.2.3. Kinetic evaluation of ROS detected by fluorometry

To determine whether any ROS generation occurred over a longer exposure period, kinetic experiments were conducted. As with fluorometric detection (described in *Section 5.2.1.*), cells were loaded with 5.7 µM DCFDA for 1 h at 37°C. The solution was then carefully aspirated and the cells washed with PBS. This was followed by the addition of 50 µl PBS and an additional 50 µl of PBS containing either DMSO (1%), AAPH (300 µM) or the relevant test compound (0.2 - 200 µM) to each well. Final concentrations of DDT, DDE and DDD were 0.01, 0.1, 1, 10 and 100 µM (0.5% DMSO final concentration). The initial concentration range was broadened to allow for the detection of ROS below 5 µM of test compound in order to determine whether lower concentrations may induce any significant ROS generation. After adding the test compounds and controls, fluorescence was determined at 30 min intervals over a period of 14 h at 37°C. Fluorescence was detected on a FluoStar Optima fluorescent plate reader using λ_{ex} = 492 nm and λ_{em} = 525 nm at a gain setting of 750.

5.2.4. Statistical analyses

Nine independent endpoint fluorometry experiments were carried out in duplicate, six with the test compounds alone (***n* =** 12) and three that included a 1 h NAC pre-treatment (***n* =** 6). Outliers were detected using Grubb's test and removed, before normality of the data distributions were evaluated with the Shapiro-Francia test. Hypothesis testing was then

performed utilising either Student's ***t***-tests or Mann-Whitney tests, to determine whether any observable differences between means were statistically significant. In addition to the endpoint ROS experiments, three independent flow cytometry experiments (***n* =** 3) and three independent kinetic experiments in quadruplicate (***n* =** 12) were performed. Flow cytometry results were tested using only Mann-Whitney tests since only three observations were available for scrutiny. All results, except those from kinetics experiments, were standardized to percentage of control and are reported as Mean ± SEM. For kinetic experiments, raw data was analysed using a two-way analysis of variance with a Bonferroni *post hoc* test to compare all groups to the control groups.

The possible effects that NAC may have on test compound-induced changes in intracellular ROS were also determined. These results were standardised to percentage of control but no preliminary tests (Grubb's and Shapiro-Francia) were performed because of the small sample size (***n* =** 6). Therefore, Mann-Whitney tests were performed without removal of outliers.

5.3. Results

5.3.1. Endpoint fluorometry

Three of the six groups of data in the DDT data set contained outliers with ***p*** < 0.05 according to Grubb's test. Similarly, 3 different groups in the DDE data set contained outliers, while the DDD data set contained 4 groups with outliers (Table 5.1). A maximum of 2 outliers were removed per group. Hypothesis testing was then performed on a minimum of 10 observations. Most of the data presented with normal distributions according to the Shapiro-Francia test (Table 5.2). Only the 50 µM group of DDT and the 10 µM group of DDE were not normally distributed, accordingly these were analysed with Mann-Whitney tests.

Table 5.1. Grubb's test results for detecting outliers in the observed ROS data. Values given in the table are p-values. Instances where $p < 0.05$ (*) indicates the presence of outliers.

Concentration	DDT	DDE	DDD
Control	0.35	0.08	0.01*
5 µM	0.05	0.00*	0.02*
10 µM	0.01*	0.00*	0.00*
50 µM	0.00*	0.06	0.00*
100 µM	0.02*	0.00*	0.08
150 µM	0.11	0.56	0.10

Table 5.2. Shapiro-Francia test normality results of the observed ROS data after removal of outliers detected with Grubb's test. Values given in the table are p-values. Instances where $p < 0.05$ are significantly non-normal. * indicates $p < 0.05$.

Concentration	DDT	DDE	DDD
Control	0.98	0.18	0.13
5 µM	0.23	0.27	0.91
10 µM	1.00	0.03*	0.29
50 µM	0.01*	0.19	0.61
100 µM	0.27	0.36	0.26
150 µM	0.19	0.45	0.64

The positive control (AAPH) yielded the large expected increase in ROS generation when compared to vehicle only treated controls (Table 5.3 and Figure 5.1). Fluorometric evaluation showed no ROS generation in HepG2 cells exposed to DDT for 3 h. Rather, results showed a trend of decreasing ROS with an increase in DDT concentration (Figure 5.3A). A

significant ($p < 0.05$) deviation from the vehicle control was only detected at the highest concentration of DDT (150 µM) where a 30% decrease in intracellular ROS levels occurred.

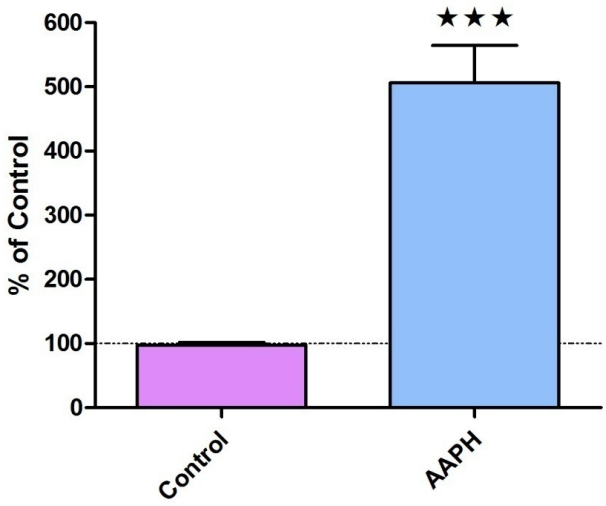

Figure 5.1. Generation of H_2O_2 in HepG2 cells following 3 h exposure to vehicle control *vs.* AAPH (150 µM) using DCFDA as ROS probe (mean ±SEM) as detected by fluorometry. *** = $p < 0.001$.

DDE exposure also decreased the amount of intracellular ROS following a dose-dependent trend. This was more pronounced than in cells exposed to DDT at all of the tested concentrations, except 50 µM, causing a significant decrease in the detected ROS of approximately 40% ($p < 0.01$), compared to controls. Similar to the other tested compounds, DDD did not induce ROS generation. DDD also produced a decrease in ROS with significant reductions at concentrations of 50 and 100 µM DDD with $p < 0.01$ and $p < 0.05$, respectively.

Table 5.3. ROS generation in HepG2 cells following 3 h exposure to DDT, DDE, DDD and AAPH (positive control). Results (% of Control) are presented as mean ±SEM. * indicates $p < 0.05$, ** $p < 0.01$ and *** $p < 0.001$ as determined by Mann-Whitney tests.

Concentration	DDT	DDE	DDD	AAPH (150 µM)
Control	100 ± 8	100 ± 10	92 ± 4	
5 µM	97 ± 12	62 ± 7**	73 ± 10	
10 µM	84 ± 10	59 ± 9**	87 ± 12	506 ± 58***
50 µM	87 ± 9	75 ± 12	64 ± 7**	
100 µM	81 ± 11	53 ± 10**	62 ± 10*	
150 µM	69 ± 11*	61 ± 9**	76 ± 11	

Table 5.4. ROS generation in HepG2 cells due to DDT, DDE, DDD, with or without 1 h pre-treatment with NAC. There were no statistically significant differences between cells pre-treated with NAC and those that were exposed to test compounds only.

	DDT		DDE		DDD	
	--	NAC	--	NAC	--	NAC
5 µM	97 ± 12	93 ± 12	62 ± 7	72 ± 8	73 ± 10	94 ± 12
10 µM	84 ± 10	87 ± 14	59 ± 9	68 ± 6	87 ± 12	87 ± 10
50 µM	87 ± 9	89 ± 12	75 ± 12	81 ± 15	64 ± 7	97 ± 24
100 µM	81 ± 12	93 ± 12	53 ± 10	73 ± 7	62 ± 10	89 ± 11
150 µM	69 ± 10	84 ± 10	61 ± 9	75 ± 6	76 ± 11	82 ± 11

NAC pre-treatment had no significant effect on test compound-induced changes in intracellular ROS levels. There is a trend in the results that NAC pre-treatment appeared to inhibit the reductions in ROS levels induced by the test compounds (Table 5.4 and Figure 5.5).

5.3.2. Flow cytometry

The positive control, AAPH, yielded expected results by significantly ($p < 0.001$) inducing ROS. AAPH produced a 2-fold increase in ROS generation when compared to the vehicle controls (Figure 5.2). Flow cytometry results support the fluorometric findings in that no significant increase in ROS generation was detected after DDT exposure. None of the flow cytometry results were significantly different from controls. A slight increase in ROS occurred in the 5 µM of DDT group but this was not a statistically significant elevation (Figure 5.3D). Flow cytometry indicated no ROS generation after DDE exposure. Similar to cells exposed to DDT, there may be a trend of decreased ROS with an increase in DDE concentration (Figure 5.3E). None of the flow cytometry results showed any significant deviation from control values. No significant DDD-induced increase in ROS generation was detected by flow cytometry but, as with DDT, results do show a slight increase in ROS generation in cells exposed to 5 µM of DDD (Figure 5.3F). A similar trend to the other test

compounds was seen, with reduced ROS production associated with increases in DDD concentration. However, none of these observations were significant (Figure 5.3F).

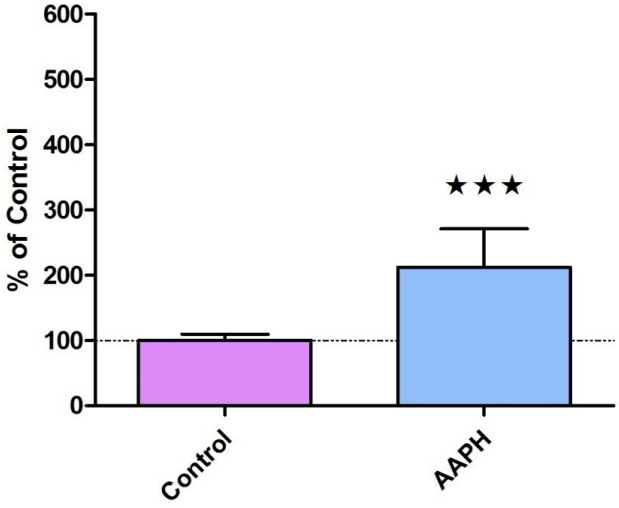

Figure 5.2. Generation of H_2O_2 in HepG2 cells following 3 h exposure to vehicle control *vs.* AAPH (150 μM) using DCFDA as ROS probe (mean ±SEM) as detected by flow cytometry. *** = $p < 0.001$.

5.3.3. Kinetic fluorometry

Kinetic evaluation of AAPH-induced ROS generation showed a sharp increase in ROS generation up to ≈ 6 h exposure, after which the rate of ROS generation decreased, reaching a plateau. AAPH significantly ($p < 0.01$) elevated intracellular ROS from 2 h of exposure onwards, compared to vehicle controls (Figure 5.4). As evident from Figure 5.4, no increase or decrease in ROS generation was observed when cells were exposed to DDT, DDE or DDD over a period of up to 14 h.

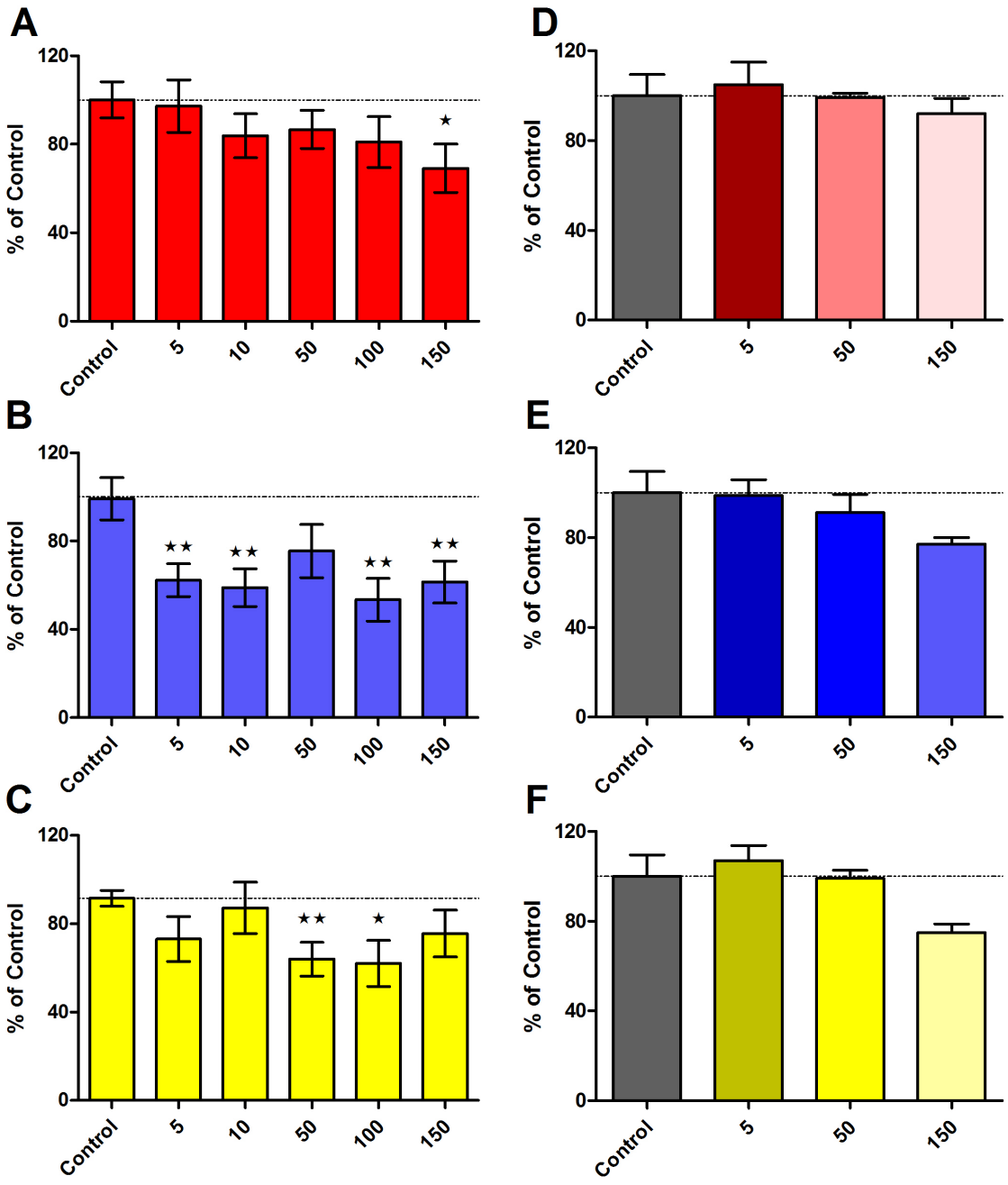

Figure 5.3. Fluorometric detection (endpoint) of H_2O_2 in HepG2 cells following 3 h exposure to DDT (A), DDE (B) and DDD (C) (mean ±SEM). * indicates $p < 0.05$ and ** $p < 0.01$ as determined by Mann-Whitney tests. Graphs (D), (E) and (F) illustrate the corresponding flow cytometry results of DDT, DDE and DDD, respectively. Dashed horizontal lines represent control values.

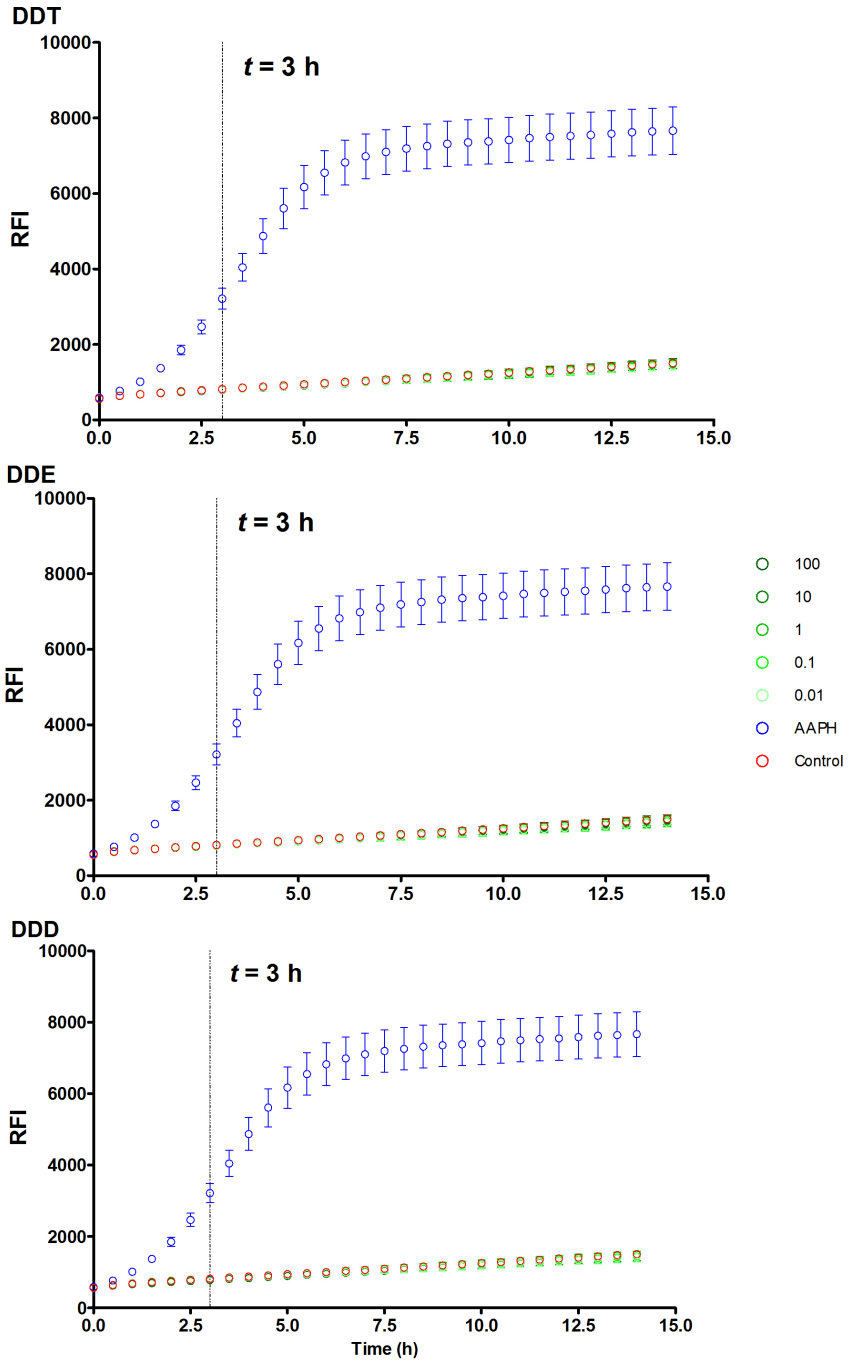

Figure 5.4. Raw data (no data manipulation) from three independent experiments showing H_2O_2 generation in HepG2 cells following exposure to various concentrations of DDT, DDE and DDD over a 14 h incubation period (mean ±SEM). Dashed vertical lines represent X = 3 h, which is the incubation period used in all other experiments. RFI = relative fluorescence intensity. AAPH (150 μM) alone induced significant ($p < 0.001$) ROS generation from 2 h onwards. All test compounds at all tested concentrations showed no significant difference from the negative control values for the same time.

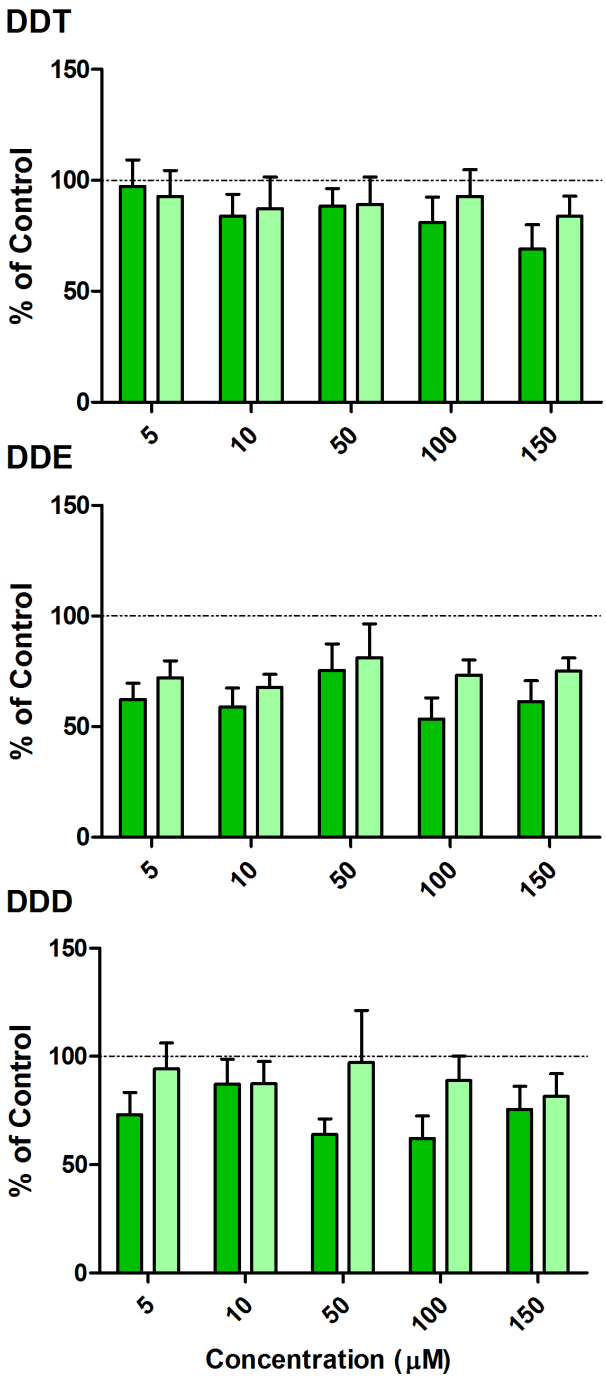

Figure 5.5. Generation of H_2O_2 in HepG2 cells following 3 h exposure to DDT, DDE and DDD (mean ±SEM), without (dark green bars) or with (light green bars) 1 h NAC pre-treatment. No significant differences were detected.

5.4. Discussion

Following the removal of outliers with the Grubb's test (Table 5.1), only 2 of the 18 data sets presented non-normal distributions (Table 5.2), indicating good reproducibility.

When comparing the results of the fluorometric and flow cytometric methods of detection of AAPH-induced ROS generation using DCFDA, fluorometry detected a 5-fold increase in fluorescence compared to a 2-fold increase observed with flow cytometry (Figure 5.1 and Figure 5.2). This would suggest that the fluorometry method is a more sensitive method than flow cytometry. However, fluorometric evaluation demonstrates a different inhibitory trend to that seen with flow cytometry (Figure 5.3).

Regarding the effect of the three test compounds on ROS levels, previous *in vitro* studies using DCFDA as probe have demonstrated DDT-induced ROS generation in various types of cells. Using fluorometry, researchers have reported DDT-induced ROS in skin tumour (Ruiz-Leal and George, 2004) and U937 monocyte lymphoma cells (Sciullo *et al.*, 2010). Studies reporting DDT-induced ROS in hepatocytes (Filipak Neto *et al.*, 2008; Shi *et al.*, 2010a) have used flow cytometry. The study by Filipak Neto *et al.* (2008) used primary hepatocytes derived from a fish species. In the human-derived L-02 hepatocyte cell line, a significant increase in intracellular ROS was observed after 24 h exposure to 10 nM and 100 nM of DDT (Shi *et al.*, 2010a). The effects of DDE and DDD on ROS generation in hepatocytes have not been reported previously. However, they have been shown to induce ROS generation in peripheral blood mononuclear cells (Perez-Maldonado *et al.*, 2004) and primary rat Sertoli cells (Song *et al.*, 2008).

In the present study neither fluorometric, nor flow cytometric methods detected any significant ROS generation caused by DDT, DDE or DDD exposure (5 - 150 µM), which may be considered contradictory to reported literature. However, flow cytometry did reveal a small increase in ROS generation at the lowest tested concentration of DDT and DDD (5 µM), which could suggest that concentrations of DDT and DDD lower than 5 µM may induce more ROS generation (Figure 5.3A). To test this hypothesis, a very wide concentration range

(0.01 - 100 µM) of all three test compounds were tested in three independent kinetic-type fluorometry experiments, each spanning 14 h of exposure, in an attempt to reproduce the reported ROS generation. The chosen concentration range included concentrations of 10 and 100 nM, which has previously been reported to induce ROS generation in cultured hepatocytes (Shi *et al.*, 2010a). Together with flow cytometry results, these experiments using the extended concentration range supported the initial endpoint fluorometry results in that no ROS generation was detected in cells exposed to any of the test compounds (Figure 5.3).

Contradictory to their first article (Filipak Neto *et al.*, 2008), a second publication reported that 50 nM of DDT caused a significant decrease in intracellular ROS in primary hepatocytes (Bussolaro *et al.*, 2010). Although the same methodology was applied, hepatocytes originating from a different fish species were employed, which could indicate a species-specific response to DDT in terms of intracellular ROS generation. This may explain why ROS generation was not seen with HepG2 cells in the present study whereas ROS generation was seen in L-02 cells (Shi *et al.*, 2010a). Although both cell lines are of human origin, the one is cancerous (HepG2) and the other not (L-02) (Guo *et al.*, 2007) so they are likely to present with different genotypic and phenotypic features and could therefore respond differently.

Another explanation for the apparent discrepancy could be the duration of exposure. In the studies conducted by Filipak Neto *et al.* (2008) and Shi *et al.* (2010a), the authors exposed hepatocytes to DDT for periods of 4 days and 24 h, respectively. Morel *et al.* (1999), who specifically studied CYP1A1-generated ROS in HepG2 cells, exposed cultures for 30 h to benzo(a)pyrene, a well-known CYP1A1 inducer, in order to detect ROS generation. In the present study cells were only exposed for 3 h, which failed to yield any elevated intracellular ROS. For this reason, the kinetics experiments were conducted over a 14 h period, but still no ROS was detected. This may indicate that the DDT-induced ROS generation seen in previous studies had its origin from the MMO system rather than mitochondria. It was shown in this study that DDT induces CYP1A1 activity, which forms part of the MMO system of enzymes. Considerable time is required for CYP1A1 up-regulation to manifest intracellularly as the relevant receptors need to be activated and translocated to the nucleus, after which transcription needs to occur, followed by translation and finally protein

synthesis. If DDT-induced ROS generation is the result of high MMO activity, all of the afore-mentioned processes need to take place before any detectable increase in ROS will present itself. If DDT-induced ROS generation was due to mitochondrial uncoupling, this would manifest much faster and would probably be detectable within 14 h of exposure as was seen with AAPH-induced ROS, which reached a maximum plateau after approximately 6 h of exposure.

CYP1A1 and intracellular ROS are also related to each other in terms of a negative-feedback autoregulatory loop, in which CYP1A1, that generates ROS during its catalytic cycle, is regulated by cytosolic ROS levels, specifically H_2O_2 (Morel and Barouki, 1998; Morel *et al.*, 1999; Barouki and Morel, 2001). ROS regulation of CYP1A1 expression occurs at a transcriptional level. The aryl hydrocarbon receptor (AhR), AhR nuclear translocator (Arnt) and Nuclear Factor I (NFI) are all required for activation and transcription of the *cyp1a1* gene and studies have shown that synergy between AhR-Arnt complex and NFI as well as NFI integrity is diminished in the presence of H_2O_2 (Morel *et al.*, 1999). The fact that CYP1A1 up-regulation was observed only after 24 h exposure to the test compounds (*Chapter 4*) provides further support for the fact that DDT does not induce ROS through a rapidly activated pathway, as observed in the present study.

NAC pre-treatment for 1 h had no significant influence on the test compound changes in intracellular ROS (Table 5.4 and Figure 5.4), which is not unexpected as initial results indicated that none of the test compounds induced ROS in the first place. This provides further support in concluding that none of the tested compounds induce ROS generation in HepG2 cells following a short 3 h exposure.

Using fluorometric detection, no elevated intracellular ROS levels were observed for any of the test compounds at any of the tested concentrations after 3 h exposure. This was confirmed by flow cytometry. After extending both the exposure period to 14 h and widening the concentration range from 0.01 – 100 µM, still no elevations in ROS levels were observed. These findings suggest that the test compounds do not induce ROS generation in these cells by a rapidly inducible reaction pathway.

Chapter 6: Mitochondrial Toxicity

6.1. Background

Mitochondria are the main source of chemical energy in a cell. They provide more than 15 times the ATP than that generated by anaerobic glycolysis (Alberts *et al.*, 2002). Mitochondria generate ATP through the action of ATP-synthase. The respiratory complexes I, III and IV of the electron transport chain are responsible for actively transporting H^+ ions into the mitochondrial intermembrane space (Figure 6.1). ATP-synthase then uses the backflow of H^+ ions from the mitochondrial intermembrane space into the mitochondrial cytosol as a driving force to synthesise ATP from adenosine diphosphate and inorganic free phosphate. Due to the constant active efflux of H^+ from the mitochondrial cytosol into the intermembrane space, a difference in H^+ concentration across the inner membrane develops, which creates an electrochemical gradient known as the mitochondrial membrane potential ($\Delta\psi_m$) (Hutteman *et al.*, 2008). In addition to H^+ re-entry into the mitochondrial matrix via ATP-synthase, all mitochondria also possess a parallel endogenous H^+ leak (Nicholls, 1977). Under normal physiological conditions the H^+ leak may serve an important purpose in limiting the $\Delta\psi_m$ to prevent dielectric breakdown of the membrane (Brand *et al.*, 1994; Rolfe and Brand, 1997).

The $\Delta\psi_m$ lies at the heart of all the major bioenergetic functions of the mitochondrion, as it provides a force that drives the influx of H^+, from the intermembrane space, by simply moving it into the mitochondria down the electrochemical potential gradient. The actions of the respiratory complexes as H^+ translocators also means that the respiratory rate is regulated by $\Delta\psi_m$ in that respiration will run faster when the membrane is depolarised as a thermodynamic consequence of the reduced energy required to move H^+ out of the intermembrane space, and will run more slowly if the membrane is hyperpolarised (Duchen, 2004).

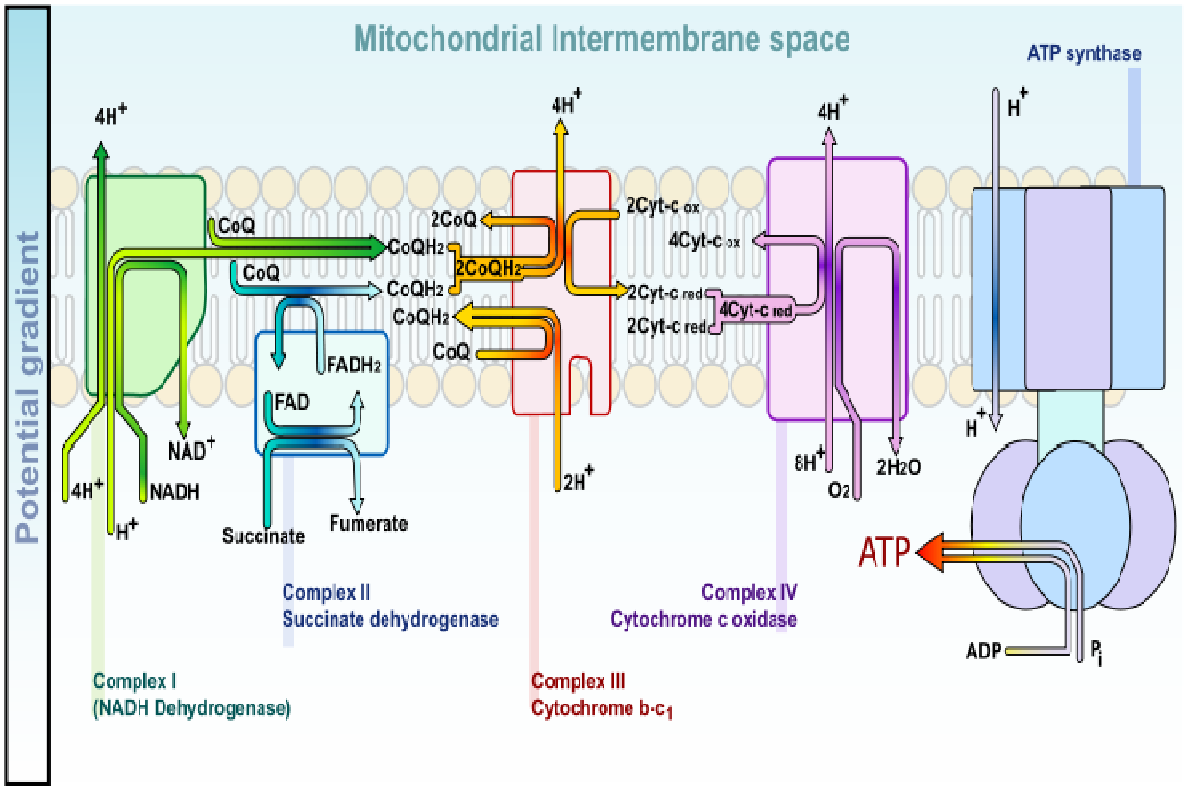

Figure 6.1. **Illustration of the electron transport chain and ATP-synthase embedded in the inner mitochondrial membrane. Electrons enter the system via reduced nicotinamide adenosine dinucleotide (NADH) and reduced flavin adenosine dinucleotide ($FADH_2$). As electrons are transferred from one respiratory complex to the next, H+ ions are driven from the mitochondrial cytosol into the intermembrane space. O_2 is the final electron receptor, which is reduced to H_2O. ATP-synthase is coupled to this system by the backflow of H+ through the proton channel of ATP-synthase, an ATPase that works in backwards, forming ATP from ADP and inorganic phosphate (Duchen, 2004) (Figure adapted from Wikipedia, 2011).**

$\Delta\psi_m$ typically ranges from -150 mV to -180 mV under normal physiological conditions. This value is negative since it is the electrochemical potential relative to the cell cytoplasm (Perry *et al.*, 2011). Cationic dyes, such as 5,5',6,6'-tetrachloro-1,1',3,3'-tetraethylbenzimidazolylcarbocyanine iodide (JC-1), have been used to evaluate $\Delta\psi_m$ in HepG2 cells (Nerurkar *et al.*, 2004; Perry *et al.*, 2011). As a positively charged molecule, this dye accumulates in mitochondria in inverse proportion to the $\Delta\psi_m$. JC-1 is unique in its ability to exist in two states, each with its own excitation-emission spectrum. When the dye is present in high concentrations within mitochondria, due to a highly negative $\Delta\psi_m$, the dye

forms J-aggregates with λ_{em} = 590 nm and when present at low concentrations, due to low $\Delta\psi_m$, the dye exists as J-monomers with λ_{em} = 520 nm (Gravance *et al.*, 2000).

Many of the cytotoxicity assays used by authors in previous attempts to detect hepatotoxicity are non-specific and fail to detect specific types of toxicity, such as mitochondrial toxicity, particularly when cell viability is not affected (Farkas & Tannenbaum, 2005). A good example of this is troglitazone, an antidiabetic drug, which was commercialised after pre-clinical *in vitro*, *in vivo* as well as clinical testing but was eventually withdrawn because it proved to be hepatotoxic due to mitochondrial toxicity that was not detected during early drug development (Labbe *et al.*, 2008). Troglitazone toxicity highlighted the importance of evaluating the mitochondrial status of cells following exposure to a certain compound. As mitochondrial effects can have an important role in cell toxicity and cell death it is prudent to assess the mitochondrial status during cytotoxicity testing as was done in the present study.

6.2. Methods

6.2.1. Evaluation of $\Delta\psi_m$ using JC-1

$\Delta\psi_m$ was evaluated using the method of Nuydens *et al.* (1999), with slight modifications. Following the 48 h seeding incubation, a 100 µl of JC-1 (20 µM) in EMEM was added to each well and cells loaded with the dye for 30 min at 37°C. Loading medium was then discarded and cells washed with 200 µl PBS. To keep cells hydrated, 50 µl of PBS was added to each well. This was followed by the addition of 50 µl of either PBS (1% DMSO), Tamoxifen (300 µM) or test compound (10 - 300 µM) to yield final concentrations of 0.5% DMSO, 150 µM Tamoxifen and 5 - 150 µM of the relevant test compounds, all diluted in PBS. Cells were then exposed for 1 h before fluorescence was measured on a FluoStar Optima at both λ_{ex} = 492 nm and λ_{em} = 525 nm (monomeric JC-1 form) and λ_{ex} = 545 nm and λ_{em} = 595 nm (aggregate JC-1 form) at a gain setting of 1000.

6.2.2. Statistical analyses

Six independent fluorometry experiments were carried out in duplicate (***n*** = 12). Relevant blank values were deducted from all values before the ratio of 595 nm/525 nm fluorescence intensities was calculated, which is used as an indication of $\Delta\psi_m$ - the more intense the fluorescence at 595 nm, the more J-aggregates are present indicating a high $\Delta\psi_m$, and *vice versa* (Nuydens *et al.*, 1999; Nerurkar *et al.*, 2004; Perry *et al.*, 2011). Data outliers were detected using Grubb's test and removed, before normality of the data distributions were evaluated with the Shapiro-Francia test. Hypothesis testing was then performed utilising either Student's ***t***-tests (normal) or Mann-Whitney tests (non-normal), to determine whether any observable differences between means were statistically significant. Results were standardized to percentage of control and are presented as Mean ± SEM.

Three additional experiments were carried out in duplicate to assess the possible effects that NAC may have on pesticide-induced changes in $\Delta\psi_m$. These results were also standardised to percentage of control but no preliminary tests (Grubb's and Shapiro-Francia) were performed. Mann-Whitney tests were performed due to the small sample size (***n*** = 6), no outliers were removed and normality of the data could not be established.

6.3. Results

One group out of each of the data sets contained outliers (Table 6.1). After removal, data distributions were tested for normality, which revealed that the data was normally distributed except for one group from both the DDT (5 µM) and DDD (100 µM) data sets (Table 6.2). Accordingly, these data groups were analysed using Mann-Whitney tests, while the rest of the data were analysed with Student's ***t***-tests to determine whether any deviations from the control mean were significant.

Table 6.1. Outliers in $\Delta\psi_m$ data, detected by Grubb's test. Values given in the table are ***p***-values. Instances where $p < 0.05$ (*) indicates the presence of outliers.

Concentration	DDT	DDE	DDD
Control	0.49	0.69	0.02*
5 µM	0.00*	0.10	0.19
10 µM	0.31	0.02*	0.09
50 µM	0.20	0.05	0.24
100 µM	0.08	0.18	0.96
150 µM	0.11	0.09	0.82

Table 6.2. Shapiro-Francia test normality results of the observed $\Delta\psi_m$ data after removal of outliers detected with Grubb's test. Values given in the table are p-values. Instances where $p < 0.05$ are significantly non-normal. * indicates $p < 0.05$.

Concentration	DDT	DDE	DDD
Control	0.24	0.56	0.46
5 µM	0.02*	0.34	0.06
10 µM	0.34	0.15	0.58
50 µM	1.00	0.41	0.71
100 µM	0.29	0.72	0.04*
150 µM	0.89	0.93	0.08

The positive control, Tamoxifen, yielded expected results as it hyperpolarised the membrane as has been previously reported for HepG2 cells (Donato *et al.*, 2009). Tamoxifen caused an approximate 7-fold increase in $\Delta\psi_m$ compared to vehicle controls (Table 6.3 and Figure 6.2). Considerable variation was seen in Tamoxifen results but hyperpolarisation was sufficiently high enough for the results to be highly significant ($p < 0.001$) (Table 6.3).

Table 6.3. Changes in $\Delta\psi_m$ in HepG2 cells following 1 h exposure to DDT, DDE, DDD and Tamoxifen (positive control). Results (% of Control) are presented as mean ±SEM. *** = $p < 0.001$ as determined by Student's *t*-tests and Mann-Whitney tests.

Concentration	DDT	DDE	DDD	Tamoxifen (150 µM)
Control	100 ± 9	100 ± 10	100 ± 4	
5 µM	86 ± 6	89 ± 5	97 ± 5	
10 µM	86 ± 6	87 ± 6	90 ± 6	688± 199***
50 µM	101 ± 7	103 ± 6	146 ± 7***	
100 µM	145 ± 13***	164 ± 15***	301 ± 20***	
150 µM	162 ± 17***	194 ± 18***	340 ± 22***	

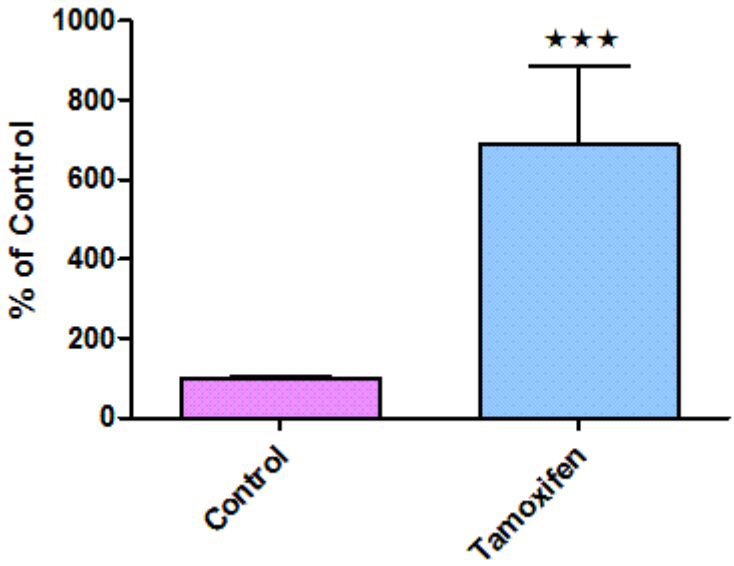

Figure 6.2. Changes in $\Delta\psi_m$ detected by JC-1 in HepG2 cells following 1 h exposure to vehicle control *vs.* Tamoxifen (150 µM) (mean ±SEM). Tamoxifen caused significant hyperpolarisation of the membrane potential with $p < 0.001$ (Student's *t*-test).

At the lower concentration range tested (5 - 10 µM), DDT reduced $\Delta\psi_m$ by 14%, although not statistically significant. At 50 µM, DDT did not affect $\Delta\psi_m$, with only a 1% difference from controls. However, highly significant increases in $\Delta\psi_m$ were seen at the higher concentration range tested, from 100 - 150 µM ($p < 0.001$), producing 45% and 62%

increases, respectively. DDT demonstrated a dose-dependent increase in $\Delta\psi_m$ from 10 - 150 µM (Table 6.3 and Figure 6.3).

A similar trend was seen with DDE. From 5 - 10 µM, there was a non-significant decrease in $\Delta\psi_m$ of approximately 12%. At 50 µM, DDE caused only a 3% increase in $\Delta\psi_m$, while 100 and 150 µM concentrations resulted in very large increases in $\Delta\psi_m$ of 64% and 94%, respectively. These increases were greater than those induced by equivalent dosages of DDT and were statistically highly significant ($p < 0.001$) (Table 6.3 and Figure 6.3).

Low concentrations of DDD (5 and 10 µM) also decreased $\Delta\psi_m$, non-significantly. However, DDD (≥ 50 µM) induced highly significant ($p < 0.001$) increases in $\Delta\psi_m$. At 50 µM, DDD caused an increase equivalent to that produced by 100 µM of DDT (46% *vs.* 45%). A 100 and 150 µM concentrations yielded 201% and 240% increases in $\Delta\psi_m$ compared to untreated controls ($p < 0.001$) (Table 6.3 and Figure 6.3).

Pre-treating cells with NAC stabilised $\Delta\psi_m$, especially at higher concentrations of the test compounds, where NAC pre-treatment significantly reduced the hyperpolarisation induced by the test compounds at concentrations of 150 µM (Table 6.4 and Figure 6.4).

Table 6.4. Changes in $\Delta\psi_m$ in HepG2 cells due to DDT, DDE, DDD, with or without 1 h pre-treatment with NAC. * indicates $p < 0.05$, ** $p < 0.01$ and *** $p < 0.001$ as determined by Mann-Whitney tests.

	DDT		DDE		DDD	
	--	NAC	--	NAC	--	NAC
5 µM	95 ± 11	109 ± 8*	89 ± 5	108 ± 5*	97 ± 5	99 ± 6
10 µM	86 ± 6	111 ± 8	93 ± 8	105 ± 6	90 ± 6	114 ± 16
50 µM	101 ± 7	112 ± 4	103 ± 6	132 ± 8*	146 ± 7	117 ± 5*
100 µM	145 ± 13	123 ± 6	164 ± 15	122 ± 10	301 ± 21	153 ± 5***
150 µM	162 ± 17	110 ± 11*	194 ± 18	116 ± 9**	340 ± 22	138 ± 14***

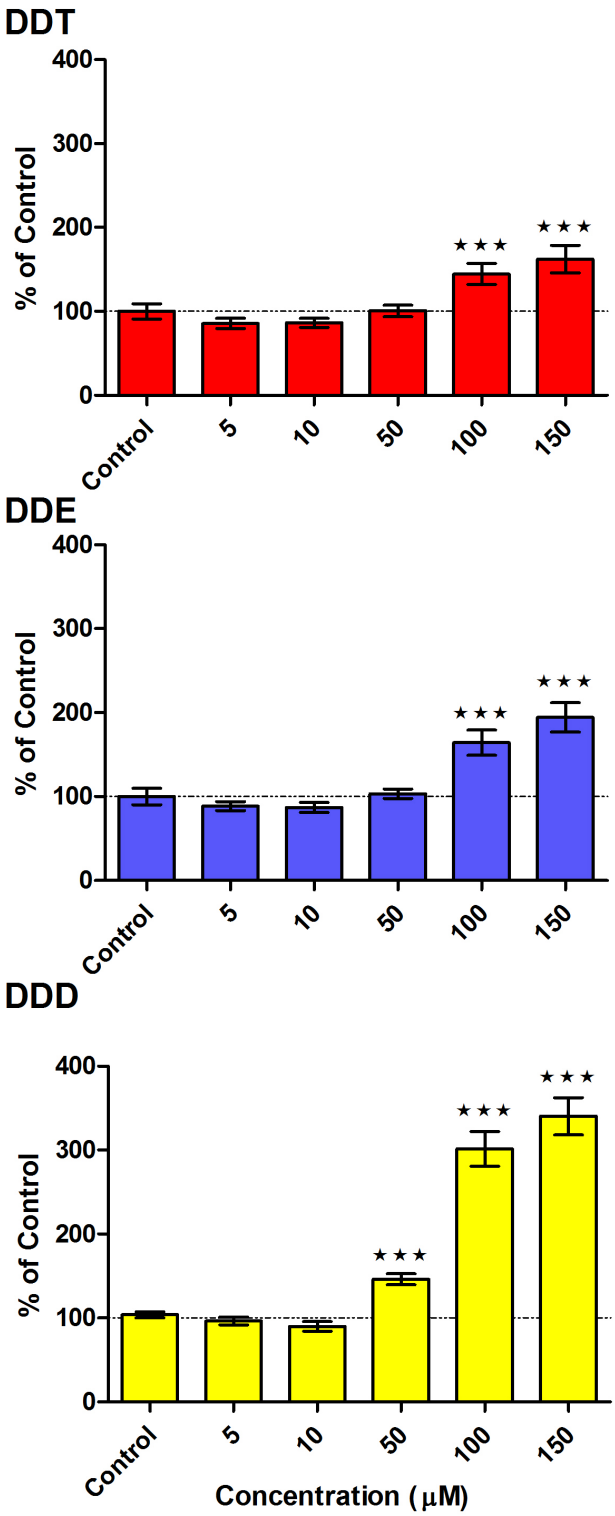

Figure 6.3. Changes in $\Delta\psi_m$ in HepG2 cells following a 1 h exposure to various concentrations of DDT, DDE and DDD (mean ± SEM) relative to untreated controls. *** = $p < 0.001$ as determined by Students *t*-tests and Mann-Whitney tests. Dashed horizontal lines represent Y = 100%.

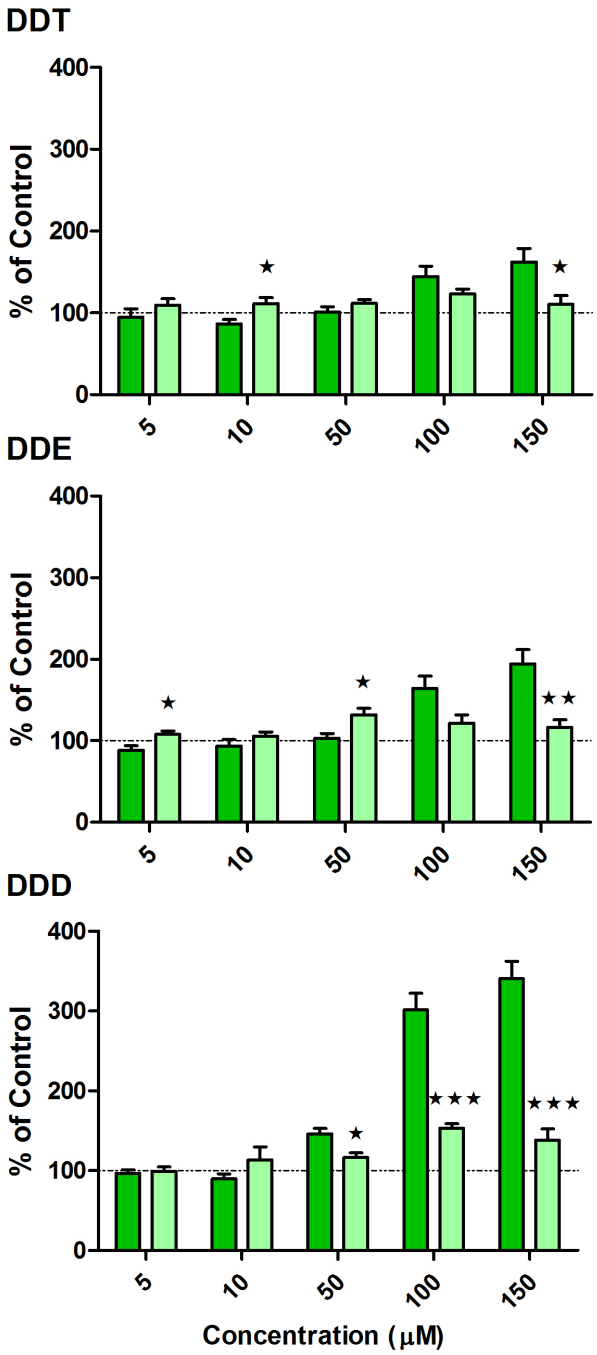

Figure 6.4. Changes in $\Delta\psi_m$ in HepG2 cells following a 1 h exposure to various concentrations of DDT, DDE and DDD relative to untreated controls. Dark green bars represent cells exposed to test compounds alone and light green bars those with a 1 h pre-treatment with NAC (mean ± SEM). * = $p < 0.05$, ** = $p < 0.01$ and *** = $p < 0.001$ as determined by Mann-Whitney tests. Dashed horizontal lines represent Y = 100%.

6.4. Discussion

Following the removal of outliers with the Grubb's test (Table 6.1), only 2 of the 18 data sets presented non-normal distributions (Table 6.2), indicating good reproducibility.

Exposure to the test compounds for 1 h produced similar trends across the tested concentration range with slight decreases in $\Delta\psi_m$ at 5 - 10 µM and significant increases from 100 - 150 µM. DDD was the most potent inducer of $\Delta\psi_m$ of the three test compounds.

No literature was found regarding the effects of the three test compounds on intact cells. To our knowledge this is the first report of the effects of DDT, DDE and DDD on the $\Delta\psi_m$ of intact, cultured hepatocytes. Due to the lack of literature for comparison, this discussion will focus on the possible reasons the observed effects may have occurred drawing on previous studies, which assessed the function of individual components of the respiratory chain and isolated mitochondria.

Elevations of $\Delta\psi_m$ are indicative of an increase in the slope of the electrochemical gradient formed by the difference in concentration of H^+ across the inner mitochondrial membrane. Results from this study suggest that all three compounds significantly increase the H^+ concentration in the intermembrane space. If the elicited response is the result of direct action of the compounds on the respiratory complexes involved in cellular respiration, this can occur in one of three ways, when considering oxidative phosphorylation:

1. by stimulating the electron transport chain, which in turn will drive more H^+ into the intermembrane space

2. by inhibiting the action of ATP-synthase, which would slow the backflow of H^+ ions into the mitochondrial cytosol

3. by inhibiting the H^+ leak that normally prevents mitochondrial hyperpolarisation under physiological conditions.

Mitochondrial hyperpolarisation observed in this study is not likely to be the result of stimulation of the electron transport chain as previous studies have shown that DDT is capable of inhibiting certain complexes of the respiratory chain including complex II (Nishihara and Utsumi, 1985) and complex III (Nishihara and Utsumi, 1985; Morena and Madeira, 1991). The same has been reported for DDE by Mota *et al.* (2011) who described inhibition of the same respiratory complexes in mitochondria isolated from rat liver, after exposure to DDE.

Observed increases in $\Delta\psi_m$ may have occurred due to decreased H^+ re-entry into the mitochondrial cytosol via ATP-synthase. Several studies in literature have described an inhibitory effect on mitochondrial ATP-synthase by DDT (Chefurka, 1983; Nishihara and Utsumi, 1985; Morena and Madeira, 1991; Donato *et al.*, 1997; Younis *et al.*, 2002). A similar ATP-synthase inhibitory action has also been described for DDE (Donato *et al.*, 1997; Mota *et al.*, 2011). Younis *et al.* (2002) demonstrated that DDT is capable of binding directly to the mitochondrial ATP-synthase of DDT-susceptible insects, inhibiting its action. The binding site, a 23 kDa protein segment, was not present in insects that were DDT-resistant and for this reason they suggested that ATP-synthase inhibition by DDT is the mechanism of action of DDT toxicity in these organisms. Furthermore, these authors also suggested that the 23 kDa protein segment was not present in mammalian mitochondria. In contradiction to this, Mota *et al.* (2011) reported inhibition of ATP-synthase by DDE in isolated rat liver mitochondria. It is not clear whether this inhibition in a mammalian species was due to the 23 kDa protein segment being present or some other mechanism that is independent of this protein segment. The aforementioned uncertainty leaves room for the argument that the inhibition of ATP-synthase may explain the mitochondrial hyperpolarisation observed in the present study.

Whether the results of the present study are due to the inhibition of the H^+ leak is also not clear. Inhibition of the H^+ leak could cause congestion by preventing H^+ from re-entering the mitochondrial cytosol, in this way increasing the electrochemical gradient and $\Delta\psi_m$. Mota *et al.* (2011) reported increases in the H^+ leak in rat liver mitochondria exposed to nanomolar concentrations of DDE. This may discredit the aforementioned hypothesis as an explanation of the results. However, those authors used DDE at concentrations in the nanomolar range. In the present study concentrations of DDE ≤ 10 µM also resulted in a decrease in $\Delta\psi_m$, which is in agreement with the report of Mota *et al.* (2011). Exposure to concentrations of 50 µM and higher of DDE elicited mitochondrial hyperpolarisation in the present study. Had Mota *et al.* (2011) tested higher concentrations of DDE (≥ 50 µM), they may have found inhibition of the H^+ leak due to DDE exposure.

Furthermore, an inhibitory action on the electron transport chain has some implications for ROS generation. The electron transport chain is the primary source of mitochondrial ROS, mainly from respiratory complexes I and III (Rhoads *et al.*, 2006). Stimulation of the electron transport chain may result in elevated ROS by free electron transfer to O_2, producing $\bullet O_2^-$, and H_2O_2 (Turrens and Boveris, 1980; Turrens *et al.*, 1985) (*Chapters 1* and *5*). DDT and DDE have been previously reported to inhibit the electron transport chain. For this reason it is unlikely to detect ROS generation by mitochondrial exposure to these compounds. This provides further support for the decrease in intracellular ROS observed in the present study.

With regards to the known hepatoprotectant, NAC, pre-treatment reversed the mitochondrial hyperpolarisation induced by high concentrations of each of the test compounds and stabilised $\Delta\psi_m$ (Figure 6.4). The ability of NAC to reverse changes in and stabilise $\Delta\psi_m$, has been reported before in A549 lung epithelial cells exposed to another pesticide, paraquat (Mitsopoulis and Suntres, 2011). The authors did not elaborate or speculate on how this may happen. A number of authors have reported a regulatory role of GSH in $\Delta\psi_m$ (Constantini *et al.*, 1996; Perl *et al.*, 2002; Nagy *et al.*, 2007). It is well known that NAC is a GSH precursor (Kurebayashi and Ohno, 2006) and that NAC treatment replenishes cellular GSH, which is why NAC is used as rescue medication in acute

acetaminophen toxicity (Ruffmann and Wendel, 1991). The fact that NAC pre-treatment was able to reverse the changes in $\Delta\psi_m$ indicates that NAC may, to some degree, protect against the toxicity induced by the test compounds. Furthermore, this suggests that the mitochondrial hyperpolarisation observed in the present study may be due to GSH depletion induced by the three test compounds. However, whether GSH depletion played a role in the observed mitochondrial hyperpolarisation is disputable, as it was observed that none of the test compounds increased intracellular ROS levels in the short time required to elevate $\Delta\psi_m$ (1 h exposure). A noteworthy observation was the fact that NAC pre-treatment elevated $\Delta\psi_m$ at low test compound concentrations but reduced excessive mitochondrial hyperpolarisation due to exposure to high concentrations of the test compounds. This trend correlates well with observations made regarding cell viability following exposure to the test compounds, where, at low concentrations of the test compounds, NAC pre-treatment exacerbated toxicity, but alleviated toxicity at higher concentrations of the test compounds.

In summary, all three of the tested compounds produced significant elevation of $\Delta\psi_m$ compared to controls, of which DDD was the most potent. This may be due to inhibition of ATP-synthase.

Chapter 7: Modes of Cell Death

7.1. Background

Cell death can follow one of two distinct pathways, apoptosis or necrosis, and can occur in response to severe stress conditions or after exposure to toxic agents. Apoptosis is a normal physiological event taking place continuously in the development of multicellular organisms or during the immune response (Samali *et al.*, 1999). Apoptosis involves activation of the intra-cellular caspase (cysteine-aspartic proteases) enzymes. Whether cell death occurs by apoptosis or necrosis is dependent on the physiologic milieu, developmental stage, tissue type, and the nature of the cell death signal (Ziess, 2003).

Sloviter (2002) recommended replacing necrosis with the term 'passive cell death', and apoptosis and programmed cell death with the term 'active cell death'. The reason for this suggested change in terminology is found in the underlying dependence/independence on cellular energy of each of these modes to manifest cell death. Apoptosis is an ordered form of cell death which depends on the ability of dying cells to initiate well-regulated, ATP-dependent self-degradation without initiating an immune response. In contrast, the core event of necrosis is rapid loss of plasma membrane integrity associated with energy depletion and release of pro-inflammatory molecules (Lin and Yang, 2008).

Apoptosis can be initiated by one of two routes: the 'intrinsic' apoptotic pathway and the 'extrinsic' apoptotic pathway. In the 'intrinsic' apoptotic pathway the mitochondria play the central role and involves the Bcl-2 family of pro-apoptotic proteins (Bad, Bid, Bax). The Bcl-2 proteins facilitate permeabilisation of the mitochondrial membrane with subsequent release of mitochondrial proteins such as cyt C and apoptotic protease activating factor-1 (Apaf-1). Cyt C and Apaf-1, in turn, form a new complex, together with po-caspase-9, known as the apoptosome, which contains active caspase-9. The cyt C/Apaf-1/Caspase-9 apoptosome then recruits effector caspases like pro-caspase-3 that is cleaved to form active caspase-3 (Cas-3) (Harwood *et al.*, 2005). Activation of Cas-3, considered by many as a final executioner protein of the apoptotic cell death sequence, leads to rapid cleavage of a

diverse spectrum of key structural and functional proteins in the cell. These targets for proteolytic attack include, amongst others, cytoskeletal components, signal transduction molecules and DNA repair enzymes (Carambula *et al.*, 2002).

The 'extrinsic' apoptotic pathway is a receptor-mediated, ordered sequence of events starting with activation of a cell surface “death receptor” such as Fas or a receptor from the tumour necrosis factor family of receptors. Receptor occupation allows interaction between receptor death domains and death effector domain on pro-caspase-8. This results in the formation of the death-inducing signalling complex or DISC (similar to the apoptosome from the 'intrinsic' pathway), followed by subsequent cleavage and activation of caspase-8, which is then able to activate the effector Cas-3 (Harwood *et al.*, 2005).

Apoptosis that follows after activation of either the mitochondria-mediated or receptor-mediated pathways rapidly leads to characteristic morphological changes associated with apoptosis including, cytoplasmic vacuolization, cellular shrinkage, an increase in cellular density, nuclear fragmentation, membrane budding and apoptotic bodies which are removed by phagocytic cells. The absence of this set of morphological changes indicates that cell death occurs by necrosis, which is characterised by chromatin flocculation and a progressive loss of plasma membrane integrity, which allows an influx of Na^{+}, Ca^{2+} and water. This constant influx causes cellular swelling, which eventually results in cell rupture and leakage of the cytoplasmic contents into the surrounding tissue. Clinically, the main difference between these modes of cell death lies in the fact that necrosis results in localised inflammation due to spillage of cytoplasmic contents, which in turn releases pro-inflammatory factors. On the other hand, apoptotic cells are broken down to apoptotic bodies with intact membranes, which are then engulfed by nearby phagocytic cells and macrophages with no subsequent inflammatory response (Harwood *et al.*, 2005).

The experiments presented in this chapter were conducted in an attempt to elucidate the mode of cell death caused by each of the test compounds, in order to provide information regarding the mechanism of toxicity of the compounds in question.

7.2. Methods

7.2.1. Assessment of cell death by apoptosis

Staurosporine, the potent inhibitor of serine/threonine kinases known to induce apoptosis in hepatocytes (Giuliano *et al.*, 2004), was used as positive control. To induce apoptosis in positive control samples, 100 µl of staurosporine working solution was added to 100 µl of cell suspesion, giving exposure to a final concentration of 11 µM for 6 h at 37°C. To quantify Cas-3 activity, the method accompanying the CASP3F Cas-3 fluorometric detection kit from Sigma-Aldrich was followed with slight modification. (The CASP3F kit was not used, just the protocol and Ac-DEVD-AMC)

Following 6 h exposure to either positive control or test compounds, plates were put on ice for 20 - 30 min to cool. As soon as the plates were not warm to the touch, medium was aspirated and replaced with 25 µl of ice-cold lysis buffer and incubated on ice for a further 20 min. After this 100 µl of assay buffer was added and the plates incubated overnight at 37°C. The following day, the cleaved 7-amino-4-methylcoumarin (AMC) was quantitated using a FluoStar Optima using λ_{ex} = 360 nm and λ_{em} = 460 nm.

7.2.2. Assessment of cell death by necrosis

The detergent Triton X-100, which is reported to disrupt most cell membranes (Tate *et al.*, 1983), was used as positive control for PI staining. To disrupt plasma membranes of the positive control sample, a 100 µl of Triton X-100 (working solution) was added to 100 µl of cells to give a final concentration of 0.5% (v/v). Cells were treated with Triton X-100 for 30 min at 37°C. Plasma membrane integrity was assessed by a modified version of PI fluorometry described by Nieminen *et al.* (1992). Prior to use, the PI stock solution was

diluted to 75 µM in PBS. Following exposure to the test compounds, a 50 µl of PI working solution was added to 200 µl of cells and stained with a final concentration of 15 µM PI for 15 min at 37°C. After staining, medium was discarded and cells washed with 200 µl of PBS, followed by the addition of 100 µl PBS before detecting the fluorescence using a FluoStar Optima at λ_{ex} = 544 nm and λ_{em} = 595 nm.

7.2.3. Statistical analyses

Six independent fluorometry experiments were carried out in duplicate (n=12). Relevant blank values were deducted from all experimental values before observed values were standardised to percentage of controls. Outliers were detected using Grubb's test and removed, before normality of the data distributions were evaluated with the Shapiro-Francia test. Hypothesis testing was then performed utilising either Student's ***t***-tests (normal) or Mann-Whitney tests (non-normal), to determine whether any observable differences between means were statistically significant. Results are presented as Mean ± SEM.

Three additional experiments were carried out in duplicate to assess the possible effects that NAC may have on the pesticide-induced mode of cell death. These results were also standardised to percentage of control but no preliminary tests (Grubb's and Shapiro-Francia) were performed. Mann-Whitney tests were performed due to the small sample size (***n*** **=** 6), no outliers were removed and normality of the data could not be established.

7.3. Results

7.3.1. Assessment of cell death by apoptosis

Analysis confirmed the presence of outliers in the 5 µM groups of both the DDE and DDD data sets, with ***p*** < 0.05 (Table 7.1). Subsequently, these were identified and removed. This

was followed by normality testing, which revealed normal distributions for most of the data except the 5, 10 and 100 µM groups of the DDE data set ($p < 0.05$) (Table 7.2.). Non-normal data was analysed using Mann-Whitney tests.

Table 7.1. Grubb's test results for detecting outliers in Cas-3 data. Values given in the table are *p*-values. Instances where $p < 0.05$ (*) indicates the presence of outliers.

Concentration	DDT	DDE	DDD
Control	0.40	0.78	0.49
5 µM	0.14	0.02*	0.00*
10 µM	0.51	0.46	0.31
50 µM	0.54	0.61	0.20
100 µM	0.44	0.77	0.08
150 µM	0.47	0.27	0.11

Table 7.2. Shapiro-Francia test normality results of the observed Cas-3 data after removal of outliers detected with Grubb's test. Values given in the table are p-values. Instances where $p < 0.05$ are significantly non-normal. * indicates $p < 0.05$.

Concentration	DDT	DDE	DDD
Control	0.74	0.38	0.42
5 µM	0.84	0.05*	0.95
10 µM	0.82	0.02*	0.92
50 µM	0.47	0.04*	0.09
100 µM	0.41	0.18	0.22
150 µM	0.22	0.23	0.57

The positive control (11 µM staurosporine) significantly ($p < 0.001$) induced Cas-3 activity when compared to controls with a mean increase of 97% (Figure 7.1). All the tested concentrations of DDT (5 - 150 µM) were found to significantly ($p < 0.001$) increase Cas-3

activity in a dose-dependent manner, ranging from a 21% increase (5 µM) to a 63% increase (150 µM). DDT-induced Cas-3 activity followed a dose-dependent trend (Figure 7.2 and Table 7.3).

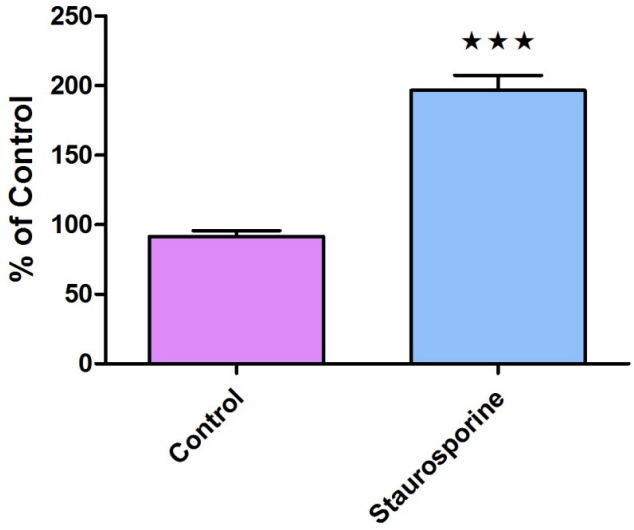

Figure 7.1. **Active caspase-3 in HepG2 cells following 6 h exposure to Control *vs.* Staurosporine (11 µM) (mean ±SEM). Staurosporine significantly induced caspase-3 activity with $p < 0.001$ (***).**

Table 7.3. **Relative Cas-3 activity in HepG2 cells following 6 h exposure to DDT, DDE, DDD and Staurosporine (positive control). Results (% of Control) are presented as mean ±SEM. ** indicates $p < 0.01$ and *** $p < 0.001$ as determined by Mann-Whitney and Student's *t*-tests.**

Concentration	DDT	DDE	DDD	Staurosporine (11 µM)
Control	100± 2	100± 2	100± 2	
5 µM	121± 4***	104± 3	119± 4***	
10 µM	128± 4***	116± 7	119± 5**	197± 11***
50 µM	143± 5***	133± 8***	141± 8***	
100 µM	149± 5***	148± 7***	182± 9***	
150 µM	163± 5***	165± 9***	239± 6***	

DDE affected Cas-3 activity in a dose-dependent manner and was also found to significantly ($p < 0.001$) increase Cas-3 activity. However, DDE was not as potent an inducer as DDT, yielding insignificant increases at the lower concentration range tested (5 - 10 µM). DDE

significantly increased Cas-3 activity at higher concentrations by 34% (50 µM), 49% (100 µM) and 66% (150 µM) (Figure 7.2 and Table 7.3).

At concentrations of 5 - 50 µM, DDD yielded results similar to that of DDT, causing significant ($p < 0.01$) increases in Cas-3 activity of between 20% and 40%. However, at concentrations of 100 and 150 µM, DDD caused highly significantly ($p < 0.001$) elevated Cas-3 activity when compared not only to the controls, but also DDT and DDE. The effect of DDD on Cas-3 activity followed a dose-dependent trend (Figure 7.2 and Table 7.3).

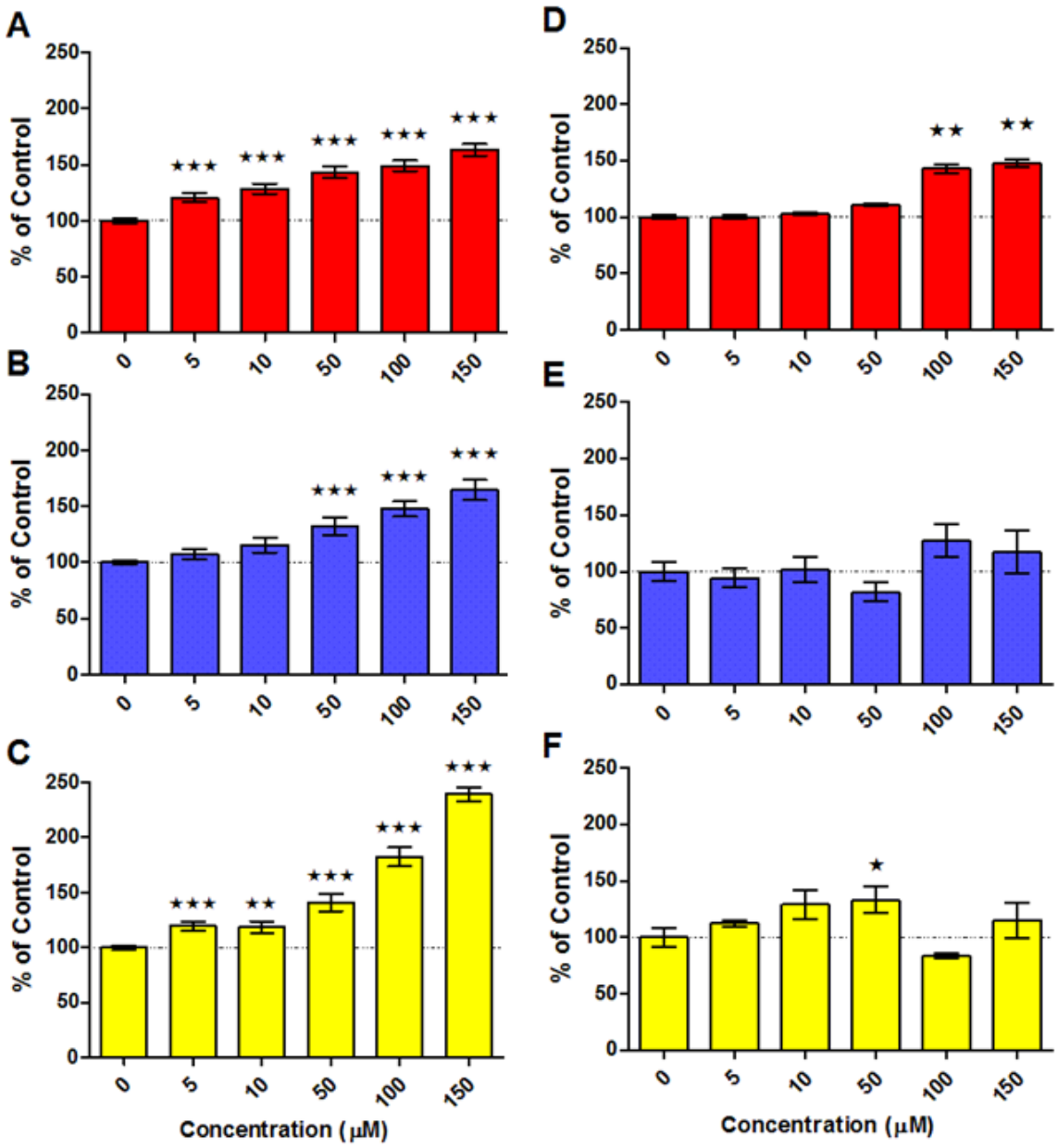

Figure 7.2. Caspase-3 activity in HepG2 cells following 6 h exposure to DDT (A), DDE (B) and DDD (C) (mean ±SEM). Caspase-3 activity was used as a measure of cell death by apoptosis. Graphs (D), (E) and (F) represent the PI staining of cells exposed to DDT, DDE and DDD, respectively. Propidium iodide was used as a measure of membrane integrity and cell death by necrosis. Dashed horizontal lines represent untreated control values. Results are given as mean ± SEM. * indicates $p < 0.05$, ** indicates $p < 0.01$ and *** $p < 0.001$ as determined by Mann-Whitney and Student's *t*-tests, where applicable.

Table 7.4. Relative Cas-3 activity in HepG2 cells after exposure to DDT, DDE, DDD, with or without 1 h pre-treatment with NAC. * = $p < 0.05$, ** = $p < 0.01$, *** = $p < 0.001$ as determined by Mann-Whitney and Student's *t*-tests.

	DDT		DDE		DDD	
	--	NAC	--	NAC	--	NAC
5 µM	121± 4	125 ± 9	104± 3	106 ± 5	119± 4	107 ± 3
10 µM	128± 4	115 ± 6	116± 7	102 ± 4	119± 5	126 ± 17
50 µM	143± 5	121 ± 12*	133± 8	100 ± 5**	141± 8	134 ± 16
100 µM	149± 5	118 ± 12*	148± 7	110 ± 7**	182± 9	166 ± 27
150 µM	163± 5	127 ± 17*	165± 9	118 ± 7**	239± 6	139 ± 16***

Results demonstrate a trend in which NAC pre-treatment significantly reduced the degree of apoptosis induction resulting from exposure to the three test compounds. This is most prominent in DDE results, where NAC pre-treatment reduced Cas-3 activity at concentrations between 50 - 150 µM ($p < 0.01$) (Table 7.4).

7.3.2. Assessment of cell death by necrosis

According to Grubb's test 5 groups out of the 3 data sets included outliers with $p < 0.05$ (5 µM DDT, 10 and 50 µM DDE and 5 and 100 µM DDD) (Table 7.5). Outliers were removed and followed by normality testing, which revealed that all of the data, except the 100 µM group from the DDE data set, was normally distributed. Subsequently all of the data were analysed with Student's *t*-tests except 100 µM DDE, which was compared to controls using the Mann-Whitney test.

Table 7.5. Grubb's test results for detecting outliers in the data from PI staining. Values given in the table are *p*-values. Instances where $p < 0.05$ (*) indicates the presence of outliers.

Concentration	DDT	DDE	DDD
Control	0.19	0.24	0.32
5 µM	0.01*	0.26	0.03*
10 µM	0.70	0.01*	0.07
50 µM	0.33	0.02*	0.69
100 µM	0.33	0.64	0.00*
150 µM	0.13	0.35	0.05

Table 7.6. Shapiro-Francia test normality results of the observed PI data after removal of outliers detected with Grubb's test. Values given in the table are p-values. Instances where $\boldsymbol{p} < 0.05$ are significantly non-normal. * indicates $\boldsymbol{p} < 0.05$.

Concentration	DDT	DDE	DDD
Control	0.68	0.11	0.06
5 µM	0.89	0.78	0.06
10 µM	0.30	0.08	0.88
50 µM	0.54	0.05	0.59
100 µM	0.43	0.05*	0.47
150 µM	0.82	0.15	0.33

Positive controls yielded an expected increase in membrane damage, causing significantly ($\boldsymbol{p} < 0.001$) higher PI staining (755%) than the untreated controls (Figure 7.3). DDT demonstrated significant loss of membrane integrity at higher concentrations (100 and 150 µM), which is indicated by the significantly higher PI staining ($\boldsymbol{p} < 0.01$). This effect followed a dose-dependent trend (Table 7.7).

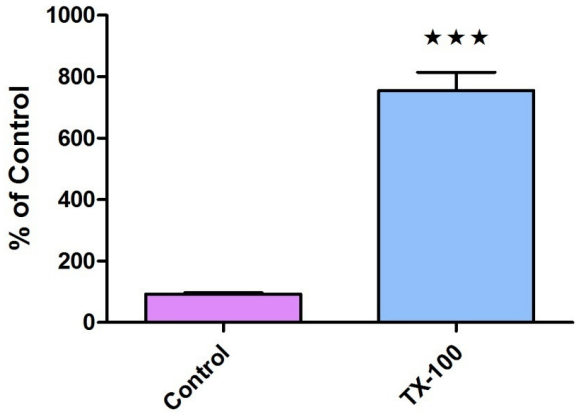

Figure 7.3. Propidium iodide staining as a measure of membrane integrity in HepG2 cells following treatment with 0.5% (v/v) Triton X-100 (TX-100) (mean ±SEM). *** = $p < 0.001$.

DDE did not have any statistically significant effect on PI staining when compared to untreated controls but higher concentrations of 100 and 150 µM did cause a slight increase in PI staining (Table 7.7).

DDD had the largest effect on membrane integrity at the lower concentration range tested increasing PI staining by 13%, 29% and 33% at concentrations of 5, 10 and 50 µM, respectively. However, only the 33% increase proved to be statistically significant. No significant influence was found at 100 and 150 µM of DDD (Table 7.7). Neither DDE nor DDD results followed any dose-response trend.

Table 7.7. PI staining in HepG2 cells following 24 h exposure to DDT, DDE, DDD and Triton X-100 (positive control). Results (% of Control) are presented as mean ±SEM. * indicates $p < 0.05$ and ** $p < 0.01$ as determined by Mann-Whitney tests.

Concentration	DDT	DDE	DDD	Triton X-100 (0.5%)
Control	100± 5	100± 8	100± 8	
5 µM	100± 4	94± 8	113± 9	
10 µM	103± 5	102± 11	129± 12	755± 60***
50 µM	111± 4	82± 8	133± 11*	
100 µM	143± 13**	127± 15	84± 7	
150 µM	148± 13**	117± 19	115± 16	

Table 7.8. PI staining in HepG2 cells due to DDT, DDE, DDD, with or without 1 h pre-treatment with NAC. * indicates $p < 0.05$ as determined by Mann-Whitney tests.

	DDT		DDE		DDD	
	--	NAC	--	NAC	--	NAC
5 µM	100± 4	94 ± 9	94± 8	96 ± 4	113± 9	98 ± 12
10 µM	103± 5	87 ± 9	102± 11	96 ± 10	129± 12	90 ± 10*
50 µM	111± 4	184 ± 41*	82± 8	136 ± 35	133± 11	115 ± 20
100 µM	143± 13	160 ± 16	127± 15	153 ± 48	84± 7	147 ± 28*
150 µM	148± 13	171 ± 23	117± 19	157 ± 51	115± 16	148 ± 14

A general trend can be observed from results where NAC pre-treatment appeared to elevate the number of cells in necrotic cell death exposed to higher concentrations of the test compounds (50 - 150 µM) (Table 7.8 and Figure 7.4).

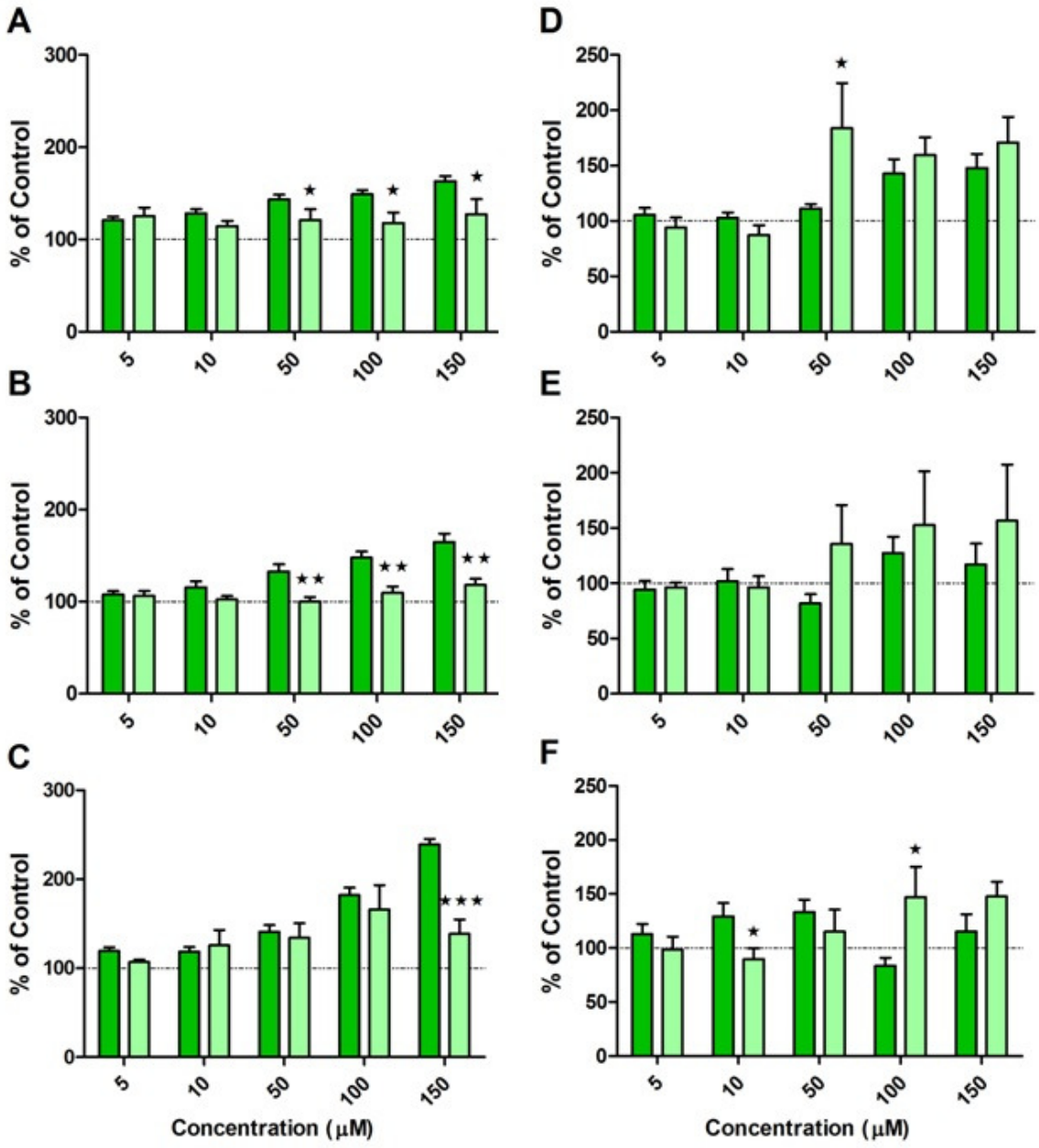

Figure 7.4. Caspase-3 activity in HepG2 cells following 6 h exposure to DDT (A), DDE (B) and DDD (C)(mean ±SEM). Graphs (D), (E) and (F) represent the propidium iodide staining of cells exposed to DDT, DDE and DDD, respectively. Caspase-3 activity and propidium iodide were used as a measure of cell death by apoptosis and necrosis, respectively. Dashed horizontal lines represent Control values. Results are given as mean ± SEM. * indicates $p < 0.05$, ** indicates $p < 0.01$ and *** $p < 0.001$ as determined by Mann-Whitney and Student's *t*-tests, where applicable. Light green bars represent 1 h pre-treatment with NAC as opposed to dark green bars, which received no pre-treatment.

7.4. Discussion

Following the removal of outliers in the Cas-3 data sets with the Grubb's test (Table 7.1), only 3 of the 18 data sets presented non-normal distributions (Table 7.2), indicating good reproducibility for the Cas-3 assay. Regarding the membrane integrity assay, only 1 of the 18 data sets presented with a non-normal distribution (Table 7.6) after removal of the relevant outliers (Table 7.5), showing good assay reproducibility.

All three tested compounds affected HepG2 cells leading to dose-dependent activation of Cas-3, implying activation of the apoptotic pathway. DDT and DDD were more potent than DDE by highly significantly ($\boldsymbol{p} < 0.001$) raising Cas-3 activity beyond baseline (controls) at concentrations as low as 5 µM. Of the three tested compounds, DDD proved to be the most potent, causing significantly more Cas-3 activity than DDT and DDE at concentrations of 100 µM (≈ +30%) and 150 µM (≈ +70%). In terms of potency the following was observed: DDD > DDT > DDE. These results correlate very well with the IC_{50} values determined during the cytotoxicity assay where a similar trend was noted.

Shi *et al.* (2010a) examined apoptosis as a possible mode of cell death of cultured hepatocytes exposed to concentrations of 10 - 100 nM of DDT. During that study the authors did not observe any DDT-induced apoptosis, probably due to a lack of cell death (94% viability). Even if that study did report some apoptotic cell death, with cell viability that high it could have been normal cell attrition and not necessarily DDT-induced. Contrarily, another study did report apoptosis in HepG2 cells exposed to 50 nM of DDT (Filipak Neto *et al.*, 2008). The discrepancy between the results from these two studies could be ascribed to the length of exposure, 24 h (Shi *et al.,* 2010a) versus 96 h (Filipak Neto *et al.*, 2008). In the present study concentrations of 5 - 10 µM were not found to induce toxicity after 24 h exposure, but significantly raised Cas-3 activity. It could be hypothesised that lower concentrations of DDT (that are not necessarily toxic) may cause significant activation of

Cas-3 following longer incubation periods such as those used in the study by Filipak Neta *et al.* (2008)

The fact that DDT is able to induce apoptosis is not confined to the liver alone. It has also been reported to induce apoptosis in human peripheral blood mononuclear cells (Perez-Maldonado *et al.*, 2004), rat thymocytes (Tebourbi *et al.*, 1998) and murine embryos (Greenlee *et al.*, 1999). DDE has also been reported to induce apoptosis in various types of tissues such as peripheral blood mononuclear cells (Perez-Maldonado *et al.*, 2004), rat Sertoli cells (Shi *et al.*, 2009) and cells from the testes of rats exposed *in vivo* (Shi *et al.*, 2010b). DDD-induced apoptosis has only been reported in peripheral blood mononuclear cells (Perez-Maldonado *et al.*, 2004). No literature is available regarding DDE/DDD-induced apoptosis in cultured hepatocytes. From their study on rat Sertoli cells, Shi *et al.* (2009) concluded that exposure to 30 and 50 µM DDE induced apoptosis via the 'extrinsic' apoptotic pathway as indicated by the up-regulation of caspase-8 activated by the Fas receptor. The authors suggested that DDE may have activated the receptor-mediated pathway by activating nuclear factor-κβ, which can exert both pro- and anti-apoptotic effect, depending on the specific cell type as well as the type of inducer. It is therefore possible that the increase in Cas-3 activity observed in the present study could also be due to upstream caspase-8 activation. However, in the liver, nuclear factor-κβ prevents apoptosis and has a positive role in regeneration (Taub, 1998). Also, observations with regard to the mitochondrial membrane potential changes after exposure to the test compounds is suggestive of Cas-3 activation via the 'intrinsic'/mitochondrial-mediated pathway in that all three test compounds (DDT, DDE and DDD) were able to significantly raise $\Delta\psi_m$, which would lead to the release of cyt C from the mitochondria, with subsequent formation of the apoptosome and Cas-3 activation. Further investigations would be necessary to confirm which of the two apoptotic pathways are responsible for the elevated Cas-3 activity after exposure to DDT, DDE and DDD.

No literature could be found with regards to necrotic effects as a result of DDT, DDE or DDD exposure *in vitro*. It would be erroneous to conclude that DDT/DDE/DDD induces cell death

through apoptosis because of a lack of *in vitro* evidence that proves otherwise. A number of previous *in vivo* studies have reported DDT-induced necrosis. DDT, DDE and DDD exposure in chicken embryo neurons *in ovo*, revealed definitive plasma and nuclear membrane damage as visualised using scanning and transmission electron microscopy, from which the authors concluded cell death by necrosis (Bornman *et al.*, 2007). Histological examination of the livers of female rats exposed to 75 and 150 ppm dietary DDT for 36 weeks revealed typical of organ necrosis (Jonsson *et al.,* 1981). In rats exposed to DDT (5 - 500 ppm) for 5 days, histological evaluation of the livers showed cytoplasmic vacuolisation, typical signs of necrosis and no DNA fragmentation, which indicates cell death by necrosis (Kostka *et al.*, 1996; Kostka *et al.*, 1999). Another study reported necrotic cell death and cellular infiltration in livers from rats that were orally exposed to two doses of 150 mg/kg body weight of DDT (Mikhail *et al.,* 1979). These authors also reported mononuclear leukocyte infiltration in the livers of these animals. They suggested that this was indicative of an inflammatory response. Inflammation should not be prevalent in the case of apoptosis because the cytoplasmic contents are contained within apoptotic bodies.

In the present study, treating HepG2 cells with NAC, prior to test compound exposure, significantly decreased the activation of Cas-3 for all three test compounds, indicating a decrease in apoptosis. These findings correlate with literature where NAC is reported to be a broad inhibitor of apoptotic death induced by various *in vitro* stressors (De Flora *et al.*, 2001). However, NAC pre-treatment did not alleviate the cytotoxic effects of any of the test compounds. Therefore, this decrease in Cas-3 activity is expected to translate to increased cell death by necrosis. Results supporting this hypothesis is visualised in Figure 7.4, where significant decreases in Cas-3 activity can be seen for DDT (Figures 7.4.A), DDE (Figure 7.4.B) and DDD (Figure 7.4.C), which are accompanied by corresponding increases in PI fluorescence representing necrotic death for DDT (Figure 7.4.D), DDE (Figure 7.4.E) and DDD (Figure 7.4.F). The decrease in test compound-induced Cas-3 activity due to NAC treatment may be explained by the stabilising effects that NAC pre-treatment had on the $\Delta\psi_m$, as transient mitochondrial hyperpolarisation is an early event preceding Cas-3 activation and membrane phosphatidylserine externalization (Nagy *et al.*, 2007).

Literature describing apoptotic death due to DDT exposure tends to originate from *in vitro* studies, whereas necrotic effects have been reported from *in vivo* studies. A possible explanation as to why DDT-induced apoptotic death has not been described *in vivo* may be the fact that it is difficult to detect apoptosis *in vivo*. The difficulty in detecting apoptosis *in vivo* has been attributed to the fast endogenous clearance of apoptotic cells from an organism (Zhang *et al.*, 2000; Nyati *et al.*, 2006). In the present study the *in vitro* tests were able to detect necrosis due to DDT exposure but not when cells were exposed to DDE and DDD. DDE and DDD results were inconsistent, not presenting any predictable dose-response trends. This is likely to be the result of experimental procedures like wash steps, aimed at reducing background fluorescence. During these wash steps necrotic cells may have been lost when aspirating the supernatant, even though particular care was taken to try and avoid this.

In summary, there seems to be no clear distinction between which mode of cell death leads to the loss of viability due to either DDT, DDE or DDD exposure since evidence exists that supports both pathways. The inflammatory response seen *in vivo* appears the most convincing, which is indicative of necrosis.

It has been reported that a switch can take place from apoptosis to necrosis due to inactivation of caspases by ROS (Samali *et al.*, 1999; Prabhakaran *et al.*, 2004). In the present study Cas-3 activity was detected after 6 h and membrane integrity was assessed after 24 h. It is therefore possible (but unlikely) that DDT may induce activation of Cas-3 but that cell death eventually occurs due to necrosis after 24 h because of Cas-3 inactivation by CYP1A1-generated ROS. The fact that DDT may inhibit ATP-synthase provides further support for this theory as apoptosis is an energy-dependent mode of death and a loss of cellular ATP would preferentially lead to cell death by necrosis, which is the hepatocyte mode of death reported *in vivo*. However, this is disputable as no test compound-induced ROS generation was observed in the present study.

Chapter 8: Concluding discussion

8.1. Procedure summary

The procedure developed during the present study aimed at miniaturising six different *in vitro* assays to be run simultaneously on a single 96 well microplate. Aspects of cellular physiology that were measured include:

- Cell viability
- CYP1A1 activity
- ROS generation
- Mitochondrial homeostasis
- Mode of cell death (apoptosis *vs*. necrosis)

Test compound exposure times for the different assays differed according to the response being measured. Cell viability, CYP1A1 activity and necrotic cell death was measured after 24 h exposure, whereas apoptotic cell death, ROS generation and mitochondrial effects were measured after exposure periods of 6 h, 3 h and 1 h, respectively. In order to perform all six assays on a single microplate, assay initiation had to be staggered, which added to the complexity of the procedure. The entire procedure, from when the first exposure starts, to obtaining the final raw data, took approximately 3 days to complete. This is considerably faster than performing each assay separately. In addition, this method yields results that are truly comparable as the experimental conditions are exactly the same for assays that are conducted on the same plate.

8.2. Test compound mechanism of toxicity

All three test compounds, DDT, DDE and DDD, proved to be cytotoxic. Following 24 h exposure DDT, DDE and DDD yielded IC_{50} values of 54 µM, 64 µM and 44 µM, respectively. Although limited literature is available on the *in vitro* hepatotoxicity, specifically for HepG2 cells, using DDT and none for the known metabolites, DDE and DDD the results from the present study correlates well with two previous studies in that the same threshold value for the onset of DDT-induced toxicity was observed; one on the same cell line (Medina-Diaz & Elizondo, 2005) and the other in a breast carcinoma cell line (Diel *et al.,* 2002).

Cyp1a1 is one of the gene batteries, whose induction is mediated by AhR through a cascade of events known as the AhR signalling pathway (Nebert *et al.*, 2000). In this classic signalling model, inactive AhR is bound to a heat shock protein (HSP90) chaperone within the cytosol. Upon ligand binding, dissociation from HSP90 takes place and activated AhR translocates into the nucleus, where the AhR can dimerise with its transcriptional partner, the Arnt. Within the nucleus, the AhR/Arnt heterodimer binds to the xenobiotic response element (XRE), leading to the transcriptional up-regulation of genes such as *cyp1a1*, which encodes the xenobiotic metabolising enzyme CYP1A1 (Nukaya *et al.*, 2010). Results from the present, and other studies (Dehn *et al.*, 2005), suggest that DDT is capable of up-regulating CYP1A1 activity. Both DDE and DDD were also capable of inducing CYP1A1 activity, which is expected as all three compounds are similar in structure. From a structural point of view CYP1A1 inducers have been classified into three groups (Navas *et al.*, 2004):

(1) Compounds having at least two aromatic rings in a plane, with a very low conformational mobility. This is the case of 2,3,7,8-tetrachlorodibenzo-*p*-dioxin (TCDD) (Safe, 1995). This compound is considered a typical AhR ligand and CYP1A1 inducer (Navas *et al.*, 2003).

(2) Molecules with conformational mobility i.e. they exist in a variety of conformers that are separated by small energy differences so that the inter-conversion between them can be readily achieved. These compounds have been described as low affinity AhR ligands and CYP1A1 inducers (Anderson *et al.*, 1996).

(3) Compounds having at least two aromatic rings linked by a sp3 carbon in their structure. Due to steric requirements of the tetrahedral carbon atom, the conformations having two aromatic rings in the same plane are energetically unfavourable.

From this classification, CYP1A1-inducing compounds are expected to have defined structures capable of binding the AhR. DDT has two aromatic rings, linked by a sp3 carbon, which would place it in the third group of Navas' classification. However, high affinity of the AhR for DDT is unlikely as the two aromatic rings in the structure of DDT are not in the same plane (Figure 8.1). DDT may also fall into the second classification as each of the two chlorobenzene rings are able to rotate around their respective single bonds with the C2 carbon allowing some degree of conformational mobility.

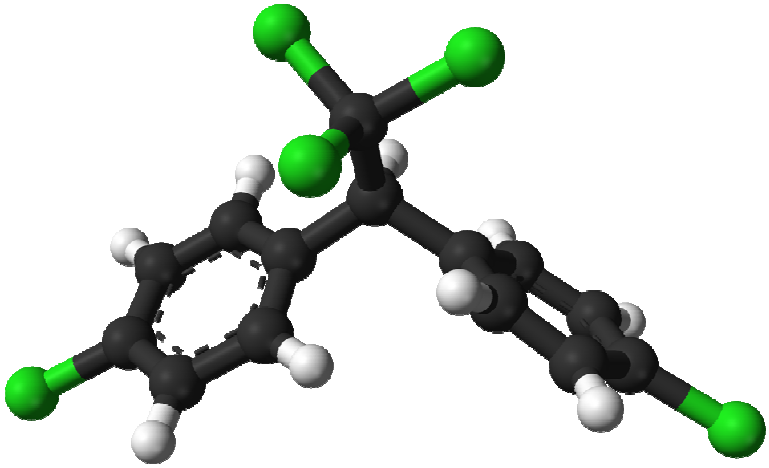

Figure 8.1. Illustration of the three dimensional structure of DDT demonstrating the two aromatic rings, which are not within the same plane (Wikipedia, 2011).

Another unlikely, but possible, explanation for how CYP1A1 was activated by the three test compounds without them binding to AhR may be that the three test compounds may cause weakening of the interactions between AhR and HSP90, facilitating dissociation of cytosolic AhR from its HSP90 chaperones thus activating AhR, which allows it to dimerise with Arnt leading to transcriptional up-regulation (Ledirac *et al.,* 1997).

Exactly how the test compounds may have up-regulated CYP1A1 activity in not known. Nonetheless, up-regulation of this enzyme has been associated with ROS generation (Schlezinger *et al.*, 2000) and DNA damage (Lin *et al.*, 2008). However, ROS evaluation revealed that no ROS generation occurred due to exposure to any of the test compounds under the test conditions (Figure 5.4.). This suggests that if toxicity was due to CYP1A1 up-regulation, it could result in subsequent DNA damage. DDT-induced DNA damage has been reported in peripheral blood mononuclear cells (Yanez *et al.*, 2004; Gajski *et al.*, 2007) and it is well established that DNA damage can result in cell death through apoptosis due to the action of p53 (Bhana and Lloyd, 2008). Activation of p53 leads to the up-regulation or post-translational modification of BH 3-only proteins such as Puma (*p53* up-regulated modulator of apoptosis), which results in apoptosis via the intrinsic apoptotic pathway (Coultas and Strasser, 2003). However, BH 3-only mediated apoptosis is reported to be caspase independent (Coultas and Strasser, 2003) and from the *in vitro* model it was evident that apoptosis was induced via Cas-3 activation, implicating a mechanism of toxicity that is independent of p53 activation and therefore not initiated by DNA damage. These findings indicate that although CYP1A1 was up-regulated by all three test compounds, CYP1A1 was not directly responsible for cell death resulting from to excessive ROS generation, as no ROS were detected. Cell death was also unlikely to have been initiated by DNA damage because Cas-3 was activated, reducing the possibility of apoptosis induction by the caspase-independent BH 3-only proteins.

None of the tested compounds elevated intracellular ROS levels at any of the tested concentrations over a 14 h exposure period. The lack of detectable concentrations of ROS makes this route of cell death unlikely.

Results from the mitochondrial assays showed that all three test compounds were potent inducers of mitochondrial hyperpolarisation, which has been described as an early apoptotic event (Matsuyama *et al.*, 2000). Observed elevations in $\Delta\psi_m$ may be due to inhibition of ATP-synthase (Younis *et al.*, 2002), intracellular GSH depletion (Nagy *et al.*, 2007) or a combination of both. Very recently, it was demonstrated that activated AhR can modulate

mitochondrial function by interacting with the ATP5α1 subunit of the ATP-synthase enzyme, which plays a major role in oxidative phosphorylation (Tappenden *et al.*, 2011). The authors demonstrated that the degree of TCDD-induced mitochondrial hyperpolarisation was not only dependent on the concentration of TCDD but also on the degree of AhR expression in different perpetual cell lines. It is therefore possible that DDT and its metabolites may have induced mitochondrial hyperpolarisation by activating AhR. However, this is unlikely for the following reasons:

(1) Structurally, the test compounds are unlikely to bind to the AhR.

(2) Although NAC pre-treatment counteracted pesticide-induced changes in $\Delta\psi_m$, it did not result in any major changes in test compound-induced CYP1A1 induction.

All three test compounds significantly induced Cas-3 activity in a dose-dependent manner, indicative of apoptotic death. In terms of potency of inducing apoptosis, the test compounds can be ranked as follows: DDD > DDT > DDE. These results correlate very well with the IC_{50} values determined, where, in terms of cytotoxicity, the same ranking was observed: DDD (44 µM) > DDT (54 µM) > DDE (64 µM). Results from NAC pre-treated cells, suggest a switch in mode of cell death from apoptosis to necrosis as Cas-3 activity was significantly decreased with a corresponding increase in PI staining, indicative of necrotic cell death pathway. These findings, coupled with those from $\Delta\psi_m$ experiments, suggest that the Cas-3 activity was possibly the result of mitochondrial hyperpolarisation as NAC was able to decrease test compound-induced changes in both $\Delta\psi_m$ and Cas-3 activation.

In conclusion, results from the developed *in vitro* assay method suggest that all three toxic test compounds, DDT, DDE and DDD, induced cell death *in vitro* in HepG2 cells, after 24 h exposure, by inducing mitochondrial hyperpolarisation, which in turn resulted in Cas-3 activation, with subsequent apoptotic death (Figure 8.2).

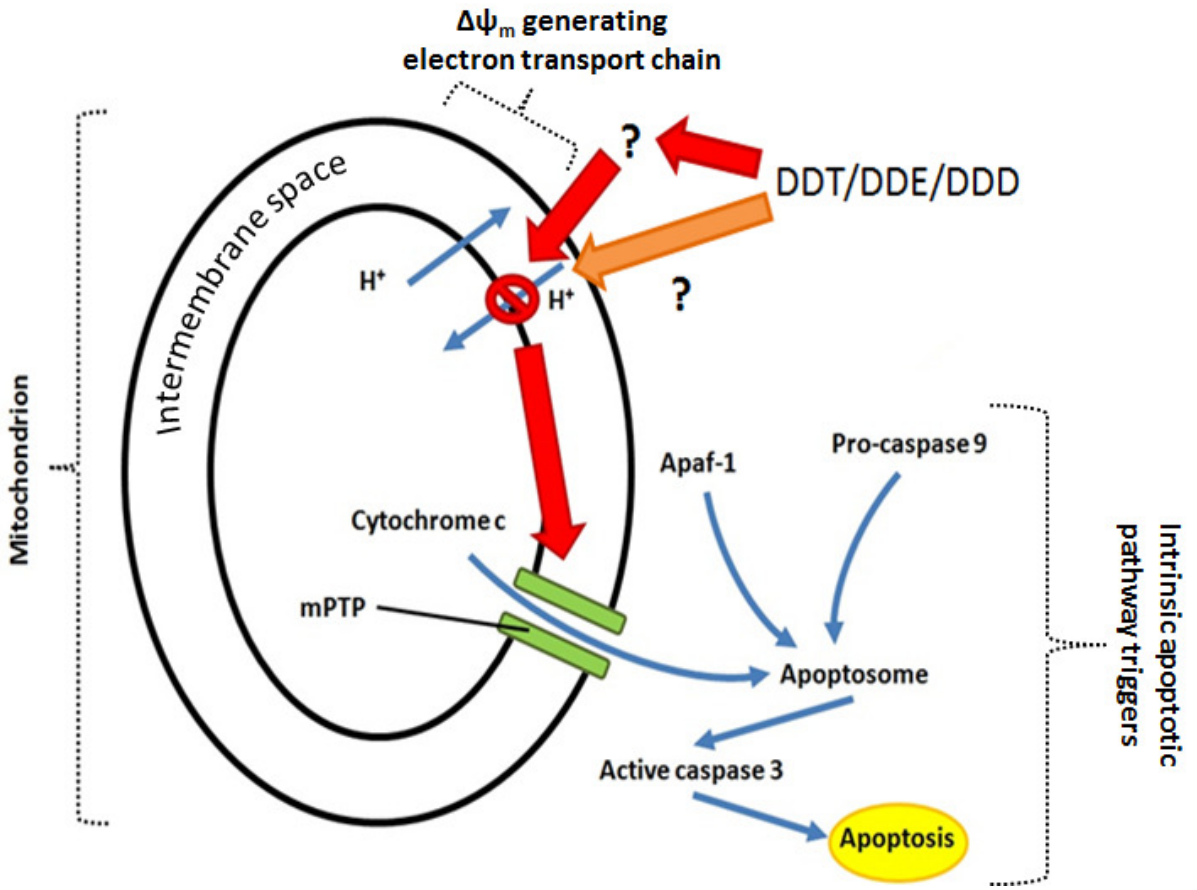

Figure 8.2. **Hypothetical mechanism of the acute toxicity of DDT, DDE and DDD in HepG2 cells after 24 h exposure to 5 - 150 μM of test compound. At high toxin concentrations (> 50 μM), the test compounds inhibit ATP synthase either directly or through some unknown mechanism(s). In turn, this elevates $\Delta\psi_m$, resulting in opening of the mPTP and cyt C release. In the cytosol, cyt C associates with Apaf-1 and pro-caspase 9 to form the apoptosome, which in turn activates Cas-3, leading to cell death by apoptosis. mPTP = mitochondrial permeability transition pore; Apaf-1 = apoptotic protease activating factor-1; $\Delta\psi_m$ = mitochondrial membrane potential.**

8.3. Advantages of the *in vitro* model

Human *in vitro* cellular models constitute valuable tools to understand the molecular and cellular processes of drug-induced liver injury (Gomez-Lechon *et al.*, 2010a). The present study aimed at developing an *in vitro*-based multiparametric screening assay, in an attempt to detect hepatotoxicity manifesting in various ways. Apart from the role this model can play in compound prioritisation and optimisation during drug development, it could enable researchers to gain some insight into the possible mechanism(s) of toxicity of a particular

compound and provide direction to further in-depth toxicity studies, demonstrating a possible role in drug development, especially in light of the three R's of animal testing: replacement, reduction and refinement.

Although this *in vitro* model was not able to pinpoint the mechanism of toxicity of the test compounds, it did identify mitochondrial hyperpolarisation as a key event that could lead to apoptotic cell death. No direct evidence was produced, but the possibility exists that this hyperpolarisation may be the result of GSH depletion without ROS generation. Further studies are needed to confirm this and, if true, determine the mechanism by which the test compounds deplete GSH.

It should be noted that the results presented in this study could be obtained within three weeks, highlighting the efficiency of the model in rapidly accumulating large quantities of cytotoxic and mechanistic data. Apart from being fast the model has a number of advantages over conventional toxicity testing:

(1) Time and infrastructure efficient
(2) Requires small quantities of test material
(3) Requires relatively few HepG2 cells, all from the same batch
(4) Assesses a broad scope of toxicity, under the same conditions
(5) It produced truly comparable data

Probably the greatest advantage of this model is listed as the 5th advantage above: the fact that results obtained from the different assays are truly comparable in that they originate from the same microplate, implying that all the assays are performed on the same passage of cells, with the same plating conditions, monitored on the same day using the same instrument. This would eliminate a considerable amount of variability that may otherwise be unavoidable.

8.4. Further development of the *in vitro* model

This proof-of-concept was successful in establishing a foundation from which further development of this model can be conducted. One of the aspects of the model that may be improved upon would be the ROS generation assay. It may be advantageous to replace the DCFDA assay with one that evaluates intracellular GSH levels rather than looking at ROS generation for two reasons: First, DCFDA only detects H_2O_2 (Gomes *et al.*, 2005), limiting the degree to which ROS generation can be assessed. Secondly, if the levels of ROS generated by a particular compound are sufficient to induce an intracellular oxidative state, it may also present as decreased levels of GSH, further increasing the chances of detecting hepatotoxic insult. Therefore, introducing a GSH assay should improve the scope of the model.

The second aspect that may be improved upon is the membrane integrity assay used to measure necrotic cell death. The method used in the present study did not produce the desired dose-dependent trends for all of the test compounds. There are other assays that rely on the same principle to evaluate a different endpoint. The LDH assay is used to determine cytotoxicity. Although this assay is not classically used to quantify necrosis, it indirectly assesses membrane integrity through measuring the leakage of LDH from cells (McKarns *et al.*, 1997). For this reason, it may be beneficial to evaluate whether or not the LDH assay can be used to quantify necrotic cell death in a microplate setup. If it proves to be successful, it can be compared to the assay used in the present study in the hope of obtaining a more accurate 'necrosis assay', which can then replace the present one.

In terms of performing the work, something that stood out was the complexity of performing this procedure. The procedure will benefit from simplification i.e. assays with fewer steps and more assays with similar exposure times. As this procedure comprises a number of individual assays, the ideal individual assay that would be conducive to this type of procedure would be an assay that:

(1) Utilises fluorescence detection to measure the endpoint

(2) Is started after exposure to the test compound

(3) Does not include any wash steps

(4) Is inert to the test compound

It may be difficult to find an assay for each parameter that satisfies all of the above-mentioned prerequisites and some compromises will have to be made.

Once these issues have been addressed, the predictive power of the model can be evaluated by accumulating data on various known hepatotoxins with different mechanisms of toxicity. A number of mathematical prediction models will then be able to be applied to the acquired data and the ability of each to accurately predict, for instance, known *in vivo* LD_{50}s or human lethal doses, can be determined.

To improve the predictive power of the model, it would probably be best to avoid the loss of assay signal, which occurred with CYP1A1 activity, where toxic concentrations of test compound induced cell death to such an extent that the CYP1A1 induction of the test compounds could not be detected any longer. This may be accomplished by lowering the tested concentration range to one that would provide more 'linear' data. In this regard 'linear' refers to data that follows a linear dose-response i.e. increasing concentration would be associated with linear dose-response, implying the use of sub-toxic concentrations (at least sub-IC_{50}) of test compound. It might also be advantageous to lengthen the toxin exposure period, which may improve assay signal/background ratios.

8.5. In conclusion

The present study set out to develop a method that can simultaneously assess a wide range of toxicity on a single 96 well microplate by measuring the effects of the known hepatotoxin DDT (and its metabolites DDE and DDD) on different parameters of cellular physiology. Furthermore, this type of cell-based procedure provides valuable mechanistic data that could direct future research into the exact mechanism(s) of toxicity of each of the test compounds. The procedure included, fundamentally, parameters suggested by the EMEA for assessing hepatotoxicity: cell viability, phase I metabolism, oxidative stress, mitochondrial homeostasis and mode of cell death (apoptosis *vs.* necrosis). Established *in vitro* assays were used to evaluate the different parameters. In order to miniaturise the relevant assays onto a single microplate required staggering of the assays in such a way that most of the endpoints can be measured at the same time. Some assay optimisation was performed to improve assay sensitivity and data quality. In addition to the test compounds, the method was tested with a known hepatoprotective agent (NAC) to evaluate the ability of the method to detect hepatoprotection. The complexity of the method was more than desired. However, this was superseded by the amount of results that were obtained in a short period of time i.e. the method was found to be highly time and infrastructure efficient. Other advantages of the method were the small amounts of test material required and relatively few cells, which makes it conducive to scalability for the purposes of higher throughput screening platforms. Although the complexity of the method does not yet allow up-scaling, it lays a solid foundation from which further method optimisation can be conducted that is directed at scalability. The quality of the obtained data was of a good standard, with small error margins and predictable dose-dependent trends in most cases. Probably the greatest advantage of this method is that data obtained from this procedure is truly comparable in that all of the assays were subjected to the same conditions and were performed on the same passage of cells, in the same plate. In conclusion, the study aims and objectives were achieved and opened the door to exciting new opportunities in further development of this method.

Annexure A: Ethical approval

UNIVERSITEIT VAN PRETORIA
UNIVERSITY OF PRETORIA
YUNIBESITHI YA PRETORIA

Faculty of Health Sciences Research Ethics Committee

DATE: 23/06/2011

TO:
Prof V Steenkamp
Dept of Pharmacology

Best Prof V Steenkamp

RE.: Commercial Lines: The use of Commercial lines ~ Mr J J van Tonder

During the meeting held on 22/06/2011, the use of Commercial Lines were discussed.

The Faculty of Health Science Ethics Committee approved the use of the cell lines for the various assays.

With regards

Dr R Sommers; MBChB; MMed (Int); MPharMed.
Deputy Chairperson of the Faculty of Health Sciences Research Ethics Committee, University of Pretoria

♦Tel:012-3541330 ♦Fax:012-3541367 / 0866515924 ♦E-Mail: manda@med.up.ac.za
♦Web: //www.healthethics-up.co.za ♦H W Snyman Bld (South) Level 2-34 ♦P.O.BOX 667, Pretoria, S.A., 0001

MS: dd 2011/06/13: C:\Documents and Settings\user\My Documents\A Letter\z-Commercial Cell Lines\Cell Lines-nTonder 5-2011.doc

Annexure B: Reagents

Bovine foetal calf serum (FCS)

FCS was procured from PAA (Pasching, Austria). Any host serum complement that may have been present was inactivated prior to use by incubation at 56□C for 45 min (Soltis *et al.*, 1979). This was added to cell culture media to a concentration of 10%.

Penicillin/streptomycin

A solution containing 10 000 U of penicillin and 10 000 µg streptomycin per millilitre was supplied by BioWhittaker (Walkersville, USA). This was added to the culture medium to a concentration of 1%.

Eagle's Minimum Essential Medium (EMEM)

EMEM powdered medium was purchased from Sigma-Aldrich (St Louis, USA). A mass of 48 g of medium powder was dissolved in 5 l sterile, deionised water. To this solution 11 g of sodium bicarbonate was added to adjust the pH to 7.4. The solution was filter sterilized twice using 0.22 µm cellulose acetate filters, dispensed into sterile 500 ml bottles, supplemented with 1% penicillin/streptomycin and stored at 4°C.

Medium was fortified with 10% (v/v) FCS prior to use.

Phosphate buffered saline (PBS)

PBS powder was obtained from BD Biosciences (Sparks, USA). A solution containing 9.23 g/l of purchased PBS powder in de-ionised water was prepared and stored at 4°C until use. Prior to use, the solution was filter-sterilised through a 0.22 µm pore size filter.

Trypsin/Versene

A trypsin/versene solution containing 0.25% (w/v) trypsin and 0.1% (w/v) ethylenediaminetetraacetic acid (EDTA) in Ca^{2+} and Mg^{2+} free PBS was obtained from Highveld Biological (Johannesburg, RSA) and stored at 4°C.

Dimethyl sulfoxide (DMSO)

DMSO was procured from Sigma-Aldrich (St Louis, USA) and used undiluted.

Trypan blue counting solution

Trypan blue in powder form was purchased from BDH Laboratories Supplies (UK). Powder (200 mg) was dissolved in 50 ml PBS to obtain a 0.4% (w/v) solution, which was then filtered through a 0.45 µm syringe filter to remove any insoluble particles.

Culturing consumables

Cellstar tissue culture flasks (25 cm^2 and 75 cm^2) were purchased from Greiner BioOne (Austria). For experimental assays, 96 well sterile white plates suitable for fluorescence were used (Nunc, Denmark).

Hepatotoxins

DDT, DDE and DDD were purchased from Supelco Analytical (Bellefonte, USA). Stock solutions (30 mM) of each toxin was prepared in DMSO and stored at -70°C.

Hepatoprotective agent

NAC was purchased from Sigma-Aldrich (St Louis, USA). A 30 mM stock solution was prepared in DMSO and stored at -70°C.

Neutral red dye

Neutral red dye was purchased from Sigma-Aldrich (St Louis, USA) and prepared fresh prior to use. The dye was made up to a final concentration of 100 µg/ml in EMEM, without FCS. To aid solubility, the solution was sonicated for 1 min, after which the pH was adjusted to 6.4 using 5 M KH_2PO_4 (Merck , Darmstadt, Germany).

Neutral red elution buffer

Elution buffer, used to dissociate bound dye, contained ethanol (Ilovo, Durban, RSA), acetic acid (Merck, Darmstadt, Germany) and distilled water in a ratio of 50:1:49 (v/v/v), respectively.

7-Ethoxyresorufin

7-Ethoxyresorufin (7-ER), NADPH and omeprazole were purchased from Sigma-Aldrich (St Louis, USA). A 100 µM 7-ER stock solution was prepared in 100% methanol. Aliquots were stored at -70°C. NADPH working solution was prepared fresh in PBS prior to use.

Omeprazole

Omeprazole stock solution (30 mM) was prepared in DMSO. Aliquots were stored at -70°C.

2',7'-Dichlorofluorescein diacetate (DCFDA)

DCFDA in powder form was procured from Sigma-Aldrich (St Louis, USA). A 1 mg/ml stock solution (2 mM) was prepared in methanol (Merck, Darmstadt, Germany) and stored at -20°C. Prior to use, the stock solution was diluted to 20 µM in PBS, 40 µl of which was added to 100 µl of medium to obtain a final concentration of 5.7 µM in each of the relevant wells.

2',2'-Azobis(2-methylpropionamidine) dihydrochloride (AAPH)

AAPH in powder form was purchased from Sigma-Aldrich (St Louis, USA). An 8 mg/ml stock solution (30 mM) was prepared in DMSO and stored at -70°C. Prior to use, the stock solution was diluted to 300 µM in PBS, 50 µl of which was added to 50 µl of PBS in each well to obtain a final concentration of 150 µM.

JC-1

JC-1 in powder form was purchased from Sigma-Aldrich (St Louis, USA). A 1 mM stock solution was prepared in DMSO and stored at -70°C. Prior to use, the stock solution was diluted to 20 µM in EMEM. Of this working solution a 100 µl was added to the relevant wells to load cells prior to exposure. Cells were loaded in a final concentration of 10 µM for 30 min at 37°C.

Tamoxifen

Tamoxifen, which causes mitochondrial membrane hyperpolarisation in HepG2 cells, was used as positive control (Donato *et al.*, 2009). Tamoxifen citrate in powder form was obtained from Sigma-Aldrich (St Louis, USA). A 30 mM stock solution was prepared in DMSO and stored at -70°C. Prior to use, the stock solution was diluted to 300 µM in PBS of which 50 µl was added to 50 µl of PBS to obtain a final concentration of 150 µM in each well.

Propidium iodide (PI)

PI in powder form was purchased from Sigma-Aldrich (St Louis, USA). A 3 mM stock solution was prepared in PBS and stored at 4°C.

t-Octylphenoxypolyethoxyethanol (Triton X-100)

Triton X-100 in liquid form was obtained from Sigma-Aldrich (St Louis, USA). Prior to use, Triton X-100 was diluted to 1% (v/v) in EMEM and stored at 4°C.

Caspase assay lysis buffer (pH 7.4)

The lysis buffer consisted of 10 mM 2-[4-(2-hydroxyethyl)piperazin-1-yl]ethanesulfonic acid (HEPES), 2mM 3-[(3-Cholamidopropyl)dimethylammonio]-1-propanesulfonate (CHAPS), 5 mM ethylenediaminetetraacetic acid (EDTA), 5 mM phenylmethylsulfonyl fluoride (All purchased from Sigma Aldrich, St Louis, USA) and 5 mM β-mercaptoethanol (Merck, Darmstadt, Germany). Phenylmethylsulfonyl fluoride and β-mercaptoethanol were added 30 min prior to use of the buffer.

Caspase assay buffer (pH 7.4)

The buffer consisted of 20 mM HEPES, 2 mM EDTA, 5 µM Cas-3-specific substrate coupled to a fluorescent probe (Acetyl-Asp-Glu-Val-Asp-7-amino-4-methylcoumarin (Ac-DEVD-AMC)) (All purchased from Sigma Aldrich, St Louis, USA) and 5 mM β-mercaptoethanol (Merck, Darmstadt, Germany). β-mercaptoethanol was added 30 min and Ac-DEVD-AMC immediately prior to initiating the assay.

Staurosporine

Staurosporine in powder form was purchased from Sigma-Aldrich (St Louis, USA). A 1 mg/ml (2.14 mM) stock solution was prepared in DMSO and stored at -70°C. Prior to use, the stock solution was diluted into EMEM to obtain a 21 µM working solution, which yielded a final concentration of 11 µM in the assay well.

Annexure C: Research outputs

National conference presentation:

Van Tonder JJ, Cromarty AD, Gulumian M, Steenkamp V. Development of an *in vitro* toxicity screening model using hepatocytes. South African Congress of Pharmacology and Toxicology, Cape Town. 3-6 October 2010. (Oral presentation)

International conference presentation:

Van Tonder JJ, Cromarty AD, Gulumian M, Steenkamp V. A microplate method for multiparametric hepatotoxicity screening. 6th International Conference of Pharmaceutical and Pharmacological Sciences. Durban, South Africa, 25-27 September 2011. (Oral presentation)

References

Abboud G, Kaplowitz N. (2007) Drug-induced liver injury. Drug Saf 30: 277-94.

Alberts B, Johnson A, Lewis J, Raff M, Roberts K, Walter P. (2002) The molecular biology of the cell. Garland Science, New York.

Alexandre E, David P, Viollon C, Wolf P, Jaeck D, Azimzadeh A, Nicod L, Boudjema K, Richert L. (1999) Expression of cytochromes P-450 2E1, 3A4 and 1A1/1A2 in growing and confluent human HepG2 hepatoma cells - Effect of ethanol. Toxicology in Vitro 13(3):427-435.

Anderson MJ, Miller MR, Hinton DE. (1996) In vitro modulation of 17-b-estradiol induced vitellogenin synthesis: effects of cytochrome P4501A1 inducing compounds on rainbow trout (Oncorhynchus mykiss) liver cells. Aquatic Toxicology 34 (4): 327-350.

Androutsopoulos VP, Tsatsakis AM, Spandidos DA. (2009) Cytochrome P450 CYP1A1: wider roles in cancer progression and prevention. BMC Cancer 9:187-203.

Atkuri KR, Mavtovani JJ, Herzenberg LA, Herzenberg LA. (2007) *N*-Acetylcysteine – a safe antidote for cysteine/glutathione deficiency. Current Opinion in Pharmacology 7: 355-359.

Attaran A, Maharaj R. (2001) Doctoring malaria, badly: the global campaign to ban DDT. British Medical Journal 321: 1403-1405.

Baiden F, Owusu-Agyei S, Webster J, Chandramohan D. (2010) The need for new antibiotics. The Lancet 375(9715): 637-638.

Bagchi D, Hassoun EA, Bagchi M, Stohs SJ. (1993) Protective effects of antioxidants against endrin-induced hepatic lipid peroxidation, DNA damage, and excretion of urinary lipid metabolites. Free Radical Biology and Medicine 15(2):217-222.

Bagchi D, Bagchi M, Hassoun EA, Stohs SJ. (1995) In vitro and in vivo generation of reactive oxygen species, DNA damage and lactate dehydrogenase leakage by selected pesticides. Toxicology 104(1-3):129-140.

Ballet F. (1997) Hepatotoxicity in drug development: detection, significance and solutions.Journal of Hepatology 26 Supplement 2: 26-36.

Banic B, Nipic D, Suput D, Millisav I. (2011) DMSO modulates the pathway of apoptosis triggering. Cellular and Molecular Biology Letters 16(2): 328-341.

Barbouti A, Doulias PT, Nousis L, Tenopoulou M, Galaris D. (2002) DNA damage and apoptosis in hydrogen peroxide-exposed jurkat cells: Bolus versus continuous generation of H_2O_2. Free Radical Biology & Medicine 33: 691-702.

Barouki R, Morel Y. (2001) Repression of cytochrome P450 1A1 gene expression by oxidative stress: mechanisms and biological implications. Biochemical Pharmacology 61: 511-516.

Baudoin R, Corlu A, Griscom, L, Legallais C., Leclerc E. (2007) Trends in the development of microfluidic cell biochips for in vitro hepatotoxicity. Toxicology In Vitro 21(4): 535-544.

Bhana S, Lloyd DR. (2008) The role of p53 in DNA damage-mediated cytotoxicity overrides its ability to regulate nucleotide excision repair in human fibroblasts. Mutagenesis 23(1): 43-50.

Bornman MS, Pretorius E, Marx J, Smit E, van der Merwe CF. (2007) Ultrastructural Effects of DDT, DDD, and DDE on Neural Cells of the Chicken Embryo Model. Toxicology 22: 328-336.

Brand MD, Chien LF, Ainscow EK, Rolfe DFS, Porter RK. (1994) The causes and functions of mitochondrial proton leak. Biochimica et Biophysica Acta 1187: 132-139.

Brini M. (2003) Ca^{2+} signalling in mitochondria: mechanism and role in physiology and pathology. Cell Calcium 34: 399-405.

Bussolaro D, Neto FF, Ribeiro CAO. (2010) Responses of hepatocytes to DDT and methyl mercury exposure. Toxicology in Vitro 24: 1491-1497.

Butterworth BE, Popp JA, Conolly RB, Goldsworthy DL. (1992) Chemically-induced cell proliferation in carcinogenesis.Mechanisms of Carcinogenesis in Risk Identification. IARC Scientific Publication No. 116: 279-305.

Carambula SF, Matikainen T, Lynch MP, Flavell RA, Dias Gonc Alves PB, Tilly J, Rueda BR. (2002) Caspase-3 Is a Pivotal Mediator of Apoptosis during Regression of the Ovarian Corpus Luteum. Endocrinology 143(4): 1495-1501.

Castell JV, Gomez-Lechin MJ, Ponsoda X, Bort R. (1997) In vitro investigation of the molecular mechanisms of hepatotoxicity. Archives of Toxicology S19: 313-321.

Carageorgiou H, Tzotzes V, Pantos C, Mourouzis C, Zarros A, Tsakiris S. (2004) *In vivo* and *in vitro* effects of cadmium on adult rat brain total antioxidant status, acetylcholine esterase (Na^{+},K^{+})-ATPase and Mg^{2+}-ATPase activities: protection by l-cysteine. Basic Clin Pharmacol Toxicol 94: 112-118.

Cederbaum AI, Lu Y, Wu D. (2009) Role of oxidative stress in alcohol-induced liver injury. Archives of Toxicology 83: 519-548.

Chefurka W. (1983) The effect of DDT and related insecticides on the mitochondrial ATPase of houseflies. Comparative biochemistry and physiology Part C, Comparative pharmacology 74(2): 259-266.

Chen Q, Cederbaum AI. (1998) Cytotoxicity and apoptosis produced by cytochrome P450 2E1 in Hep G2 cells. Molecular Pharmacology53: 638-648.

Chen Z, Maartens F, Vega H, Kunene S, Gumede J, Krieger RI. (2009) 2,2-bis(4-Cholorphenyl)Acetic Acid (DDA), a Water-Soluble Urine Biomarker of DDT Metabolism in Humans. International Journal of Toxicology 28(6): 528-533.

Committee for medicinal products for human use.(2008) Non-clinical guideline on drug-induced hepatotoxicity.Retrieved from: http://www.emea.europa.eu/pdfs/human/swp/15011506en.pdf.

Costantini P, Chernyak BV, Petronilli V, Bernardi P. (1996) Modulation of the mitochondrial permeability transition pore by pyridine nucleotides and dithiol oxidation at two separate sites.Journal of Biological Chemistry 271 (12): 6746-6751.

Coultas, L., Strasser, A. (2003) The role of the Bcl-2 protein family in cancer. Seminars in Cancer Biology 13(2): 115-123.

Dambach DM, Andrews BA, Moulin F. (2005) New technologies and screening strategies for hepatotoxicity: Use of in vitro models. Toxicologic Pathology 33(1): 17-26.

Dashti N, Wolfbauer G, Koren E. (1984) Catabolism of human low density lipoproteins by human hepatoma cell line HepG2. Biochimica et Biophysica Acta - Lipids and Lipid Metabolism 794(3):373-384.

Davila JC, Rodriguez RJ, Melchert RB, Acosta D. (1998) Predictive value of in vitro model systems in toxicology.Annual Review of Pharmacology and Toxicology 38: 63-96.

De Flora S, Izzotti A, D'Adostini F, Balansky RM. (2001) Mechanisms of N-acetylcysteine in the prevention of DNA damage and cancer, with special reference to smoking-related end-points. Carcinogenesis 22(7): 999-1013.

Dehn PF, Allen-Mocherie S, Karek J, Thenappan A. (2005) Organochlorine insecticides: Impacts on human HepG2 cytochrome P4501A, 2B activities and glutathione levels. Toxicology in Vitro 19(2):261-273.

Delescluse C, Ledirac N, de Sousa G, Pralavorio M, Lesca P, Rahmani R. (1998) Cytotoxic effects and induction of cytochromes P450 1A1:2 by insecticides, in hepatic or epidermal cells: binding capability to the Ah receptor. Toxicology Letters 96: 33-39.

Delescluse C, Lemaire G, de Sousa G, Rahmani R. (2000) Is CYP1A1 induction always related to AHR signaling pathway? Toxicology 153: 73-82.

Denison MS, Whitlock JP. (1995) Xenobiotic-inducible transcription of cytochrome P450 genes.The Journal of Biological Chemistry270: 18175-78.

Dickerson RL, McMurry CS, Smith EE, Taylor MD, Nowell SA, Frame LT. (1999) Modulation of endocrine pathways by 4,49-DDE in the deer mouse *Peromyscus maniculatus*. The Science of the Total Environment 233: 97-108.

Diel P, Olff S, Schmidt S, Michna H. (2002) Effects of the environmental estrogens bisphenol A, *o*,*p*_-DDT, *p*–*tert*-octylphenol and coumestrol on apoptosis induction, cell proliferation and the expression of estrogen sensitive molecular parameters in the human breast cancer cell line MCF-7. Journal of Steroid Biochemistry and Molecular Biology 80(1): 61-70.

Dierickx PJ. (1987) Inhibition of glutathione-dependent uridine uptake in cultured human hepatoma cells. Medical Science Research 15(21): 1349-1350.

Donato MM, Jurado AS, Atunes Madeira MC, Madeira VMC. (1997) Comparative Study of the Toxic Actions of 2,2-Bis- (*p*-Chlorophenyl)-1,1,1-Trichloroethane and 2,2-Bis(*p*-chlorophenyl)- 1,1-Dichloroethylene on the Growth and Respiratory Activity of a Microorganism Used as a Model. Applied and Environmental Microbiology 63(12): 4948-4951.

Donato MT, Martínez-Romero A, Jiménez N, Negro A, Herrera G, Castell JV, O'Connor J-E, Gómez-Lechón MJ. (2009) Cytometric analysis for drug-induced steatosis in HepG2 cells. Chemico-Biological Interactions 181: 417-423.

Droge W. (2002) Free radicals in the physiological control of cell function. Physiological Reviews 82: 47-95.

Dubois M, Plaisance H, Thome J-P, Kremers P. (2006) Hierarchical cluster analysis of environmental pollutants through P450 induction in cultured hepatic cells: Indications for a toxicity screening test. Ecotoxicology and Environmental Safety 34: 205-215.

Duchen MR. (2004) Mitochondria in health and disease: perspectives on a new mitochondrial biology. Molecular Aspects of Medecine 25(4): 365-451.

Ekwall B, Barile FA, Castano A, Clemedson C, Clothier RH, Dierickx P *et al*. (1998) MEIC Evaluation of Acute Systemic Toxicity: Part VI. The Prediction of Human Toxicity by Rodent LD50 Values and Results from 61 In Vitro Methods. Alternatives to Laboratory Animals 26 S2: 617-658.

Elbekai RH, El-Kadi AOS. (2005) The role of oxidative stress in the modulation of aryl hydrocarbon receptor-rgulated genes by As^{3+}, Cd^{2+}, and Cr^{6+}. Free Radical Biology and Medicine 39: 1499-1511.

Eisenbrand G, Pool-Zobel B, Baker V, Balls M, Blaauboer BJ, Boobis A, *et al*. (2002) Methods of *in vitro* toxicology. Food and Chemical Toxicology 40: 193-236.

Farber E. (1991) Hepatocyte proliferation in stepwise development of experimental liver cell cancer. Digestive Diseases and Sciences 36(7):973-978.

Flodstrom S, Hemming H, Warngard L, Ahlborg UG (1990). Promotion of altered hepatic foci development in rat liver, cytochrome P450 enzyme induction and inhibition of cell-cell communication by DDT and some structurally related organohalogen pesticides. Carcinogenesis 11(8):1413-1417.

Farkas D, Tannenbaum SR. (2005) In vitro methods to study chemically-induced hepatotoxicity: A literature review. Current Drug Metabolism 6(2): 111-125.

Ferro M, Doyle A. (2001) Standardisation for In Vitro Toxicity Tests. Cell Biology and Toxicology 17: 205-212.

Filipak Neto F, Zanata SM, Silva de Assis HC, Naka LS, Randi MAF, Oliveira Ribeiro CA. (2008) Toxic effects of DDT and methyl mercury on the hepatocytes from *Hoplias malabaricus*. Toxicology in Vitro 22: 1705-1713.

Finch R, Hunter PA. (2006) Antibiotic resistance--action to promote new technologies: report of an EU Intergovernmental Conference held in Birmingham, UK, 12-13 December 2005. Journal of Antimicrobial Chemotherapy 58 S1: i3-i22.

Flynn TJ, Ferguson MS. (2008) Multiendpoint mechanistic profiling of hepatotoxicants in HepG2/C3A human hepatoma cells and novel statistical approaches for development of a prediction model for acute hepatotoxicity. Toxicology in Vitro 22: 1618-1631.

Fotakis G, Timbrell JA. (2006) In vitro cytotoxicity assays: Comparison of LDH, neutral red, MTT and protein assay in hepatoma cell lines following exposure to cadmium chloride. Toxicology Letters 160(2):171-177.

Fujii-Kuriyama Y, Imitaka H, Sogawa K, Yasumoto K-I, Kikuchi Y. (1992) Regulation of CYP1A expression. The FASEB Journal 6: 706-710.

Fujii-Kuriyama Y, Kawajiri Y. (2010) Molecular mechanisms of the physiological functions of the aryl hydrocarbon (dioxin) receptor, a multifunctional regulator that senses and responds to environmental stimuli. Procedings of the Japan Academy, Ser. B, Physical and Biological Sciences 86: 40-53.

Funk D, Schrenk H-H, Frei E. (2007) Serum albumin leads to false-positive results in the XTT and the MTT assay.BioTechniques 43:178-186.

Gajski G, Ravlic S, Capuder Z, Garaj-Vrhovac V. (2007) Use of sensitive methods for detection of DNA damage on human lymphocytes exposed to p,p'-DDT: Comet assay and new criteria for scoring micronucleus test. Journal of Environmental Science and Health: Part B 42(6): 607-613.

Giuliano M, Bellavia G, Lauricella M, D'Anneo A, Vassallo B, Vento R, Tesoriere G. (2004) Staurosporine-induced apoptosis in Chang liver cells is associated with down-regulation of Bcl-2 and Bcl-XL. International Journal of Molecular Medicine 13(4): 565-71.

Gomes A, Fernandes E, Lima JLFC. (2005) Fluorescence probes used for detection of reactive oxygen species. Journal of Biochemical and Biphysical Methods 65: 45-80.

Gómez-Lechón MJ, Lahoz A, Gombau L, Castell JV, Donato MT. (2010a) *In Vitro* Evaluation of Potential Hepatotoxicity Induced by Drugs. Current Pharmaceutical Design 16: 1963-1977.

Gómez-Lechón MJ, Tolosa L, Castell JV, Donato MT. (2010b) Mechanism-based selection of compounds for the development of innovative in vitro approaches to hepatotoxicity studies in the LIINTOP project. Toxicology In Vitro 24(7): 1879-1889.

Gravance CG, Garner DL, Baumber J, Ball BA.(2000) Assessment of equine sperm mitochondrial function using JC-1. Theriogenology 53(9): 1691-1703.

Greenlee AR, Quail CA, Berg RL. (1999) The antiestrogen ICI 182,780 abolishes developmental injury for murine embryos exposed in vitro to *o,p*-DDT. Reproductive Toxicology 14: 225-234.

Guengerich FP (2001). Common and uncommon cytochrome P450 reactions related to metabolism and chemical toxicity. Chemical Research in Toxicology 14(6): 611-650.

Guo R, Wang T, Shen H, Ge H-m, Sun J, Huang Z-h, Shu Y-q. (2010) Involvement of mTOR and survivin inhibition in tamoxifen-induced apoptosis in humanhepatoblastomacell line HepG2. Biomedicine and Pharmacotherapy 64(4): 249-253.

Guo SY, Shen X, Yang J, Yang RL, Mao K, Zhao DH, Li CJ. (2007) TIMP-1 mediates the inhibitory effect of interleukin-6 on the proliferation of a hepatocarcinoma cell line in a STAT3-dependent manner. Brazilian Journal of Medical and Biological Research 40(5): 621-31.

Gwathmey JK, Tsaioun K, Hajjar RJ. (2009) Cardionomics: a new integrative approach for screening cardiotoxicity of drug candidates. Expert Opinion on Drug Metabolism & Toxicology 5(6): 647-660.

Hakimelahi GH, Khodarahmi GA. (2005) The Identification of Toxicophores for the Prediction of Mutagenicity, Hepatotoxicity and Cardiotoxicity. Journal of the Iranian Chemical Society 2(4): 244-267.

Halliwell B, Gutteridge JMC. (2007) Free radicals in biology and medicine.4th Ed. Oxford, UK.Oxford University Press.

Harada T, Ohtsuka R, Takeda M, Yoshida T, Enomoto A, Kojima S, Tamiyama N, Nakashima N, Ozaki M. (2006) Hepatocarcinogenesis by DDT in rats. Journal of Toxicologic Pathology. 19(4):155-167.

Hardisty JF, Brix AE. (2005) Comparative hepatic toxicity: prechronic/chronic liver toxicity in rodents. Toxicologic Pathology 33: 35-40.

Harwood SM, Yaqoob MM, Allen DA. (2005) Caspase and calpain function in cell death: bridging the gap between apoptosis and necrosis. Annals of Clinical Biochemistry 42: 415-431.

Hewitt NJ, Gómez-Lechón MJ, Houston JB, Hallifax D, Brown HS, Maurel P,Kenna JG, Gustavsson L, Lohmann C, Skonberg C, Guillouzo A, Tuschl G, Li AP, Lecluyse E, Groothuis GMM, Hengstler JG. (2003) Primary hepatocytes: current understanding of the regulation of metabolic enzymes and transporter proteins, and pharmaceutical practice for the use of hepatocytes in metabolism, enzyme induction, transporter, clearance, and hepatotoxicity studies. Drug Metabolism Reviews 39: 159-234.

Horvath S. (1980) Cytotoxicity of drugs and diverse chemical agents to cell cultures. Toxicology 16: 59-66.

Hüttemann M, Lee I, Pecinova A, Pecina P, Karin Przyklenk K, Doan JW (2008) Regulation of oxidative phosphorylation, the mitochondrial membrane potential, and their role in human disease. Journal of Bioenergetics and Biomembranes 40: 445-456.

Ikeda, T. (2011) Drug-induced idiosyncratic hepatotoxicity: Prevention strategy development afterafter the troglitazone case. Drug Metabolism and Pharmackinetics 26(1): 60-70.

Ioannides C, Lewis DF. (2004) Cytochromes P450 in the bioactivation of chemicals. Current Topics in Medicinal Chemistry 4: 1767-1788.

Iyer KR, Sinz MW. (1999) Characterization of Phase I and Phase II hepatic drug metabolism activities in a panel of human liver preparations. Chemico-Biological Interactions 118(2): 151-169.

Jakoby WB, Ziegler DM. (1990) The enzymes of detoxication. Journal of Biological Chemistry 265(34): 20715-20718.

Jezek P, Hlavata L. (2005) Mitochondria in homeostasis of reactive oxygen species in cells, tissues and organism. The International Journal of Biochemistry and Cell Biology 37: 2478-2503.

James LP, McCullough SS, Lamps LW, Hinson JA. (2003) Effect of N-Acetylcysteine on Acetaminophen Toxicity in Mice: Relationship to Reactive Nitrogen and Cytokine Formation. Toxicological Sciences 75:458-467.

Jonsson EM, Abrahamson A, Brunstrom B, Brandt I. (2006) Cytochrome P4501A induction in rainbow trout gills and liver following exposure to waterborne indigo, benzo[*a*]pyrene and 3,3,4,4,5-pentachlorobiphenyl. Aquatic Toxicology 79: 226-232.

Jonsson HT, Walker EM, Greene WB, Hughson MD, Hennigar GR. (1981) Effects of prolonged exposure to dietary DDT and PCB on rat liver morphology.Archives of Environmental Contamination and Toxicology 10(2): 171-183.

Kalgutkar AS, Soglia JR. (2005) Minimising the potential for metabolic activation in drug discovery. Expert Opinion on Drug Metabolism and Toxicology 1: 91-142.

Katsura N, Ikai I, Mitaka T, Shiotani T, Yamanokuchi S, Sugimoto S, Kanazawa A, Terajima H, Mochizuki Y, Yamaoka Y. (2002)Long-Term Culture of Primary Human Hepatocytes with Preservation of Proliferative Capacity and Differentiated Functions. Journal of Surgical Research 106**:** 115–123

Kennedy SW, Jones SP. (1994) Simultaneous measurement of cytochrome P450 1A catalytic activity and total protein concentration with a fluorescence plate reader. Analytical Biochemistry 223: 217-23.

Kiang TKL, Teng XW, Surendradoss J, Karagiozov S, Abbott FS, Chang TKH. (2011) Glutathione depletion by valproic acid in sandwich-cultured rat hepatocytes: Role of biotransformation and temporal relationship with onset of toxicity. Toxicology and Applied Pharmacology 252: 318-324.

Klaassen CD (2001). Casarett and Doull's toxicology: the basic science of poisons. 6 ed. Philadelphia, McGraw-Hill.

Klaunig JE, Ruch RJ. (1987) Strain and species effects on the inhibition of hepatocyte intercellular communication by liver tumor promoters. Cancer Letters 36(2):161-168.

Knowles BB, Howe CC, Aden DP. (1980) Human hepatocellular carcinoma cell lines secrete the major plasma proteins and hepatitis B surface antigen. Science 209(4455):497-499.

Kostka G, Kopec-Szelzak J, Palut D. (1996) Early hepatic changes induced in rats by two hepatocarcinogenic organohalogen pesticides: Bromopropylate and DDT. Carcinogenesis 17(3):407-412.

Kostka G, Palut D, Kopec-Szlezak J, Ludwicki JK. (1999) Early hepatic changes in rats induced by permethrin in comparison with DDT. Toxicology 142(2):135-143.

Kruhlak NL, Contrera JF, Benz RD, Matthews EJ. (2007) Progress in QSAR toxicity screening of pharmaceutical impurities and other FDA regulated products. Advanced Drug Delivery Reviews 59: 43–55.

Kurebayashi H, Ohno Y. (2006) Metabolism of acrylamide to glycidamide and their cytotoxicity in isolated rat hepatocytes: Protective effects of GSH precursors. Archives of Toxicology 80 (12): 820-828.

Labbe G, Pessayre D, Fromenty B. (2008) Drug-induced liver injury through mitochondrial dysfunction: mechanisms and detection during preclinical safety studies.Fundamental & Clinical Pharmacology 22: 335-353.

Lasser KE, Allen PD, Woolhandler SJ, Himmelstein DU, Wolfe SM, Bor DH. (2002) Timing of new black box warnings and withdrawals for prescription medications. Jounral of the Amarican Medical Association287: 2215-2220.

Ledirac N, Delescluse C, De Sousa G, Pralavorio M, Lesca P, Amichot M, Bergé JB, Rahmani R. (1997) Carbaryl induces CYP1A1 gene expression in HepG2 and HaCaT cells but is not a ligand of the human hepatic Ah receptor. Toxicology and Applied Pharmacology 144(1): 177-182.

Lemaire B, Beck M, Jaspart M, Debier C, Calderon PB, Thomé J-P, Rees J-F. (2011) Precision-Cut Liver Slices of Salmo salar as a tool to investigate the oxidative impact of CYP1A-mediated PCB 126 and 3-methylcholanthrene metabolism. Toxicology in Vitro 25: 335-342.

Lewis DFV. (2003) Human Cytochromes P450 Associated with the Phase 1 Metabolism of Drugs and other Xenobiotics: A Compilation of Substrates and Inhibitors of the CYP1, CYP2 and CYP3 Families. Current Medicinal Chemistry 10: 1955-1972.

Lin P-H, Lin C-H, Huang C-C, Fang J-P, Chuang M-C. (2008) 2,3,7,8-Tetrachlorodibenzo-p-dioxin modulates the induction of DNA strand breaks and poly(ADP-ribose) polymerase-1 activation by 17β-estradiol in human breast carcinoma cells through alteration of CYP1A1 and CYP1B1 expression. Chemical Research in Toxicology 21(7): 1337-1347.

Lin T, Yang MS. (2008) Benzo[a]pyrene-induced necrosis in the HepG2 cells via PARP-1 activation and NAD^+ depletion. Toxicology 245: 147-153.

Lindén J, Lensu S, Tuomisto J, Pohjanvirta R. (2010) Dioxins, the aryl hydrocarbon receptor and the central regulation of energy balance. Frontiers in Neuroendocrinology 31: 452-478.

Liu Y, Fiskum G, Schubert D. (2002) Generation of reactive oxygen species by the mitochondrial electron transport chain. Journal of Neurochemistry 80: 780-787.

Liu Q, Yu H, Tan Z, Cai H, Ye W, Zhang M, *et al*. (2011) In vitro assessing the risk of drug-induced cardiotoxicity by embryonic stem cell-based biosensor. Sensors and Actuators B: Chemical 155(1): 214-219.

Livermore DM. (2004) The need for new antibiotics. Clinical Microbiology and Infection 10 S4: 1-9.

Ma Q. (2001) Induction of CYP1A1. The AhR/DRE paradigm: transcription, receptor regulation, and expanding biological roles. Current Drug Metabolism2: 149-164.

Ma Q, Lu AYH. (2007) CYP1A Induction and Human Risk Assessment: An Evolving Tale of in Vitro and in Vivo Studies. Drug Metabolism and Disposition 35(7): 1009-1016.

Mandenius C-F, Steel D, Noor F, Meyer T, Heinzle E, Asp J, *et al*. (2011) Cardiotoxicity testing using pluripotent stem cell-derived human cardiomyocytes and state-of-the-art bioanalytics: a review. Journal of Applied Toxicology 31: 191-205.

Marselos M, Strom SC, Michalopoulos G. (1987) Effect of phenobarbital and 3-methylcholanthrene on aldehyde dehydrogenase activity in cultures of HepG2 cells and normal human hepatocytes. Chemico-Biological Interactions 62(1):75-88.

Marzullo L. (2005) An update of N-acetylcysteine treatment for acute acetaminophen toxicity in children. Current Opinion in Pediatrics 17: 239-245.

Masubuchi Y, Nakayama S, Horie T. (2002) Role of Mitochondrial Permeability Transition in Diclofenac-Induced Hepatocyte Injury in Rats. Hepatology 35(3): 544-551.

Matsuyama S, Llopis J, Deveraux QL, Tsien RY, Reed JC. (2000) Changes in intramitochondrial and cytosolic pH: Early events that modulate caspase activation during apoptosis. Nature Cell Biology 2(6): 318-325.

Meister A, Anderson ME.(1983) Glutathione. Annual Review of Biochemistry 52: 711-760.

Mikhail TH, Aggour N, Awadallah R, Boulos MN, El-Dessoukey EA, Karima AI. (1979) Acute toxicity of organophosphorus and organochlorine insecticides in laboratory animals. Zeitschrift für Ernährungswissenschaft18(4): 258-268.

Mitsopoulis P, Suntres ZE. (2011) Protective Effects of Liposomal N-Acetylcysteine against Paraquat-Induced Cytotoxicity and Gene Expression. Journal of Toxicology Volume 2011: Article ID 808967.

Medina-Diaz IM, Elizondo G. (2005) Transcriptional induction of CYP3A4 by o,p'-DDT in HepG2 cells. Toxicology Letters 157(1): 41-47.

Morena AJM, Madeira VMC. (1991) Mitochondrial bioenergetics as affected by DDT. Biochimica et Biphysica Acta 1060(2): 166-174.

Moreno-Sanchez R, Bravo C, Vasquez C, Ayala G,Silveira LH, Martinez-Lavin M. (1999) Inhibition and Uncoupling of OxidativePhosphorylation by NonsteroidalAnti-inflammatory DrugsBiochemical Pharmacology 57: 743-752.

Morel Y, Barouki R. (1998) Down-regulation of Cytochrome P450 1A1 Gene Promoter by Oxidative Stress. The Journal of Biological Chemistry 273(4): 26969-26976.

Morel Y, Mermod N, Barouki R. (1999) An Autoregulatory Loop Controlling CYP1A1 Gene Expression: Role of H_2O_2 and NFI. Molecular and Cellular Biology Oct: 6825-6832.

Mota PC, Cordeiro M, Pereira SP, Oliveira PJ, Moreno AJ, Ramalho-Santos J. (2011) Differential effects of p,p_-DDE on testis and liver mitochondria:Implications for reproductive toxicology. Reproductive Toxicology 31: 80-85.

Murakami T. (2000) Cytotoxicity testing through cell adhesion to a pattern of collagen matrix. Analytica Chemica Acta 415(1-2): 201-207.

Nagy G, Koncz A, Fernandez D, Perl A. (2007) Nitric oxide, mitochondrial hyperpolarization, and T cell activation. Free Radical Biology and Medicine 42 (11): 1625-1631.

Nakamura H, Ariyoshi N, Okada K, Nakasa H, Nakazawa K, Kitada M. (2005) CYP1A1 Is a Major Enzyme Responsible for the Metabolism of Granisetron in Human Liver Microsomes. Current Drug Metabolism 6: 469-480.

Navas JM, Chana A, Herradon B, Segner H, (2003) Induction of CYP1A by the N-imidazole derivative, Ibenzylimidazole. Environmental Toxicology and Chemistry 22: 830-836.

Navas JM, Chana A, Herradon B, Segner H. (2004) Induction of cytochrome P4501A (CYP1A) by clotrimazole, a non-planar aromatic compound. Computational studies on structural features of clotrimazole and related imidazole derivatives. Life Sciences 76: 699–714.

Nebert DW, Roe AL, Dieter MZ, Solis WA, Yang Y, Dalton TP. (2000) Role of the aromatic hydrocarbon receptor and [Ah] gene battery in the oxidative stress response, cell cycle control and apoptosis. Biochemical Pharmacology 59: 65-85.

Nerurkar PV, Dragull K, Tang C-S. (2004) In Vitro Toxicity of Kava Alkaloid, Pipermethystine, in HepG2 Cells Compared to Kavalactones. Toxicological Sciences 79:106-111.

Nicholls DG. (1977) The effective proton conductance of the inner membrane of mitochondria from brown adipose tissue. Dependency on proton electrochemical potential gradient. European Journal of Biochemistry 77: 349-356.

Nieminen AL, Gores GJ, Bond JM, Imberti R, Herman B, Lemasters JJ. (1992) A novel cytotoxicity screening assay using a multiwell fluorescence scanner. Toxicology and Applied Pharmacology 115(2): 147-155.

Niles AL, Moravec RA, Riss TL.(2009) *In Vitro* Viability and Cytotoxicity Testing and Same-Well Multi-Parametric Combinations for High Throughput Screening. Current Chemical Genomics 3: 33-41.

Nims RW, Lubet RA, Fox SD, Jones CR, Anita, Thomas PE, Reddy AB, Kocarek TA.(1998) Comparative pharmacodynamics of CYP2B induction by DDT, DDE, and DDD in male rat liver and cultured rat hepatocytes. Journal of Toxicology and Environmental Health, Part A 53(6): 455-477.

Nishihara Y, Utsumi K. (1985) Effects of 1,1,1-trichloro-2,2-bis-(*p*-chlorophenyl)ethane (DDT) on ATPase-linked functions in isolated rat-liver mitochondria. Food and Chemical Toxicology 23(6): 599-602.

Nukaya M, Lin BC, Glover E, Moran SM, Kennedy GD, Bradfield CA. (2010) The aryl hydrocarbon receptor-interacting protein (AIP) is required for dioxin-induced hepatotoxicity but not for the induction of the Cyp1a1 and Cyp1a2 genes. Journal of Biological Chemistry 285(46): 35599-35605.

Nuydens R, Novalbos J, Dispersyn G, Weber C, Borgers M, Geerts H. (1999) A rapid method for the evaluation of compounds with mitochondria-protective properties. Journal of Neuroscience Methods 92: 153-159.

Nyati MK, Feng FY, Kanade VD, Nayak R. (2006) Chloroquine treatment increases detection of 5-fluorouracil-induced apoptosis index in vivo. Molecular Imaging 5 (3): 148-152.

Oh SH, Lima SC. (2006) A rapid and transient ROS generation by cadmium triggers apoptosis via caspase-dependent pathway in HepG2 cells and this is inhibited through *N*-acetylcysteine-mediated catalase upregulation. Toxicology and Applied Pharmacology 212: 212-213.

Panas MW, Xie Z, Panas HN, Hoener MC, Vallender EJ, Miller GM. (2011) Trace amine associated receptor 1 signalling in activated lymphocytes. Journal of Neuroimmune Pharmacology *In Press*.

Parekh AB. (2003) Mitochondrial regulation of intracellular Ca^{2+} signalling:More than just simple Ca^{2+} buffers. News in Physiological Sciences 18: 252-256.

Park BK, Kitteringham NR, Maggs JL, Pirmohamed M, Williams DP. (2005) The role of metabolic activation in drug-induced hepatotoxicity.Annual Review of Pharmacology and Toxicology 45: 177-202.

Park JE, Yang JH, Yoon SJ, Lee JH, Yang ES, Park JW. (2002) Lipid peroxidation-mediated cytotoxicity and DNA damage in U937 cells. Biochimie 84: 1199-1205.

Pauli-Magnus C, Meier PJ (2006).Hepatobiliary transporters and drug-induced cholestasis. Hepatology 44(4): 778-787.

Perez-Maldonado IN, Diaz-Barriga F, De la Fuente H, Gonzalez-Amaro R, Calderon J, Yanez L. (2004) DDT induces apoptosis in human mononuclear cells in vitro and is associated with increased apoptosis in exposed children. Environmental Research 94: 38-46.

Pearl GM, Livingston-Carr S, Durham SK, (2001) Integration of computational analysis as a sentinel tool in toxicological assessments, Current Topics in Medicinal Chemistry 1: 247–255.

Perl A, Gergely, P, Puskas F, Banki K. (2002) Metabolic switches of T-cell activation and apoptosis. Antioxidants and Redox Signaling 4 (3): 427-443.

Perret A, Pompon D. (1998) Electron shuttle between membranebound cytochrome P450 3A4 and b5 rules uncoupling mechanisms. Biochemistry 37: 11412-11424.

Perry SW, Norman JP, Barbieri J, Brown EB, Gelbard HA. (2011) Mitochondrial membrane potential probes and the proton gradient: a practical usage guide. BioTechniques 50: 98-115.

Peters TS. (2005) Do Preclinical Testing Strategies Help Predict Human Hepatotoxic Potentials?Toxicologic Pathology 33: 146-154.

Polaniak R, Buldak RJ, Karon M, Birkner K, Kukla M, Zwirska-Korcala K, Birkner E. (2010) Influence of an Extremely Low Frequency Magnetic Field (ELF-EMF) on Antioxidative Vitamin E Properties in AT478 Murine Squamous Cell Carcinoma Culture In Vitro. International Journal of Toxicology 29(2): 221-230.

Powers SK, Jackson MJ. (2006) Exercise-induced oxidative stress: Cellular mechanisms and impact on muscle force production. Physiological Reviews 88: 1243-1276.

Prabhakaran K, Li L, Borowitz JL, Isom GE. (2004) Caspase inhibition switches the mode of cell death induced by cyanide by enhancing reactive oxygen species generation and PARP-1 activation. Toxicology and Applied Pharmacology 195: 194-202.

Ray SD, Kumar MA, Bagchi D. (1999) A Novel Proanthocyanidin IH636 Grape Seed Extract Increases in Vivo Bcl-X Expression and Prevents Acetaminophen-Induced Programmed and Unprogrammed Cell Death in Mouse Liver. Archives of Biochemistry and Biophysics 369(1):42-58.

Ray SD, Parikh H, Hickey E, Bagchi M, Bagchi D. (2001) Differential effects of IH636 grape seed proanthocyanidin extract and a DNA repair modulator 4-aminobenzamide on liver microsomal cytochrome 4502E1-dependent aniline hydroxylation. Molecular and Cellular Biochemistry 218(1):27-33.

Reid Y, Gaddipati JP, Yadav D, Kantor J. (2009) Establishment of a human neonatal hepatocyte cell line In Vitro Cellular & Developmental Biology – Animal 45: 535-542.

Reliene R, Fischer E, Schiestl RH. (2004) Effect of *N*-acetylcysteine on oxidative DNA damage and the frequency of DNA deletions in atm-deficient mice. Cancer Research 64: 5148-5153.

Rhoads DM, Umbach AL, Subbaiah CC, Siedow JN. (2006) Mitochondrial Reactive Oxygen Species.Contribution to Oxidative Stress and Interorganellar Signaling. Plant Physiology 141: 357-366.

Riffat AF, Masood A. (2006) *Allium cepa* derived EROD as a potential biomarker for the presence of certain pesticides in water. Chemosphere 62: 527-537.

Riss T, Moravec R. (2004) Use of multiple assay endpoints to investigate the effects of incubation time, dose of toxin, and plating density in cell-based cytotoxicity assays. Assay and Drug Development Technologies 2: 51-62.

Rolfe DFS, Brand MD. (1997) The physiological significance of mitochondrial proton leak in animal cells and tissues. Bioscience Reports 17: 9-16.

Rudzok S, Schmückinga E, Graebsch C, Herbarth O, Bauer M. (2009) The inducibility of human cytochrome P450 1A by environmental-relevant xenobiotics in the human hepatoma derived cell line HepG2. Environmental Toxicology and Pharmacology 28: 370-378.

Ruffmann R, Wendel A. (1991) GSH rescue by N-acetylcysteine. Klinische Wochenschrift 69 (18): 857-862.

Ruiz-Leal M, George S. (2004) An in vitro procedure for evaluation of early stage oxidative stress in an established fish cell line applied to investigation of PHAH and pesticide toxicity. Marine Environmental Research 58: 631-635.

Safe S. (1995) Modulation of gene expression and endocrine response pathways by 2,3,7,8-tetrachlorodibenzo-p-dioxin and related compounds. Pharmacology and Therapeutics 67: 247-281.

Sahu SC. (2003) Hepatocyte culture as an in vitro model for evaluating the hepatotoxicity of food-borne toxicants and microbial pathogens: A review. Toxicology Mechanisms and Methods 13(2): 111-119.

Samali A, Nordgren H, Zhivotovsky B, Peterson E, Orrenius S. (1999) A Comparative Study of Apoptosis and Necrosis in HepG2 Cells: Oxidant-Induced Caspase Inactivation Leads to Necrosis. Biochemical and Biophysical Research Communications 255: 6-11.

Santos NAG, Medina WSG, Martins NM, Carvalho Rodrigues MA, Curti C, Santos AC. (2008) Involvement of oxidative stress in the hepatotoxicity induced by aromatic antiepileptic drugs. Toxicology in Vitro 22: 1820-1824.

Sassa S, Sugita O, Galbraith RA, Kappas A. (1987) Drug metabolism by the human hepatoma cell, Hep G2. Biochemical and Biophysical Research Communications 143(1):52-57.

Schlezinger JJ, Keller J, Verbrugge LA, Stegeman JJ. (2000) 3,3',4,4'-Tetrachlorobiphenyl oxidation in fish, bird and reptile species: Relationship to cytochrome P450 1A inactivation and reactive oxygen production. Comparative Biochemistry and Physiology - C Pharmacology Toxicology and Endocrinology 125(3): 273-286.

Schlezinger JJ, Struntz WDJ, Goldstone JV, Stegeman JJ. (2006) Uncoupling of cytochrome P450 1A and stimulation of reactive oxygenspecies production by co-planar polychlorinated biphenyl congeners. Aquatic Toxicology 77: 422-432.

Schuster D, Laggner C. Langer T. (2005) Why drugs fail—a study on side effects in new chemical entities. Current Pharmaceutical Design11: 3545-3559.

Sciullo EM, Christoph Vogel CF, Wu D, Murakami A, Ohigashi H, Matsumura F. (2010) EVects of selected food phytochemicals in reducing the toxic actions of TCDD and *p,p_*-DDT in U937 macrophages. Archives of Toxicology 84: 957-966.

Shi Y, Song Y, Wang Y, Liang X, Hu Y, Guan X, Cheng J, Yang K. (2009) *p,p'*-DDE Induces Apoptosis of Rat Sertoli Cells via a FasL-Dependent Pathway. Journal of Biomedicine and Biotechnology Volume 2009, Article ID 181282.

Shi Y, Zhang J-H, Jiang M, Zhu L-H, Tan H-Q, Lu B. (2010a) Synergistic Genotoxicity Caused by Low Concentration of Titanium Dioxide Nanoparticles and p,p0-DDT in Human Hepatocytes. Environmental and Molecular Mutagenesis 51: 192-204.

Shi Y-Q, Wang Y-P, Song Y, Li H-W, Liu C-J, Wu Z-G, Yang K-D. (2010b) p,p-DDE induces testicular apoptosis in prepubertal rats via the Fas/FasL pathway. Toxicology Letters 193: 79-85.

Shiizaki K, Ohsako S, Kawanishi M, Yagi T. (2008) Omeprazole Alleviates Benzo[a]pyrene Cytotoxicity by Inhibition of CYP1A1 Activity in Human and Mouse Hepatoma Cells.Basic & Clinical Pharmacology &Toxicology 103: 468-475.

Shimada T, Yamazaki H, Mimura M, Inui Y, Guengerich FP. (1994) Interindividual variations in human liver cytochrome P-450 enzymes involved in the oxidation of drugs, carcinogens and toxic chemicals: studies with liver microsomes of 30 Japanese and 30 Caucasians. Journal of Pharmacology and Experimental Therapeutics 270(1): 414-423.

Sierra-Santoyo A, Hernandez M, Albores A, Cebria ME.(2000) Sex-Dependent Regulation of Hepatic Cytochrome P-450 by DDT. Toxicological Sciences 54:81-87.

Silber PM, Ruegg CE, Myslinski N. (1994) *In vitro* methods for predicting human toxicity. Laboratory Animals23: 33-37.

Silva JP, Couthino OP. (2010) Free radicals in the regulation of damage and cell death – basic mechanisms and prevention. Drug Discoveries & Therapeutics. 4(3): 144-167.

Simon HU, Haj-Yehia A, Levi-Schaffer F. (2000) Role of reactive oxygen species (ROS) in apoptosis induction. Apoptosis 5: 415-418.

Sloviter RS (2002). Apoptosis: a guide for the perplexed. Trends in Pharmacological Sciences 23: 19-24.

Smilkstein MJ, Bronstein AC, Linden C, Augenstein WL, Kulig KW, Rumack BH. (1991) Acetaminophen overdose: a 48-hour intravenous N-acetylcysteine treatment protocol. Annals of Emergency Medicine20: 1058-1063.

Soltis RD, Hasz D, Morris MJ, Wilson ID. (1979) The effect of heat inactivation of serum on aggregation of immunoglobulins. Immunology 36(1): 37-45.

Song Y, Liang X, Hu Y, Wang Y, Yu H, Yang K. (2008) *p,p*-DDE induces mitochondria-mediated apoptosis of cultured rat Sertoli cells. Toxicology 253: 53-61.

Souza V, Escobar Md Mdel C, Gómez-Quiroz L, Bucio L, Hernández E, Cossio EC, Gutiérrez-Ruiz MC. (2004) Acute cadmium exposure enhances AP-1 DNA binding and induces cytokines expression and heat shock protein 70 in HepG2 cells. Toxicology 197(3): 213-228.

Sukata T, Uwagawa S, Ozaki K, Ogawa M, Nishikawa T, Iwai S *et al*. (2002) Detailed low-dose study of 1,1-bis(p-chlorophenyl)-2,2,2-trichloroethane carcinogenesis suggests the possibility of a hormetic effect. International Journal of Cancer 99(1):112-118.

Swift B, Pfeifer ND, Brouwer KLR. (2010) Sandwich-cultured hepatocytes: An in vitro model to evaluate hepatobiliary transporter-based drug interactions and hepatotoxicity. Drug Metabolism Reviews 42(3): 446-471.

Tappenden DM, Lynn SG, Crawford RB, Lee K, Vengellur A, Kaminski NE, Thomas RS, LaPres JJ. (2011) The aryl hydrocarbon receptor interacts with ATP5α1, a subunit of the ATP synthase complex, and modulates mitochondrial function. Toxicology and Applied Pharmacology *In Press.*

Tate EH, Wilder ME, Cram LS, Wharton W. (1983) A method for staining 3T3 cell nuclei with propidium iodide in hypotonic solution. Cytometry 4(3): 211-5.

Taub R. (1998) Blocking NF-κB in the liver: The good and bad news. Hepatology 27: 1445-1446.

Tebourbi O, Rhouma KB, Sakli M. (1998) DDT induces apoptosis in rat thymocytes. Bulletin of Environmental Contamination and Toxicology 61: 216-223.

Tsui WMS (2003). Drug-associated changes in the liver. Current Diagnostic Pathology 9(2): 96-104.

Turrens JF, Boveris A. (1980) Generation of superoxide anion by the NADH dehydrogenase of bovine heart mitochondria. Biochemical Journal 191: 421-427.

Turrens JF, Alexandre A, Lehninger AL. (1985) Ubisemiquinone is the electron donor for superoxide formation by complex III of heart mitochondria. Archives of Biochemistry and Biophysics 237: 408-414.

Vrzal R, Stejskalova L, Monostory K, Maurel P, Bachleda P, Pavek P, Dvorak Z. (2009) **D**examethasone controls aryl hydrocarbon receptor (AhR)-mediated CYP1A1 and CYP1A2 expression and activity in primary cultures of human hepatocytes. Chemico-Biological Interactions 179(2-3): 288-296.

Wallace KB, Starkov AA. (2000) Mitochondrial targets of drug toxicity. Annual Review of Pharmacology and Toxicology 40: 353-388.

Wang T, Weinman SA. (2006) Causes and consequences of mitochondrial reactive oxygen species generation in hepatitis C. Journal of Gastroenterology and Hepatology 21: S34-37.

Wang X, Martindale JL, Holbrook NJ.(2000) Requirement for ERK activation in cisplatin-induced apoptosis.The Journal of Biological Chemistry 275: 39435-39443.

Weisiger RA. (2010) Isoniazid Hepatotoxicity.eMedicine 10-28-0100.

Westerink WMA, Schoonen WGEJ. (2007) Cytochrome P450 enzyme levels in HepG2 cells and cryopreserved primary human hepatocytes and their induction in HepG2 cells. Toxicology in Vitro 21: 1581-1591.

Whitlock JP. (1999) Induction of cytochrome P4501A1.Annual Reviews on Pharmacology and Toxicology39: 103-125.

Wikipedia. (2011) Degradation of DDT to form and DDE (by elimination of HCl, left) and DDD (by reductive dechlorination, right). Retrieved on 25/06/2011 from http://upload.wikimedia.org/wikipedia/commons/thumb/a/a1/DDT_to_DDE_and_DDD.svg/500px-DDT_to_DDE_and_DDD.svg.png.

Wikipedia.(2011) Mitochondrion.Retrieved on 28 May 2011 from: http://en.wikipedia.org/wiki/File:ETC_electron_transport_chain.svg.

World Health Organization.(1979) DDT and its derivatives.

Wu D, Cederbaum AI. (2003) Alcohol, oxidative stress and free radical damage. Alcohol Research and Health 27(4): 277-284.

Wu J-P, Chang LW, Yao H-T, Chang H, Tsai H-T, Tsai M-H, Yah T-K, Lin P. (2009) Involvement of oxidative stress and activation of aryl hydrocarbon receptor in elevation of CYP1A1 expression and activity in lung cells and tissues by arsenic: an *in vitro* and *in vivo* study. Toxicological Sciences 107(2): 385-393.

Wu Y, Connors D, Barber L, Jayachandra S, Hanumegowda UM, Adams SP. (2009) Multiplexed assay panel of cytotoxicity in HK-2 cells for detection of renal proximal tubule injury potential of compounds. Toxicology in Vitro 23: 1170-1178.

Ximenes VF, Pessoa AS, Padovan CZ, Abrantes DC, Gomes FHF, Maticoli MA, de Menezes ML. (2009) Oxidation of melatonin by AAPH-derived peroxyl radicals: Evidence of a pro-oxidant effect of melatonin. Biochimica et Biophysica Acta 1790: 787-792.

Yáñez L, Borja-Aburto VH, Rojas E, de la Fuente H, González-Amaro R, Gómez H, Jongitud AA, Díaz-Barriga F. (2004) DDT induces DNA damage in blood cells. Studies in vitro and in women chronically exposed to this insecticide. Environmental Research 94(1): 18-24.

You L, Chan SK, Bruce JM, Archibeque-Engle S, Casanova M, Corton JC *et al*. (1999) Modulation of testosterone-metabolizing hepatic cytochrome P-450 enzymes in developing Sprague-Dawley rats following in utero exposure to p,p'-DDE. Toxicology and Applied Pharmacology 158(2):197-205.

Younis HM, Abo-El-Saad MM, Abdel-Razik RK, Abo-Seda SA. (2002) Resolving the DDT target protein in insects as a subunit of the ATP synthase. Biotechnology and Applied Biochemistry 35(1): 9-17.

Yu, BP. (1994) Cellular defences against damage from reactive oxygen species. Physiological Reviews 74: 139-162.

Zangar RC, Davydov DR, Verma S. (2004) Mechanisms that regulate production of reactive oxygen species by cytochrome P450. Toxicology and Applied Pharmacology 199 : 316-331.

Zeiss CJ. (2003) The Apoptosis-Necrosis Continuum: Insights from Genetically Altered Mice. Veterinary Pathology 40:481-495.

Zhang Y, Goodyer C, LeBlanc A. (2000) Selective and protracted apoptosis in human primary neurons microinjected with active caspase-3, -6, -7, and -8. The Journal of Neuroscience. 20(22): 8384-8389.

Zhang L, Seitz LC, Abramczyk AM, Chan C. (2009) Synergistic effect of cAMP and palmitate in promoting altered mitochondrial function and cell death in HepG2 cells. Experimental Cell Research 316: 716-727.

Zhang R, Kang KA, Piao MJ, Kim KC, Kim AD, Chae S, Park JS, Young UJ, Hyun JW. (2010) Cytoprotective effect of the fruits of *Lycium chinense* Miller against oxidative stress-induced hepatotoxicity. Journal of Ethnopharmacology 130: 299-306.

Zhao C, Dodin G, Yuan C, Chen H, Zheng R, Jia Z, Fan BT. (2005) "In vitro" protection of DNA from Fenton reaction by plant polyphenol verbascoside. Biochimica et Biopysica Acta 1723(1-3): 114-123.